Chem Soc Rev

REVIEW ARTICLE

View Article Online
View Journal | View Issue

Cite this: *Chem. Soc. Rev.*, 2018, **47**, 8842

Excited-state intramolecular proton-transfer (ESIPT) based fluorescence sensors and imaging agents

Adam C. Sedgwick, [ab] Luling Wu, [a] Hai-Hao Han, [c] Steven D. Bull, *[a] Xiao-Peng He, *[c] Tony D. James, *[ad] Jonathan L. Sessler, *[b] Ben Zhong Tang, *[e] He Tian *[c] and Juyoung Yoon *[f]

Received 4th September 2018

DOI: 10.1039/c8cs00185e

rsc.li/chem-soc-rev

In this review we will explore recent advances in the design and application of excited-state intramolecular proton-transfer (ESIPT) based fluorescent probes. Fluorescence based sensors and imaging agents (probes) are important in biology, physiology, pharmacology, and environmental science for the selective detection of biologically and/or environmentally important species. The development of ESIPT-based fluorescence probes is particularly attractive due to their unique properties, which include a large Stokes shift, environmental sensitivity and potential for ratiometric sensing.

Introduction

Fluorescence based sensors and imaging agents have been routinely used in biology, physiology, pharmacology, and environmental science for the selective detection of biologically and/or environmentally important species for around 150 years. The use of fluorescent probes has revolutionised our understanding of a range of physiological or pathological processes and have provided

[a] *Department of Chemistry, University of Bath, Bath, BA2 7AY, UK. E-mail: s.d.bull@bath.ac.uk, t.d.james@bath.ac.uk*
[b] *Department of Chemistry, University of Texas at Austin, 105 E 24th street A5300, Austin, TX 78712-1224, USA. E-mail: sessler@cm.utexas.edu*
[c] *Key Laboratory for Advanced Materials and Joint International Research Laboratory of Precision Chemistry and Molecular Engineering, Feringa Nobel Prize Scientist Joint Research Center, School of Chemistry and Molecular Engineering, East China University of Science and Technology, 130 Meilong Rd, Shanghai 200237, China. E-mail: xphe@ecust.edu.cn, tianhe@ecust.edu.cn*
[d] *Department of Materials and Life Sciences, Faculty of Science and Technology, Sophia University, 7-1 Kioi-cho, Chiyoda-ku, Tokyo 102-8554, Japan*
[e] *Department of Chemistry, The Hong Kong University of Science & Technology (HKUST), Clear Water Bay, Kowloon, Hong Kong, China. E-mail: tangbenz@ust.hk*
[f] *Department of Chemistry and Nano Science, Ewha Womans University, Seoul 120-750, Korea. E-mail: jyoon@ewha.ac.kr*

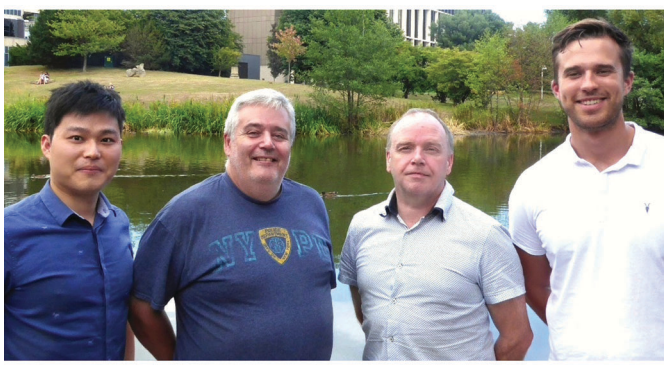

From left to right: Luling Wu, Tony D. James, Steven D. Bull and Adam C. Sedgwick

Luling Wu received his MSc in 2017 from Shanghai Normal University. In 2017, he was awarded a scholarship by the China Scholarship Council (CSC) to carry out a PhD at the University of Bath. Tony D. James is a Professor at the University of Bath, Fellow of the Royal Society of Chemistry and holds a Royal Society Wolfson Research Merit Award (2017–2022). His BSc was from the University of East Anglia (1986), PhD from the University of Victoria (1991), Postdoctoral Research with Seiji Shinkai (1991–1995) and Royal Society University Research Fellow at the University of Birmingham (1995–2000). He was awarded the Daiwa-Adrian Prize (2013), the inaugural CASE Prize (2015) and MSMLG Czarnik Award (2018). Steven D. Bull received a BSc Joint Hons from the University of Cardiff, a PhD from University of Cardiff (1990), and was post-doctoral fellow at the University of Queensland (1991–1993) and University of Oxford with Professor S. G. Davies (1994–2000). He joined the University of Bath in 2000 where he is a Professor of Organic Chemistry. He was awarded a Royal Society Industrial Fellowship (2002–2006), the Daiwa-Adrian Prize (2013) and University of Bath prize for outstanding PhD supervision (2013). Adam C. Sedgwick, received his MChem from the University of Bath in 2014, during which he undertook an industrial placement at BioFocus (now Charles River) working as a medicinal chemist. He recently finished his PhD studies at the University of Bath. He has just moved to University of Texas at Austin to carry out a Post. Doctoral Fellowship under the supervision of Jonathan L. Sessler.

effective sensing protocols for the detection of harmful species that may have been released into the environment (aqueous and gaseous). Despite the significant progress made in this exciting field, a number of challenges, including ease-of-use, selectivity, and sensitivity, still remain. The challenges are compounded by the increasingly stringent requirements for detection that have been introduced by regulatory bodies, which means that current fluorescent probes may not be suitable for use in a real-world setting.[1,2a,b]

Fluorescent probes use either specific host–guest interactions, or a selective chemical reaction to produce a change in the fluorescence properties of the system. When the binding between the host and guest is non-covalent and reversible, then the fluorescent probe is known as a chemosensor. However,

Hai-Hao Han

Hai Hao Han received his BSc in Applied Chemistry (2015) from SDUT and is currently pursuing his PhD degree in Applied Chemistry with Professor Xiao-Peng He at School of Chemistry and Molecular Engineering, ECUST.

Xiao-Peng He

Xiao-Peng He received his BSc in Applied Chemistry (2006) and PhD in Pharmaceutical Engineering (2011) from ECUST. He then completed a co-tutored doctoral program at ENS Cachan (France). He carried out his postdoctoral research with Professor Kaixian Chen (SIMM, CAS) at ECUST from 2011 to 2013. He is now professor at School of Chemistry and Molecular Engineering at ECUST.

Jonathan L. Sessler

Jonathan L. Sessler received a BSc degree in Chemistry in 1977 from the University of California, Berkeley. He obtained his PhD from Stanford University in 1982. After postdoctoral stays in Strasbourg and Kyoto, he accepted a position at the University of Texas at Austin, where he is currently the Doherty-Welch Chair. He was a co-founder of Pharmacyclics, Inc. and Cible, Inc. He was also a WCU Professor at Yonsei University and recently accepted a laboratory directorate at Shanghai University.

Ben Zhong Tang

Ben Zhong Tang is Chair Professor of Chemistry at Hong Kong University of Science & Technology. His PhD was from Kyoto University (1988). He was elected to Chinese Academy of Sciences in 2009. He has published >1100 papers, which have been cited >60 000 times, with a h-index of 116. He received State Natural Science Award (1st Class) from Chinese Government in 2017. He is currently serving as Editor-in-Chief of Materials Chemistry Frontiers.

He Tian

He Tian was appointed Cheung Kong Distinguished Professor by the Education Ministry of China in 1999. In 2011, he was selected as a member of the Chinese Academy of Science. In 2013, he became a Fellow of the TWAS (the World Academy of Science) for the advancement of science in developing countries. He has been listed as a Highly Cited Researcher in Chemistry (2014–2018) by Clarivate.

Juyoung Yoon

Juyoung Yoon received his PhD (1994) from The Ohio State University. After completing postdoctoral research at the University of California, Los Angeles and at The Scripps Research Institute, he joined the faculty at Silla University in 1998. In 2002, he moved to Ewha Womans University, where he is currently Professor of Department of Chemistry and Nano Science. He was listed as a highly cited researcher in chemistry from 2014–2017.

if the interaction between the host and guest produces an irreversible chemical reaction, then the fluorescent probe is referred to as a chemidosimeter.[3–6] Over the years, these two definitions, as well as the term 'fluorescent probe', have been used interchangeably (and ambiguously), therefore for the purpose of this review both types of sensor will be referred to as fluorescent probes. Traditionally, three classic fluorescence mechanisms have been exploited to generate a fluorescence response, namely PET (Photoinduced Electron Transfer), FRET (Förster Resonance Energy Transfer) and ICT (Internal Charge Transfer). In this review, we will focus on probes that use excited-state intramolecular proton transfer (ESIPT), or a combination of fluorescence mechanisms (AIE/ESIPT, PET/ESIPT, ICT/ESIPT or FRET/ESIPT) for the detection of biologically and/or environmentally important species.

The process of excited-state intramolecular proton transfer (ESIPT) was first reported by Weller in the 1950s for salicylic acid.[7] Since then, the photophysics of ESIPT has been extensively studied and applied to a range of applications.[8–11] In general, molecules can exhibit ESIPT fluorescence if their structures incorporate an intramolecular hydrogen bonding interaction between a hydrogen bond donor (–OH and NH_2) and a hydrogen bond acceptor (=N– and C=O). The most common ESIPT fluorophores are analogues of 2-(2′-hydroxyphenyl)benzimidazole (HBI), 2-(2′-hydroxyphenyl)benzoxazole (HBO) and 2-(2′-hydroxyphenyl)benzothiazole (HBT). Additional ESIPT fluorophores that have been reported include quinoline,[12] benzophenones,[13] flavones,[14] anthraquinones,[15] benzotriazoles,[16] *N*-salicylideneaniline,[17] and quinoxalines,[18] as illustrated in Fig. 1.

ESIPT is a unique four-level photochemical process, with the electronic ground state of ESIPT fluorophores typically existing in an enol (E) form. Upon photoexcitation, the electronic charge of such molecules can be redistributed, resulting in greater acidity for the hydrogen bond donor group and increased basicity for the hydrogen bond acceptor within the E form. As a result, an extremely fast enol to keto phototautomerization ($k_{ESIPT} > 10^{12}$ s^{-1}) event takes place, with the excited state enol form (E*) rapidly converting to its excited keto form (K*). After decaying radiatively back to its electronic ground state, a reverse proton transfer (RPT) takes place to produce the original E form (see Scheme 1).

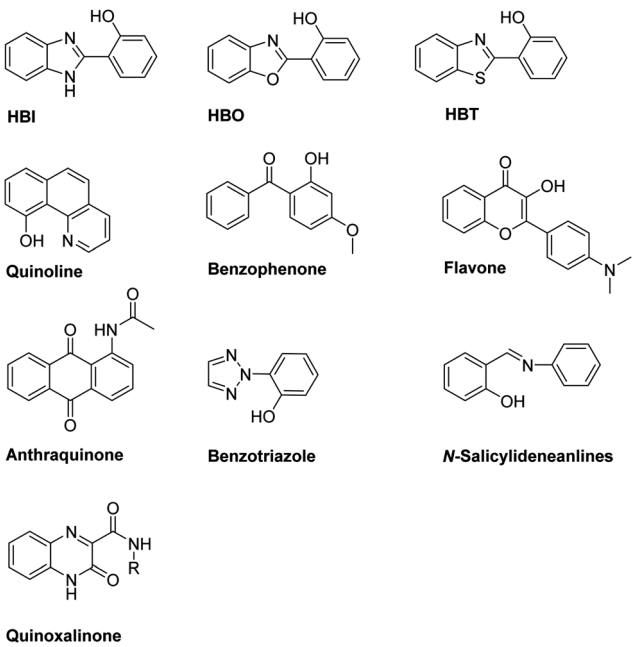

Fig. 1 Representative examples of commonly used ESIPT fluorophores.

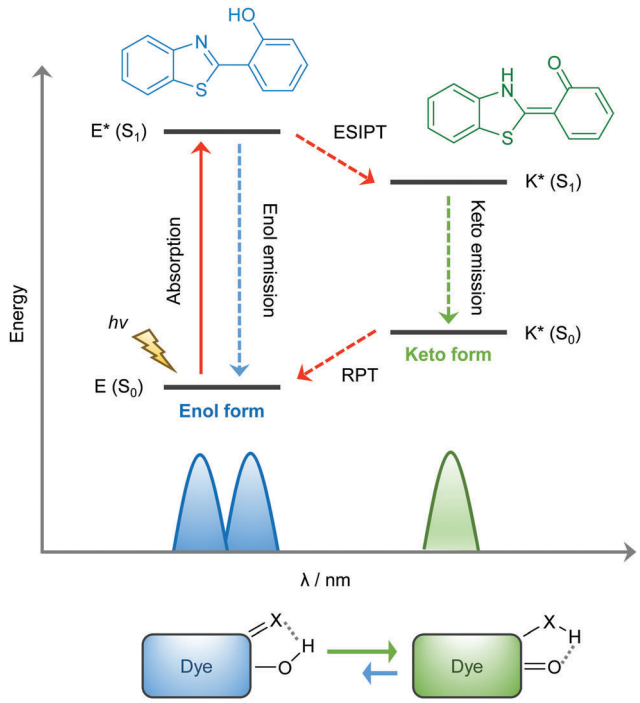

Scheme 1 Diagrammatic description of the ESIPT process.

Because of this rapid four-level photochemical process, ESIPT fluorophores are characterized by several particularly attractive features that make them useful as fluorescent probes and imaging agents. For instance, ESIPT fluorophores have an unusually large Stokes shift (~200 nm) when compared to traditional fluorophores (fluorescein, rhodamine, *etc.*). This helps avoid unwanted self-reabsorption and inner-filter effects. Moreover, due to the transient nature of the four-level photochemical process, the ESIPT emission is highly sensitive to its local surroundings. Consequently, the presence of polar and hydrogen bond donating solvents can result in inhibition of the ESIPT process with the keto (K*) emission often not being observed. Therefore, many ESIPT fluorescent probes require a large ratio of organic solvent, or cetyltrimethylammonium bromide (CTAB), to create a sufficiently hydrophobic micellar environment to produce a fluorescence response.[19,20] Due to the importance of the environment in ESIPT fluorescence, in this review we have reported the measurement conditions in the text and for all figures and schemes. Most ESIPT fluorophores can be used for ratiometric sensing because they exhibit dual-emission spectra arising from the excited state enol (E*) and the excited state keto (K*) emissions. This is particularly useful for fluorescence detection of biologically and/or environmentally

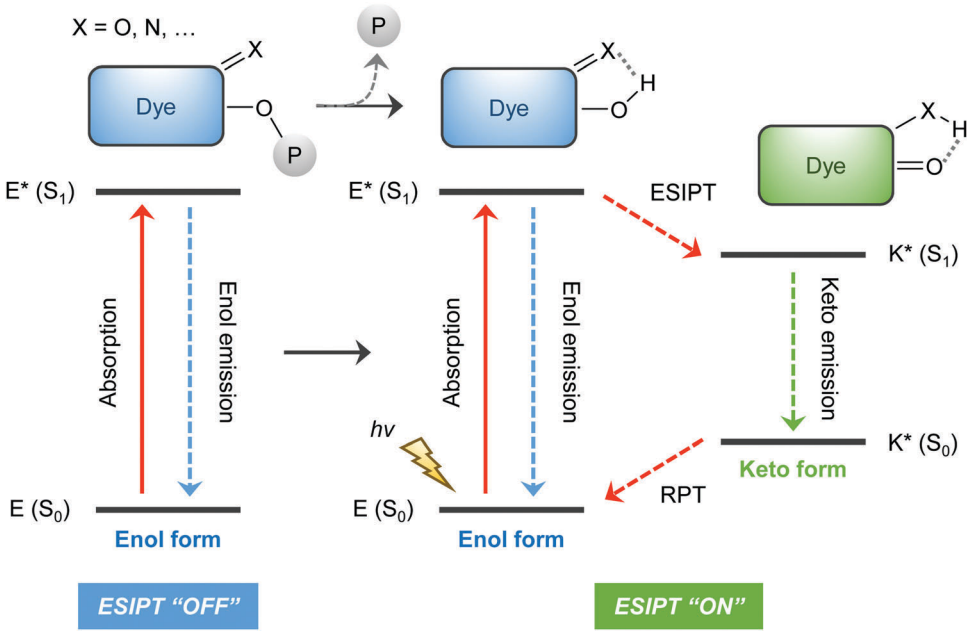

Scheme 2 Diagrammatic representation of the most common strategy underlying the design of ESIPT-based fluorescent probes.

important species, because ratiometric probes provide direct information about the concentration of the target analyte without the need for calibration.[21]

The general strategy for the development of ESIPT-based fluorescent probes is based on a design that involves blocking the hydrogen bond donor of the ESIPT fluorophore with a reactive unit specific that prevents the ESIPT process. As a result, only enol emission is observed, because no exchangeable protons are available. However, exposure of a reactive unit in the probe to a specific analyte allows access to the keto form which results in the ESIPT process being turned on (Scheme 2).

ESIPT fluorescence-based sensors for cations

Proton (H^+)

The proton (H^+) is the smallest but most important cationic species involved in physiological and pathological processes. Damage to transporters that maintain pH homeostasis is known to result in cellular dysfunction and metabolic disruption that can lead to disease.[22,23] Therefore, monitoring changes in the pH of biological systems can provide important insight into the development of different disease states.

Sekar *et al.* combined HBI and HBT with fluorescein to afford ESIPT-fluorescein pH-based fluorescent probes (Fig. 2),[24,25] that were able to detect pH values between 6–13. Fluorescein has a remarkably small Stokes shift of 18 nm; however, HBT-fluorescein and HBI-fluorescein displayed a remarkably large K* Stokes shift of 248 and 267 nm, respectively, at pH 7, thus demonstrating the benefit of the ESIPT fluorescent probe approach.

Shuang *et al.* developed a series of oxime-appended spirobenzopyrans as fluorescent pH ratiometric probes **1-R** that

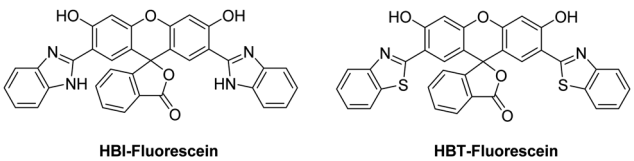

Fig. 2 HBI-fluorescein and HBT-fluorescein for the use as pH fluorescent probes. Measurement conditions: 100% aqueous solution.

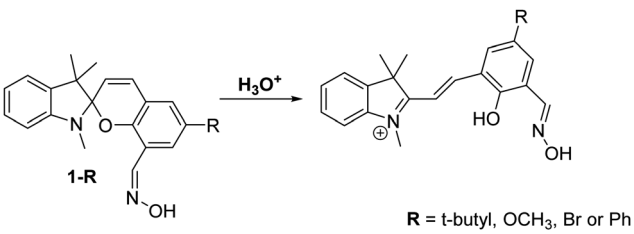

Scheme 3 Oxime-appended spirobenzopyrans **1-R** for the use as pH fluorescent probes. Measurement conditions: HEPES/ACN (8 : 2) buffer solution.

work in HEPES/ACN (8 : 2) buffer solutions – Scheme 3. Transformation of the acidochromic spirobenzopyran (closed) form to the merocyanine (open) form results in the ESIPT process taking place to provide a dual emission spectrum. Spirobenzopyran (R = ^{t}Bu) provided a 68-fold increase in ratiometric intensities (I_{645}/I_{522}) when the pH decreased from 8.0 to 4.0 (pK_a = 5.90).[26]

Lysosomes are membrane-bound organelles with internal acidic environments (pH = 5), which enable a range of digestive enzymes to function. However, small changes to lysosomal pH can result in adverse effects that are associated with a number of diseases.[27–29]

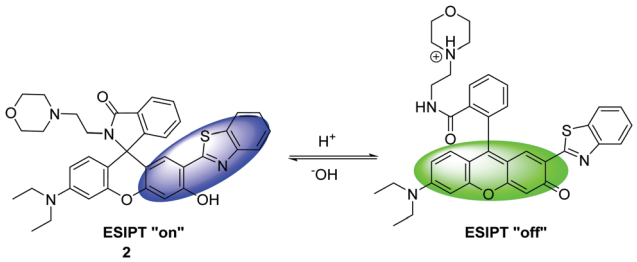

Scheme 4 HBT-based rhodol fluorescent probe **2** for the monitoring of changes in pH in lysosomes. Measurement conditions: 100% PBS buffer (10 mM).

Zhang *et al.* have developed a new lysosome-targeted ratiometric fluorescent probe **2** (FR-Lys) by attaching morpholine to an ESIPT rhodol HBT fluorophore. The morpholine group serves as a targeting unit for the lysosome. Concurrently, the rhodol fragment can undergo a pH-modulated open/close reaction of its spirocyclic fragment; this enables the HBT moiety to provide a pH modulated ESIPT response (Scheme 4).[30]

Interestingly, Singh *et al.* have reported a theranostic ESIPT pH probe **3** incorporating a HBT-7-hydroxy-coumarin fluorophore, which was then functionalised with a photocleavable unit containing the anticancer drug chlorambucil (Fig. 3). Probe **3** exhibited good ESIPT photophysical properties with a large Stokes shift of 151 nm. Moreover, this theranostic probe was shown to be pH sensitive. At physiological pH, the phenol is deprotonated, and no ESIPT takes place with only blue emission from the coumarin unit being observed. At the slightly acidic pH levels that are present in many cancer cells,[31] the phenolate anion becomes protonated, thus turning on the ESIPT process that results in an increase in fluorescence emission at 516 nm. Photolysis of **3** using UV light at 365 nm was shown to result in efficient release of chlorambucil. Probe **3** was shown to internalize into cancer cells, while an MTT assay revealed low cytotoxicity towards the MDA-MB-231 cell line. Exposure to UV light, resulted in probe **3** demonstrating enhanced cytotoxicity due to the release of chlorambucil inside the cancer cell.[32]

Magnesium (Mg^{2+})

Magnesium (Mg^{2+}) is an abundant element that plays a vital role in a number of cellular processes including cellular proliferation, a range of enzymatic reactions, cell death, DNA stabilisation and signal transduction.[33] Changes in the concentrations of Mg^{2+} have been linked to a number of serious illnesses, including hypertension, diabetes, osteoporosis, renal failure and cardiac arrest. Consequently, it is of great importance to develop simple and efficient probes that allow for the monitoring of Mg^{2+} levels in real time.[34]

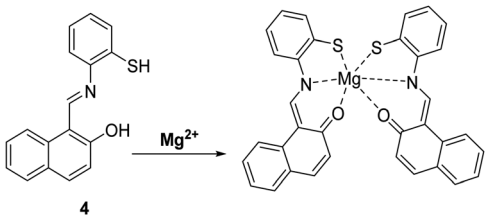

Scheme 5 A simple naphthalene Schiff base ESIPT fluorescent probe **4** for the detection of Mg^{2+}. Measurement conditions: THF/H_2O (9 : 1).

Callan and co-workers designed a simple ESIPT probe **4** for the ratiometric detection of Mg^{2+}. The Schiff base of **4** undergoes ESIPT to generate a keto tautomer, which enables efficient binding of Mg^{2+} (Scheme 5). Probe **4** was shown to display good selectivity and high sensitivity for the detection of low concentrations of Mg^{2+} (2 μM) in a THF/H_2O (9 : 1) solvent system. It was shown to bind to Mg^{2+} with a 2 : 1 stoichiometry and an association constant (K_{21}) of $(1.4 \pm 0.1) \times 10^4\ M^{-2}$, meaning that it could be used potentially as a diagnostic probe for hypermagnesaemia (high level of Mg^{2+} in blood).[35]

Zinc (Zn^{2+})

Zinc (Zn^{2+}) is the second most abundant transition metal in nature, which acts as an essential element in a number of physiological processes.[36,37] Changes in Zn^{2+} levels are closely associated with the onset of a number of diseases, including breast cancer, cerebral ischemia, Alzheimer's disease, Parkinson's disease, hypoxia-ischemia and epilepsy.[38,39] Furthermore, a decrease in Zn^{2+} levels has been reported as a potential biomarker for the diagnosis of prostate cancer.[40] Therefore, the ability to visualise Zn^{2+} in biological systems could potentially aid the understanding of its role in disease progression.

Pang *et al.* developed a bis-HBO fluorescent probe **5** functionalised with the Zn^{2+}-chelating di-(2-picolyl)amine (DPA) ligand. In the presence of Zn^{2+}, probe **5** was shown to exhibit a large increase in enol fluorescence emission intensity (10-fold),

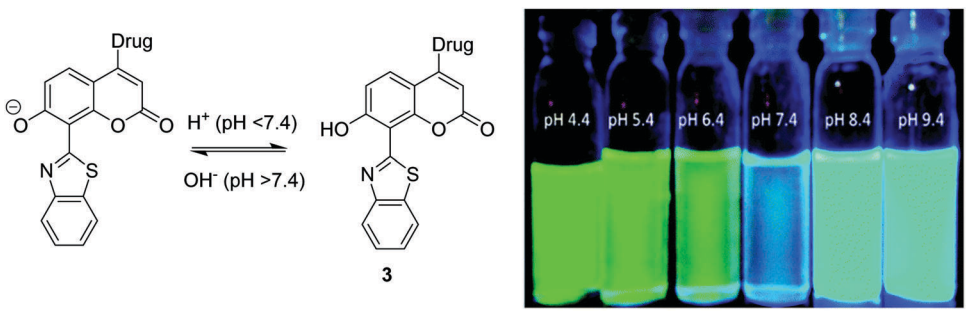

Fig. 3 A HBT-coumarin theranostic pH probe **3** for the monitoring of pH in cancer cells with UV activated drug release of chlorambucil. Measurement conditions: HEPES/ACN (7 : 3) buffer solution. Adapted with permission from (*J. Mater. Chem. B*, 2015, **3**, 3490–3497). Copyright (2015) the Royal Society of Chemistry.

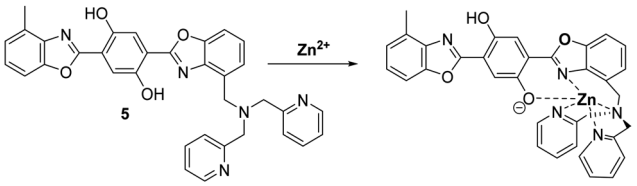

Scheme 6 A bis-HBO fluorescent probe **5** for the detection of Zn^{2+} using the chelating ligand DPA. Measurement conditions: HEPES (50 mM, pH 7.2, 0.1 M KNO_3 containing 5% DMSO).

which coincided with the appearance of a strong NIR keto emission peak at 710 nm (Scheme 6).[41]

Tang *et al.* developed an ESIPT HBI-derived fluorescent probe **6** containing the Zn^{2+}–ligand DPA, which had two fluorescence emission features due to a presumed ESIPT process. Addition of Zn^{2+} resulted in a significant ratiometric change in the fluorescence intensity due to inhibition of this ESIPT process (Scheme 7). Additionally, probe **6** overcame the limitations of other Zn^{2+}-based probes by being able to clearly discriminate Zn^{2+} over Cd^{2+}. Furthermore, the **6**–Zn^{2+} complex exhibited a highly selective and ratiometric response towards S^{2-}, caused by displacement of Zn^{2+} ions. This feature led to the suggestion that probe **6** could be used as a ratiometric probe to effect the sequential recognition of Zn^{2+} and S^{2-} in aqueous media.[42]

More recently, Yin and co-workers developed a thymolphthalein-HBI fluorophore **7**, with hydroxyl and amino groups that provide a binding pocket for Zn^{2+} coordination – see Scheme 8. Probe **7** was shown to detect low concentrations of Zn^{2+} producing a rapid increase in fluorescence intensity within 5 seconds. In addition, probe **7** demonstrated excellent selectivity for Zn^{2+}

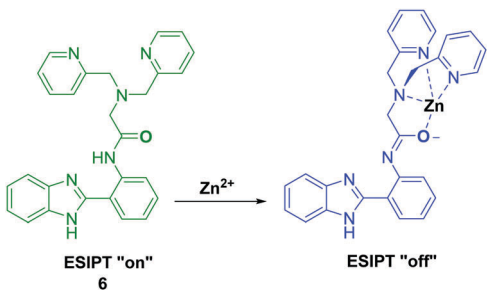

Scheme 7 Inhibition of the ESIPT process of **6** through the binding of Zn^{2+} using ligand DPA. Measurement conditions: HEPES/ACN (8 : 2) (10 mM, pH 7.4).

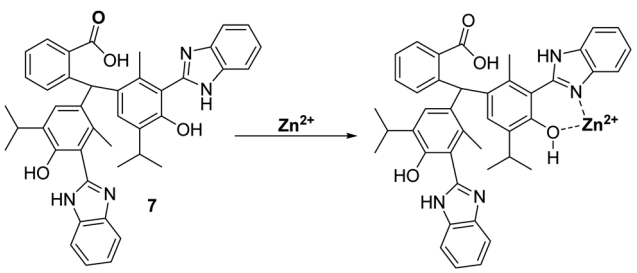

Scheme 8 Thymolpthalein-based ESIPT fluorescent probe **7** for the detection of Zn^{2+} in A549 cells. Measurement conditions: EtOH.

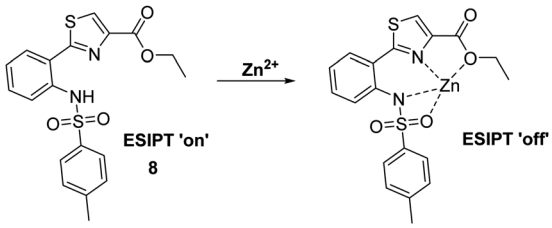

Scheme 9 A thiazole-based ESIPT fluorescent probe **8** for the detection of Zn^{2+} through the inhibition of the ESIPT process. Measurement conditions: EtOH.

over other metal ions and was shown to be able to image Zn^{2+} in living A549 cells.[43]

Kim *et al.* have developed a highly selective 2-(2′-tosylamidophenyl)thiazole fluorescent probe **8** for the detection of Zn^{2+} in ethanol (Scheme 9). It was shown to bind Zn^{2+} selectively in a 1 : 1 stoichiometry; however, it was also responsive to the presence of Cd^{2+}. Bound Zn^{2+} could be displaced by the sequential addition of either hydrogen pyrophosphate or hydrogen phosphate, which led to an overall decrease in fluorescence intensity.[44]

Copper (Cu^{+} and Cu^{2+})

Copper is an essential element for all living species that acts as a redox active co-factor for a range of physiological processes, including respiration, cellular defence, signalling, metabolism and neurotransmitter biosynthesis.[45] Dysregulation of copper has been associated with a number of diseases including neurodegeneration, which means the development of fluorescent probes for imaging copper in biological systems is highly desirable.[46,47]

Govindaraju and co-workers developed a reaction-based HBT fluorescent probe **9** for the selective detection of Cu^{+} and Cu^{2+} (Scheme 10). Initially, the ESIPT process of probe **9** is blocked; however, the presence of Cu^{+}/Cu^{2+} results in copper-mediated oxidative benzylic ether cleavage to release the HBT fluorophore. Probe **9** was shown to have a high sensitivity and

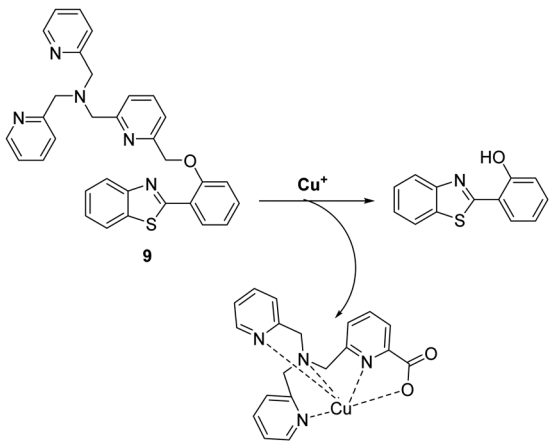

Scheme 10 Reaction-based ESIPT fluorescent probe for the selective deprotection of probe **9** for the detection of Cu^{+}. Measurement conditions: 50 mM HEPES, pH 7.2, 2 mM GSH.

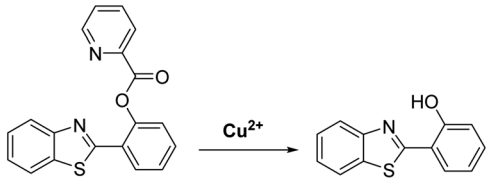

Scheme 11 Selective hydrolysis of picolinoyl ester of probe **10** and its use for the fluorescence detection of Cu^{2+}. Measurement conditions: PBS/ACN (8 : 2) – pH 7.4.

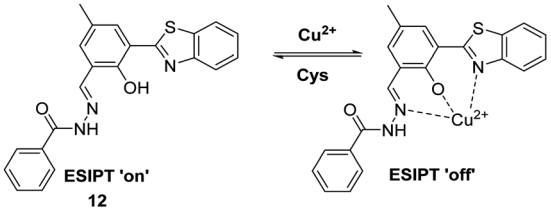

Scheme 13 An ESIPT-based fluorescent probe **12** for the reversible detection of Cu^{2+} and Cys. Measurement conditions: PBS/ACN (8 : 2), pH 7.4.

an excellent selectivity for Cu^{+} (1 μM) in the presence of 2 mM glutathione (GSH), under conditions that mimic the reducing environment of the cell. Additionally, copper-mediated cleavage of probe **9** resulted in a large ratiometric change in the fluorescence intensity. This was taken as support for the notion that **9** could be used as a probe for copper in biological environments.[48]

Similarly, Han *et al.* developed a reaction-based probe containing a HBT fluorophore for the selective detection of Cu^{2+}. This system incorporates a picolinoyl ester unit that can undergo copper-mediated hydrolysis (Scheme 11). ESIPT of probe **10** is initially blocked; however, in the presence of Cu^{2+} a large increase in fluorescence intensity is observed. Probe **10** was shown to be selective and sensitive (LOD = 16.1 nM) for Cu^{2+} allowing it to be detected in living cells.[49]

Guo *et al.* reported a reversible ESIPT fluorescent probe for the detection of Cu^{2+} and the sequential detection of S^{2-} (Scheme 12). Probe **11** was shown to successfully bind to Cu^{2+} (10 μM), which resulted in quenching of the fluorescence emission intensity. Interestingly, the addition of S^{2-} to Cu^{2+}–**11** restored the fluorescence emission due to displacement of Cu^{2+}. Remarkably, a fluorescence "ON–OFF–ON" cycle could be repeated 5 times *via* the alternating addition of Cu^{2+} and S^{2-}. Probe **11** displayed excellent selectivity for Cu^{2+} and a rapid response time. Excellent water solubility was conferred by the presence of its hydrophilic trihydroxyl group. A combination of these desirable features, enabled probe **11** to be used successfully to visualise Cu^{2+} and S^{2-} in A549 cells.[50]

Similarly, Li *et al.* developed a HBT-derived fluorescent probe **12** for the reversible detection of Cu^{2+} and cysteine (Cys) (Scheme 13). Probe **12** was shown to coordinate Cu^{2+} in a 1 : 1 stoichiometry. This binding results in its fluorescence emission intensity being quenched due to the deactivation of its ESIPT process. Cys was shown to react with Cu^{2+}–**12** complex within 1 min to restore the initial fluorescence emission intensity, thus enabling probe **12** to be used to detect selectively exogenously administered Cu^{2+} and Cys in HeLa cells.[51]

Cobalt (Co^{2+})

Cobalt (Co^{2+}) is an essential trace element that is present in cobalamins and metalloenzymes that catalyse a range of biological functions. Unfortunately, the high free redox activity of Co^{2+} makes it highly toxic to living cells. Therefore, the development of fluorescent probes for the detection of relatively low concentrations of free cobalt species is highly desirable.[52]

Govindaraju *et al.* have developed a reaction-based HBT-based fluorescent probe **13** whose ESIPT process is initially blocked. In the presence of Co^{2+} oxidative cleavage at its benzylic position is facilitated (Scheme 14). This results in a remarkable ratiometric change in fluorescence intensity through the release of the HBT fluorophore. In fact, probe **13** demonstrates an excellent selectivity over other metal ions. Moreover, a minimum detection level for Co^{2+} of 20 μM was noted.[48]

Iron (Fe^{2+} and Fe^{3+})

Iron is the most abundant transition metal found in the human body. It is essential to the functioning of numerous physiological processes. Iron homeostasis is normally tightly regulated, because excess levels of iron result in severe cell damage and organ damage through metal cation-mediated generation of excess reactive oxygen species (ROS).[53] In fact, abnormal iron concentrations have been associated with several diseases including neurodegenerative diseases, anaemia, cancer and hepatitis.[54,55]

Menges and co-workers developed a selective imidazole-based fluorescent ESIPT probe **14**. This system was shown to bind to Fe^{3+} with a 1 : 1 stoichiometry and "turn-off" the initial fluorescence (Scheme 15). These results suggest that this ESIPT fluorophore may be a highly promising sensing platform for the development of sensors for other analytes.[56]

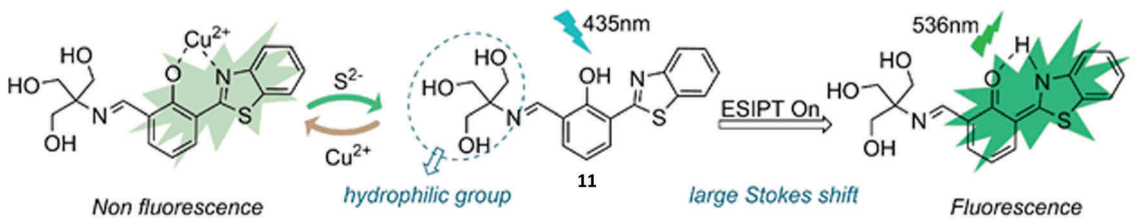

Scheme 12 Development of a reversible ESIPT fluorescent probe **11** for the detection of copper or S^{2-}. Measurement conditions: PBS solution (10 mM, pH 7.4). Reproduced with permission from (*Sens. Actuators, B*, 2018, **256**, 600–608). Copyright (2018) Elsevier.

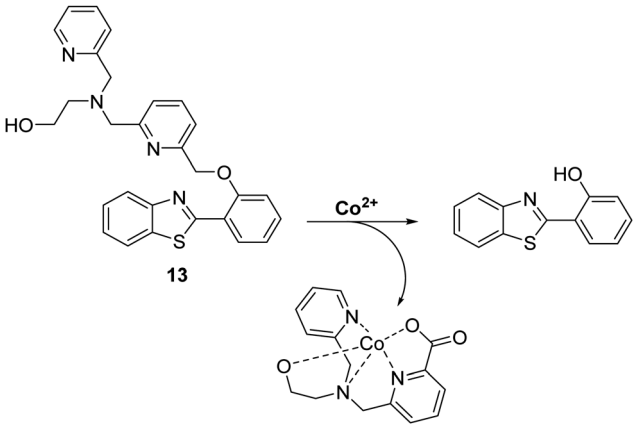

Scheme 14 Reaction-based ESIPT fluorescent probe for Co^{2+} (**13**) and the selective deprotection events that underlie its efficacy. Measurement conditions: 50 mM HEPES, pH 7.2, 2 mM GSH.

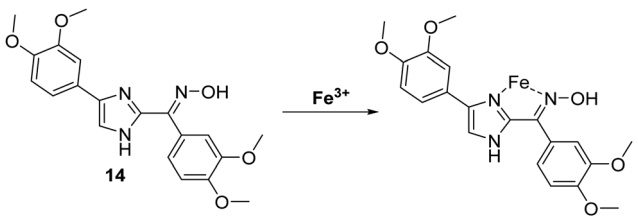

Scheme 15 An imidazole-based ESIPT fluorescent probe **14** used for the fluorescence detection of Fe^{3+}. Measurement conditions: DMSO.

Pang and co-workers have developed a single ESIPT based fluorescent probe **15**, that was used to selectively detect and discriminate between the trivalent metal ions Cr^{3+}, Al^{3+}, and Fe^{3+} in an H_2O/EtOH (8 : 2) solvent system (Scheme 16). Probe **15** was functionalised with two hydrazine "Schiff bases", which enabled selective binding of trivalent cations over divalent cations. A large increase in the fluorescence emission intensity was observed in the presence of an M^{3+} cation (Cr^{3+} and Al^{3+}). Interestingly, an initial fluorescence increase was observed in the presence of Fe^{3+}; however, the fluorescence emission was found to decrease over time, presumably as the result of tautomerisation. Probe **15** was shown to be effective at monitoring intracellular Cr^{3+} and Al^{3+} levels in human mesenchymal stem cells.[57]

Mercury (Hg^{2+})

Mercury is a naturally occurring element found in the earth's crust that the World Health Organisation (WHO) considers to be one of the top ten chemicals with major public health concerns. Natural geographical events, such as erosion and volcanic eruptions, or industrial activities, such as smelting or chemical synthesis, are potential routes for the release of mercury into the environment.[58] Mercury consumption can have devastating consequences to human health, as witnessed in Japan with the consumption of mercury species in contaminated fish that occurred in the Minamata incident.[59] Therefore, it is extremely important to have access to methods for the qualitative and quantitative detection of mercury in drinking water.

Ahn *et al.* developed a ratiometric fluorescent HBT ESIPT probe **16** for the detection of mercury species. The mode of action is based on mercury-promoted deprotection of a vinyl ether group to afford its corresponding phenol (Scheme 17). In the presence of mercury, the vinyl ether was found to be selectively hydrolysed. This turns on the ESIPT process, which resulted in a ratiometric change in fluorescence from blue to cyan emission. Probe **16** was shown to have high sensitivity (LOD = 20 ppb) and have an excellent selectively in detecting mercury species over various other metal ions. These attributes make probe **16** suitable for the analysis of drinking water. In fact, it was shown to react with mercury in a 2 : 1 stoichiometry, thus indicating its potential for detecting highly toxic methylmercury.[60]

Yao *et al.* developed a novel ratiometric Hg^{2+} fluorescent probe **17** based on the ESIPT fluorophore, 2-(1-(*p*-tolyl)-1*H*-phenanthro[9,10-*d*]imidazol-2-yl)phenol, which incorporated a similar Hg^{2+} cleavable vinyl ether group (Scheme 18). The presence of Hg^{2+} resulted in a ratiometric change in the fluorescence intensity (I_{477}/I_{380}). A high sensitivity (LOD = 7.8 nM), in addition to an excellent selectively for Hg^{2+} over other metal ions, was seen. Additionally, it was shown that probe **17** has good cell permeability and could be used to visualise exogenously added Hg^{2+} in HeLa cells.[61]

Palladium (0, +2 and +4)

Palladium is used in a wide range of applications, including in dental appliances, as a catalyst for organic synthesis, and automotive emission control catalysts.[62] Unfortunately, palladium at high concentrations is known to have toxic effects on biological systems, with low doses promoting allergic reactions.[63] Therefore, given the potential occurrence of palladium in food, medicines, and water, there is significant interest in developing analytical methods to determine the concentrations of potential palladium contaminants.

Bai *et al.* developed a ratiometric ESIPT flavone-based fluorescent probe **18** for the detection of Pd species that was shown to have good sensitivity (LOD for Pd(II) = 87 nM) and excellent selectivity over a range of other metal ions (Scheme 19). Probe **18** undergoes a Pd-catalysed depropargylation reaction to release the fluorophore whose phenolic group enables the ESIPT process to take place. Remarkably, probe **18** could be used to detect Pd(IV), Pd(II) and Pd(0) oxidation states, with Pd(II) and Pd(IV) producing the largest ratiometric changes in fluorescence intensity (I_{517}/I_{412}).[64]

Chen *et al.* developed two HBT-derived ESIPT-based fluorescent probes **19** and **20**. Both rely on similar depropargylation reactions that are triggered by Pd^{2+}. Again, this liberates a phenol, which allows the ESIPT process to occur (Fig. 4). Exposure to Pd^{2+}, resulted in large increases in the fluorescence emission intensities of both probes. Interestingly, probe **20** showed greater sensitivity to Pd^{2+} than probe **19** (LOD = 14.6 nM *vs.* LOD = 285 nM, respectively). Both probes could be successfully incorporated into test strips that were able to detect low concentrations of Pd^{2+} (15 ppm) by eye.[65]

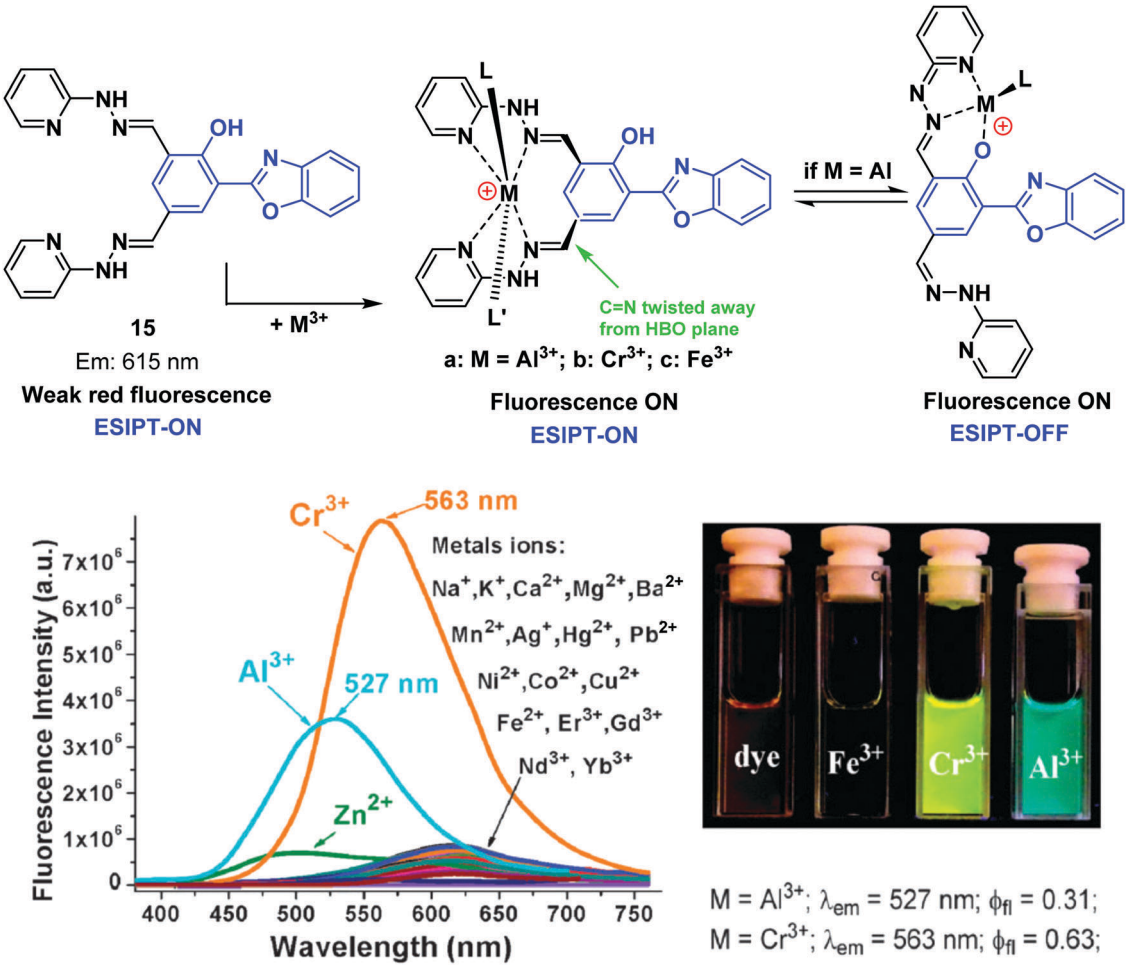

Scheme 16 A single fluorescent ESIPT probe **15** with the ability to distinguish between Fe^{3+}, Cr^{3+}, and Al^{3+} in solution and in live cells. Measurement conditions: H_2O/EtOH (8 : 2). Reproduced with permission from (*Chem. Commun.*, 2014, **50**, 12258–12261). Copyright (2014) The Royal Society of Chemistry.

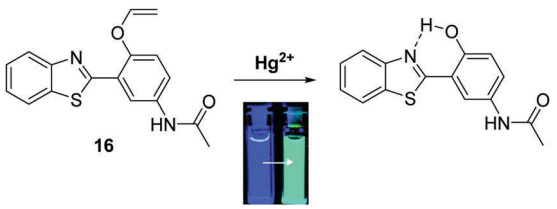

Scheme 17 Vinyl-ether protected ESIPT probe **16**, a species that proved useful for the selective detection of Hg^{2+}. Meaurement conditions: PBS (pH 7.4) containing 1% ACN. Adapted with permission from (*Org. Lett.*, 2011, **13**, 3422–3425). Copyright (2011) American Chemical Society.

Zeng *et al.* combined a HBT fluorophore with the electron acceptor 1,4-dimethylpyridin-1-ium iodide to develop a long-wavelength ESIPT fluorescent probe **21** that contains an extended π-electron framework. In the presence of Pd^{2+}, probe **21** undergoes a palladium-mediated depropargylation reaction, resulting in a ratiometric change in fluorescence intensity (I_{635}/I_{495}) (Scheme 20). Probe **21** was shown to have the ability to detect multiple oxidation states of palladium (0, +2, +4). In the case of Pd^{2+}, excellent selectivity and high sensitivity was seen with a LOD = 57 nM being recorded in a purely aqueous medium.[66]

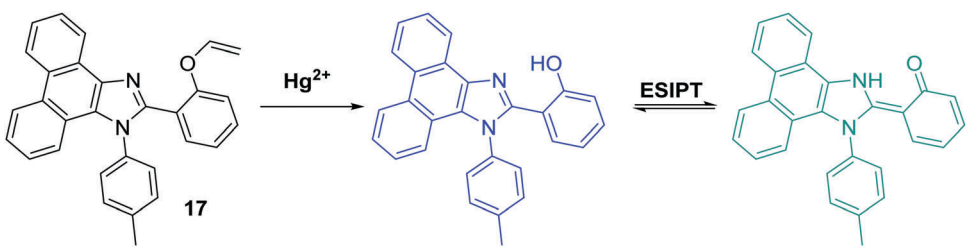

Scheme 18 Vinyl protected probe **17** used for the ratiometric fluorescence detection of Hg^{2+} in aqueous solution and HeLa cells. Measurement conditions: PBS (pH 7.4) containing 1% ACN.

Scheme 19 Propargyl-protected probe **18** for the ratiometric fluorescence detection of Pd^{2+}. Measurement conditions: HEPES/ACN (4 : 1).

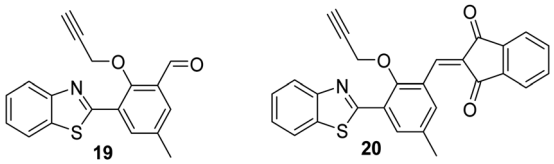

Fig. 4 Two ESIPT-based probes **19** and **20** that allow the detection of Pd^{2+}. Measurement conditions: HEPES/THF (5 : 2).

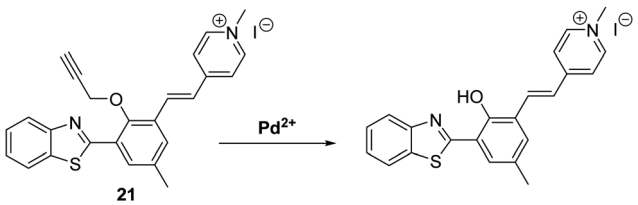

Scheme 20 Propargyl-protected **21**, a probe developed for the ratiometric fluorescence detection of Pd^{2+}. Measurement conditions: PBS (10 mM, pH = 7.4).

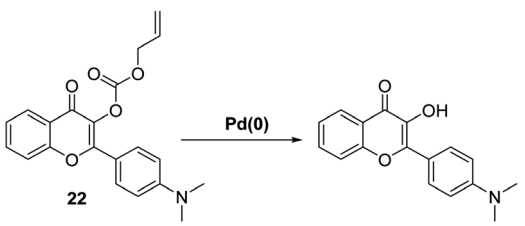

Scheme 21 Pd catalysed decarboxylative deprotection of probe **22**, a process that allows for the ratiometric fluorescence detection of 0, +2 and +4 Pd species. Measurement conditions: PBS/THF (9 : 1) pH = 7.4.

A different approach to palladium sensing was introduced by Liu *et al.* These researchers developed an allyl containing ESIPT dimethylamino-flavone probe **22** with the ability to detect a range of palladium (0, +2, and +4) species (Scheme 21). Probe **22** was found to react with Pd(0) in a 1 : 1 stoichiometry. This led to the suggestion that Pd(0) initially coordinates to the double bond to form a π-allyl complex that underwent decarboxylative elimination of the fluorophore, which allows the ESIPT process to take place. Probe **22** exhibited a large and rapid ratiometric change in fluorescence intensity (I_{522}/I_{470}) in response to Pd(0), with a LOD = 9.0 nM (1.5 min). This probe could be used to visualise Pd(0) in HeLa cells using two-photon fluorescence spectroscopy.[67]

ESIPT fluorescence based sensors for anions

Pyrophosphate ($P_2O_7^{4-}$)

Pyrophosphate (PPi) is a biologically important anion, which is central to a number of biological processes, including ATP hydrolysis, DNA and RNA polymerisation, and a number of enzymatic reactions. Moreover, unregulated PPi production, degradation, and transport is associated with a range of diseases.[68]

Pang and co-workers designed and synthesised an ESIPT-based fluorescent probe **23** containing a binuclear Zn^{2+} system. Coordination of PPi to Zn^{2+} triggers a large ratiometric fluorescence response, due to the ESIPT pathway being turned on (Scheme 22). Job plot analysis revealed that probe **23** is bound to PPi with a 1 : 1 stoichiometry, a conclusion that was further supported by electrospray mass spectrometric studies. Probe **23** displayed excellent selectivity and was used to detect PPi released over the course of a PCR experiment, thus demonstrating its usefulness as a tool for bioanalytical applications.[69]

Superoxide ($O_2^{\cdot-}$)

Superoxide ($O_2^{\cdot-}$) is known as the "primary" reactive oxygen species that is ultimately responsible for generating other ROS/RNS species, such as H_2O_2 and $ONOO^-$. The production of

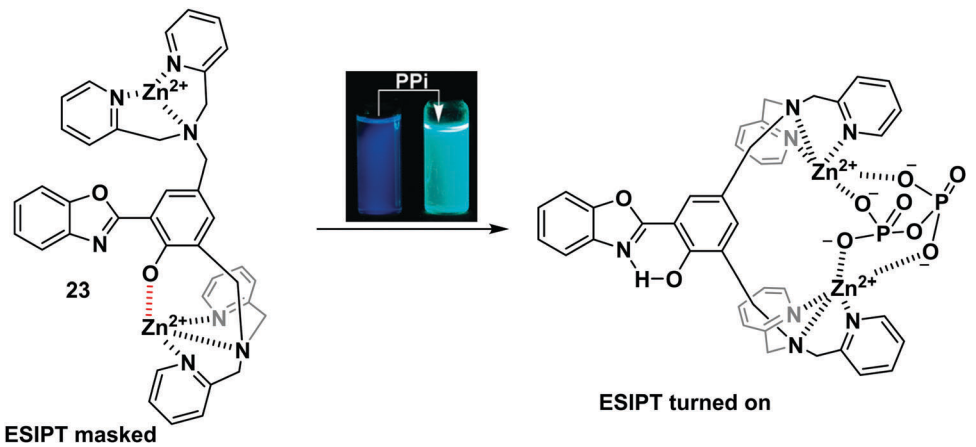

Scheme 22 A binuclear Zn^{2+} ESIPT based probe **23** for the ratiometric detection of pyrophosphate. Measurement conditions: HEPES buffer (10 mM, pH = 7.4). Reproduced with permission from (*Org. Lett.*, 2011, **13**, 1362–1365). Copyright (2011) American Chemical Society.

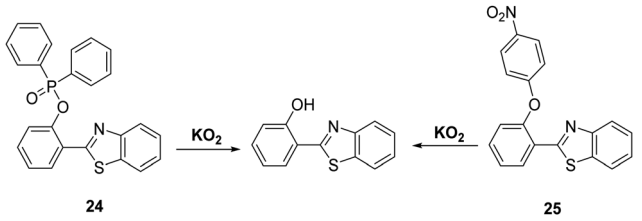

Scheme 23 Reaction-based ESIPT fluorescent probes **24** and **25** for the detection of KO_2. These probes operate *via* two different deprotection strategies. Measurement condtions: probe **24** – HEPES/DMSO 50 : 50, pH = 7.2. Probe **25** – H_2O/DMSO 50 : 50, pH = 7.2.

superoxide mostly occurs in mitochondria, due to leakage of electrons from the electron transport chain to molecular oxygen. The high reactivity and short half-life of O_2^- makes it difficult to detect.[70,71] O_2^- has been shown to be involved in a range of pathological conditions such as inflammation, aging, and ischemia-reperfusion injury.[72,73] Therefore, the development of analytical tools for its real-time detection is highly desirable.

Churchill and co-workers developed two HBT-derived fluorescent probes **24** and **25**, that are functionalised with phosphinate and 4-nitrophenyl ether groups, respectively (Scheme 23). Initially, the ESIPT processes of both probes are blocked; however, reaction with O_2^- results in the phosphino group of **24** and the *p*-nitrophenyl group of **25** being cleaved to give the same free phenolic unit that turns on the ESIPT process. Exposure of probe **24** to O_2^- led to a 60-fold increase in fluorescence intensity, which enabled it to be used for cellular imaging studies. An MTT assay for probe **24** in SH-SY5Y cells provided initial evidence that this probe was not neurotoxic.[74]

Peroxynitrite ($ONOO^-$)

Peroxynitrite ($ONOO^-$), is a highly reactive nitrogen species (RNS) that is formed *via* the diffusion controlled reaction between superoxide ($^-O_2$) and nitric oxide (NO).[75,76] Peroxynitrite is known for its destructive properties, causing irreversible damage to a range of biological molecules, such as lipids, proteins, and DNA.[77] Peroxynitrite has been implicated as a key pathogenic factor for a number of diseases, including inflammation, cancer, ischemia-reperfusion injury, and neurodegenerative diseases.[78–80] Therefore, the development of probes for peroxynitrite detection could allow for important advances in diagnostics and allow for improved staging of various medical conditions.

Li *et al.* reported a simple and effective HBT-based ESIPT probe **26** that allows for the detection of $ONOO^-$ with a good selectivity profile and a fast response time (Scheme 24). Probe **26** was shown to be capable of crossing the blood–brain barrier (BBB) and could be used for two-photon fluorescence spectroscopy. This enabled probe **26** to be used for the visualisation of $ONOO^-$ in neurovascular ischemia progression in a live mouse brain.[81] The excellent properties of probe **26** led to suggestion that it may have utility in visualising other pathophysiological processes that result in $ONOO^-$ formation.

James and co-workers developed a boronate-based HBT probe for peroxynitrite **27**. This system exploits the rapid $ONOO^-$-mediated oxidation of a boronate ester fragment that

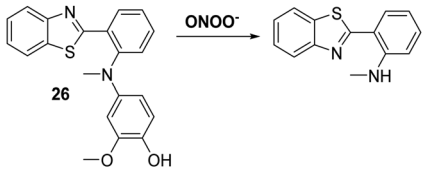

Scheme 24 A reaction-based fluorescent probe **26** that allows for the rapid detection of $ONOO^-$ in cells and within a live mouse brain. Measurement conditions: PBS solution (10 mM, pH = 7.4).

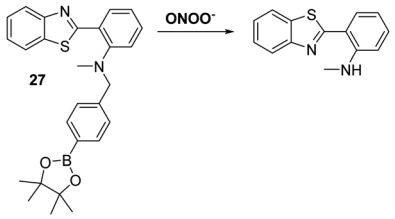

Scheme 25 A boronate-based fluorescent probe **27** for the rapid detection of $ONOO^-$ that was found to be effective in both HeLa and RAW 264.7 cells. Measurement conditions: PBS solution containing 52.1% MeOH, pH = 8.2.

is selective for $ONOO^-$ over hypochlorite and hydrogen peroxide (Scheme 25).[82] A benzyl boronic ester ''protecting'' unit was used to block the ESIPT process initially. Exposure to $ONOO^-$ results in oxidative deprotection of the benzyl boronic ester fragment and leads to an increase in the fluorescence intensity. Probe **27** was shown to be cell permeable, which enabled it to be used to visualise $ONOO^-$ in live cell imaging experiments involving the HeLa and RAW 264.7 cell lines.[83] More recently, James and co-workers developed a ratiometric boronate-based ESIPT probe for the visualisation of $ONOO^-$ within the endoplasmic reticulum.[84]

Sulfites (SO_3^{2-}/HSO_3^-)

Sulfur dioxide (SO_2) is a toxic pollutant that is produced by a variety of industrial processes,[85–87] SO_2 is also produced enzymatically in the cytosol and mitochondria of cells. It then equilibrates to form HSO_3^-, or SO_3^{2-}. Endogenously generated SO_2 acts as a signalling molecule in several physiological processes; however, elevated levels of SO_2 have been associated with a number of diseases, including cardiovascular disease, cancer, and ischemia-reperfusion injury.[88]

Song and co-workers have developed a levulinate ester-functionalised HBT fluorescent probe **28** for the ratiometric detection of SO_3^{2-}. Exposure of probe **28** to this latter dianion triggers a cyclisation reaction that leads to cleavage of the levulinate ester fragment and release of the HBT fluorophore (Scheme 26). A large change in ratiometric fluorescence intensity (I_{468}/I_{373}) was observed when SO_3^{2-} (0–1000 μM) was added. Moreover, probe **28** demonstrates excellent selectivity over other anions, illustrating its potential for the detection of SO_3^{2-}.[89]

Hypochlorite ($HOCl/ClO^-$)

Myeloperoxidase (MPO) in leukocytes catalyses the reaction between chloride anions and H_2O_2 to generate hypochlorous

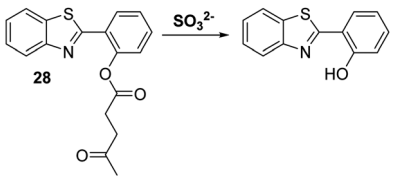

Scheme 26 Levulinate-functionalised HBT fluorescent probe **28**, which allows for the triggered release of HBT and the detection of SO_3^{2-}. Measurement conditions: PBS/CAN (50 : 50) pH = 7.4.

acid ($HOCl/ClO^-$), which is a biologically important reactive oxygen species generated by the immune system for its microbiocidal properties.[90] Unfortunately, excess production of $HOCl/ClO^-$ can lead to uncontrolled damage of a range of biomolecules, such as amino acids, proteins, carbohydrates and lipids.[91,92] As a consequence, $HOCl/ClO^-$ has been associated with cell and tissue damage, as well as a number of diseases.[93] These deleterious properties provide an incentive to develop probes allowing for the effective detection of $HOCl/ClO^-$.

Yoon and co-workers have synthesised a diaminomaleonitrile (DMN)-based ESIPT fluorescent probe **29** for the detection of $HOCl/ClO^-$ (Scheme 27). Probe **29** undergoes $HOCl/ClO^-$ mediated imine hydrolysis to release the corresponding aldehyde (as confirmed by high resolution mass spectrometry). It is this release that responsible for the observed increase in fluorescence intensity. Probe **29** was shown to display excellent selectivity over other ROS/RNS, including $ONOO^-$ and H_2O_2. It also displayed high sensitivity, reacting fully with $HOCl/ClO^-$ in less than a minute. This enabled it to be used to monitor exogenous and endogenous $HOCl/ClO^-$ production in living cells and tissues using two-photon microscopic analyses.[94]

Goswami *et al.* designed a thiosemicarbazide HBT-based fluorescent probe **30** for the ratiometric detection of $HOCl/ClO^-$. These latter species were proposed to disrupt the hydrogen bonding network of the probe, resulting in inhibition of the ESIPT process (Scheme 28). Probe **30** demonstrated high selectivity and sensitivity for $HOCl/ClO^-$ exposure which was accompanied by a colorimetric change from orange to blue. Probe **30** was shown to be able to detect different concentrations of $HOCl/ClO^-$ in tap water, illustrating its potential utility in monitoring the quality of drinking water.[95]

Chen and co-workers developed a dithiolane functionalised HBT-based fluorescent probe **31** for the detection of $HOCl/ClO^-$. In this case advantage was taken of the ability of hypochlorite to

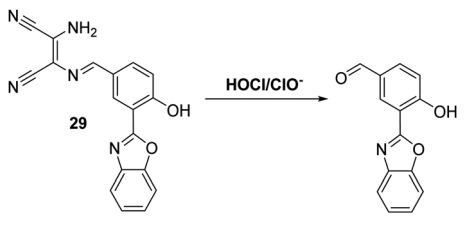

Scheme 27 A two-photon diaminomaleonitrile (DMN)-based ESIPT fluorescent probe **29** for the selective detection of $HOCl/ClO^-$ in RAW 264.7 cells and hippocampal brain slices. Measurement conditions: PBS/DMF (8 : 2) pH = 7.4.

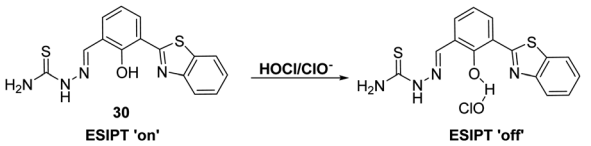

Scheme 28 A thiosemicarbazide HBT-based probe **30** for the selective detection of hypochlorite ($HOCl/ClO^-$), including in tap water. Measurement conditions: ACN/H_2O (50 : 50).

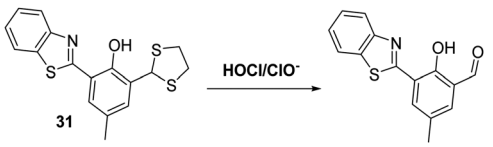

Scheme 29 Fluorescent probe **31** that exploits the oxidation of a dithiolane functionalised HBT to permit the detection of hypochlorite. Measurement conditions: PBS (pH = 7.4, 10 mM).

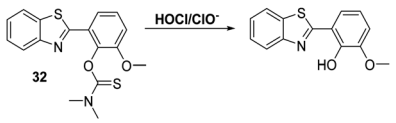

Scheme 30 Selective oxidation of a dimethylthiocarbamate moiety is exploited to generate the HBT-based fluorescent probe **32**, which was used for the detection of hypochlorite. Measurement conditions: PBS (pH = 7.4, 10 mM, 1% DMSO) containing 1 mM CTAB.

oxidise the dithiolane functionality to its corresponding fluorescent aldehyde (Scheme 29). This reactivity profile, which is reflected in a colour change from yellow to blue, enabled probe **31** to be used as a highly selective and sensitive probe for $HOCl/ClO^-$ with a LOD = 8.9 nM. Probe **31** was shown to be cell permeable and capable of detecting both exogenous and endogenous $HOCl/ClO^-$ in HeLa cells.[96]

More recently, James and co-workers have developed a thiocarbamate functionalised HBT-OMe fluorescent probe **32** for the detection of $HOCl/ClO^-$ (Scheme 30). Addition of $HOCl/ClO^-$ resulted in rapid hydrolysis (<10 s) of the thiocarbamate linker resulting in a large increase in fluorescence intensity (>40-fold). This probe demonstrated high sensitivity (LOD = 0.16 nM) and excellent selectivity for hypochlorite over other ROS/RNS. It was capable of detecting exogenous and endogenous $HOCl/ClO^-$ in HeLa cells. Test strips impregnated with **32** were prepared and shown to be useful for the qualitative detection of different concentrations of $HOCl/ClO^-$ in water. Alternatively, **32** was shown to be capable of performing as a dual input logic gate for detecting Hg^{2+} and H_2O_2. Exposure of **32** to Hg^{2+} led to a significant increase in fluorescence intensity after 30 min; however, due to the large difference in response rates, no interference from Hg^{2+} was observed when probe **32** was used to test for $HOCl/ClO^-$ in drinking water.[97]

Cyanide (CN^-)

Cyanide (CN^-) is used extensively for industrial applications, including gold mining; however, it is one of the deadliest anionic poisons known. Its toxicity is ascribed to its ability to

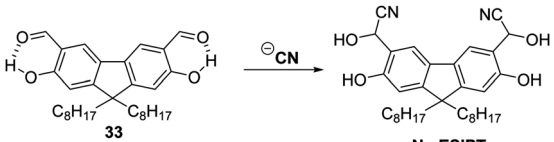

Scheme 31 A salicylaldehyde functionalised fluorene fluorescent probe **33** for the detection of CN^-. Measurement conditions: ACN only.

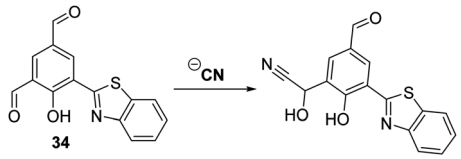

Scheme 32 A selective HBT fluorescent probe **34** for the detection of CN^-. Measurement conditions: ACN only.

inhibit cytochrome-*c* oxidase, the final oxidase of the electron transport chain. Ultimately, this deactivates the electron transport chain and results in the inhibition of cellular respiration.[98,99] Consequently, the ability to detect low levels of CN^- in the environment and biological systems is extremely important.

Malik *et al*. synthesised a salicylaldehyde functionalised fluorene ESIPT probe **33** for CN^-. This system relies on reaction of CN^- with the aldehyde group in **33**. This affords a stable cyanohydrin product (Scheme 31) and results in a large increase in fluorescence intensity. With a calculated LOD of 0.06 ppm, it was found that probe **33** could be used to image CN^- in living SH-SY5Y cells.[100]

Similarly, Nandi and co-workers developed a HBT-functionalised ratiometric fluorescent probe **34** for the detection of CN^-. In this case the cyanide anion selectively reacts with the *ortho*-aldehyde functionalilty of **34** to afford a cyanohydrin that inhibits the ESIPT process (Scheme 32). The net result is a ratiometric change (I_{436}/I_{521}) in fluorescence intensity. The detection limit of probe **34** for the cyanide anion was 1.6 μM, a value that is below the WHO recommended level for CN^- in drinking water (*i.e.*, 1.9 μM).[101]

Fluoride (F^-)

Fluoride (F^-) occurs naturally at trace levels in all-natural water sources; however, an ability to detect F^- has garnered considerable interest in recent years due to the significant health and environmental impact that can occur when this halide anion is present at higher concentrations.[102]

Silyl ethers are widely used for the protection of alcohol and phenol functionalities, with silyl-ether protecting groups known to be selectively removed by the action of F^- to afford their corresponding alcohols. Several research groups have exploited this reactivity profile to develop reaction-based fluorescent probes suitable for the detection of F^-. For example, Yang and co-workers employed *tert*-butyldiphenylsilyl ether (TBDPS) to block the phenol group of probe **35** and inhibit the ESIPT process (Scheme 33). Exposure to a F^- source results in cleavage of the O–Si bond which 'turned on' the ESIPT process leading to a ratiometric change in the fluorescence intensity (I_{560}/I_{418}).

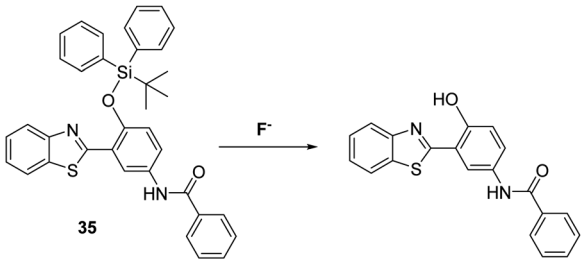

Scheme 33 A silyl ether protected HBT-based fluorescent probe **35** for the detection of the fluoride anion. Measurement conditions: 100% H_2O solution containing 2 mM CTAB.

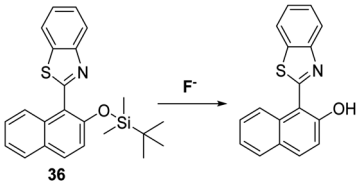

Scheme 34 A silyl ether protected naphthalene HBT fluorescent probe **36** for the fluoride anion. Measurement conditions: HEPES/CAN (2 : 8) pH = 7.4.

Probe **35** was shown to have excellent selectivity over other anions making it suitable for use in practical applications.[103]

Saha *et al.* also blocked the phenol functionality of a HBT-derived naphthalene fluorophore with a *tert*-butyldimethylsilyl group to afford probe **36** (Scheme 34). In this case, the addition of F^- led to a significant ratiometric change in the fluorescence intensity, an effect ascribed to deprotection of the O–Si bond, which allows an ESIPT process to occur efficiently. Test strips containing probe **36** were prepared and were shown to be effective for the qualitative detection of F^-. Probe **36** was also found to be cell permeable and to be capable of imaging exogenously added F^- in HeLa cells.[104a,b]

Interestingly, Wu *et al.* developed two distinct HBT-based ESIPT fluorescent probes (**37** and **38**) for the detection of F^-. Both systems displayed good selectivity and sensitivity[105] to the fluoride anion and gave rise to a ratiometric response (Scheme 35). Probe **38** is believed to capable of detecting F^- *via* formation of an N–H–F bonding interaction. This interaction stabilises the keto form involved in the ESIPT process, as shown in Scheme 35.

Wang and co-workers synthesised a benzoselenadiazole-based diarylamine-based ESIPT probe **39** for F^- (Scheme 36). This highly selective probe contains a strong electron withdrawing 4-nitrophenyl group, whose presence increases the acidity of the N–H bond. Addition of excess F^- to probe **39** leads to deprotonation of the N–H proton (observed by ^{1}H NMR spectroscopy). This results in a ratiometric change in the fluorescence intensity (I_{478}/I_{671}) of probe **39**, as well as an easily-visualized colour change.[106]

Peng and co-workers developed two HBO-based anion fluorescent probes for the detection of F^- (Scheme 37). The first HBO derivative was functionalised with a *p*-toluenesulfonyl unit to afford probe **40**. This system could be used to detect F^-,

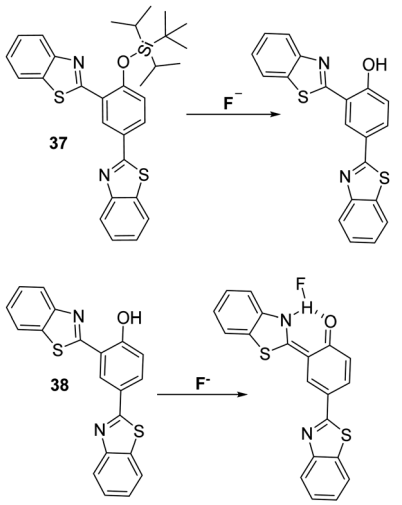

Scheme 35 Two HBT fluorescent probes **37** and **38**, which employ two different strategies for the detection of the fluoride anion. Measurement conditions: THF.

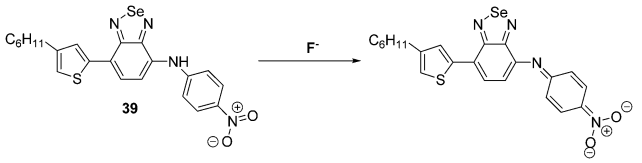

Scheme 36 A benzoselenadiazole-based diarylamine ESIPT fluorescent probe **39**. This system permits detection of the fluoride as the result of a deprotonation event. Measurement conditions: DMSO.

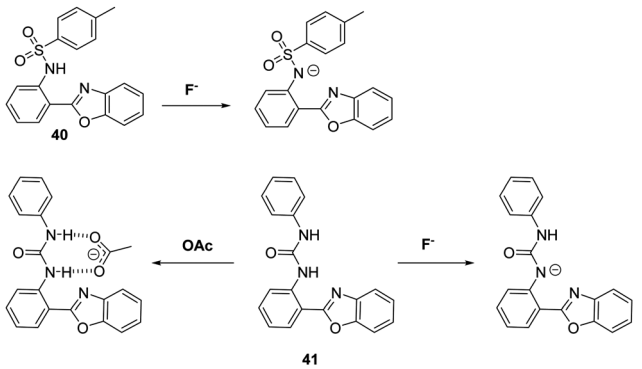

Scheme 37 Two HBO-based fluorescent probes **40** and **41** that permit the detection of the fluoride anion as the result of deprotonation. A response to other anions was also seen as detailed in the text. Measurement conditions: DMSO.

CH_3COO^-, and $H_2PO_4^-$ salts *via* deprotonation of the sulfonamide group and a corresponding inhibition of the ESIPT process. In the case of probe **41** the inherent ESIPT process could be inhibited either by F^--promoted deprotonation of the urea unit, or *via* formation of a strong CH_3COO^-–urea intermolecular hydrogen bond complex. Interestingly, exposure of probe **41** to a F^- or CH_3COO^- source resulted in different ratiometric responses, thus allowing these two anions to be distinguished.[107]

ESIPT fluorescence based sensors for small neutral molecules

Hydrogen sulphide (H_2S)

Hydrogen sulphide (H_2S) has recently been reported as an endogenous gaseous transmitter that regulates several physiological and pathological processes, including those involved in neurotransmission, vasodilation, inflammation, atherosclerosis, oxidative stress, and inhibition of insulin signaling.[108–111] Therefore, the development of a fluorescent probe for the intracellular detection of H_2S could help advance our fundamental understanding of its role in pathophysiological processes.

Qian and co-workers developed and designed a fluorescent probe **42** for the detection of H_2S through the functionalisation of the ESIPT fluorophore HMBT with a H_2S reactive unit, namely 2-(pyridin-2-yl-disulfanyl)benzoic acid (Scheme 38). Exposure of probe **42** to H_2S results in cleavage of the S–S bond. This produces a free –SH intermediate, which subsequently cyclises to release HMBT. Probe **42** was shown to exhibit high sensitivity (LOD = 0.12 μM) towards H_2S, producing a 30-fold fluorescence enhancement within 2 minutes. Probe **42** was also shown to display excellent selectivity over other biologically relevant species, including other thiol-containing analytes (GSH, HCys, and Cys), presumably because these latter species are unable to form the requisite –SH intermediate. The potential utility of probe **42** for biological applications was demonstrated through fluorescence imaging of H_2S in HeLa cells containing CTAB.[112]

An alternative strategy for the detection of H_2S involves exploitation of the well-known H_2S-mediated reduction reactions of aryl azides to the corresponding amines to generate a fluorescence response.[113,114] This approach is embodied in the azide-functionalised HBT derivative **43** prepared by Guo *et al.* (Scheme 39). Initially, probe **43** was found to be non-fluorescent; however, addition of H_2S resulted in a remarkably large fluorescence increase (~1150-fold). Probe **43** was shown to be extremely sensitive (LOD = 0.78 nM) for H_2S with relatively fast response times (3–10 min). It also exhibited excellent selectivity against other biologically relevant analytes. Probe **43** could be used to image exogenous and endogenously H_2S in B16 cells in the presence of CTAB.[115]

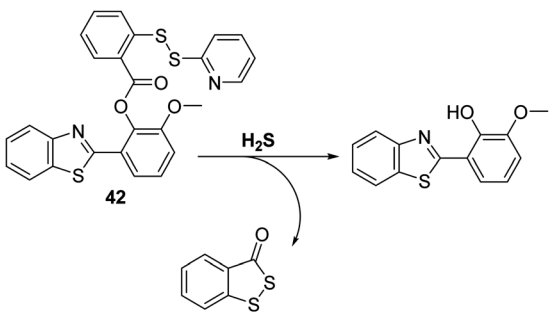

Scheme 38 HMBT-based fluorescent probe **42**, a system that permits the selective detection of H_2S in HeLa cells. Measurement conditions: Tris–HCl buffer (20 mM, pH = 7.4) containing 1 mM CTAB.

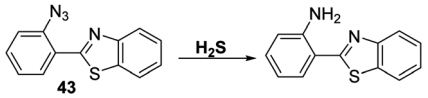

Scheme 39 The selective detection of H_2S *via* a H_2S-mediated azide reduction of probe **43**. This reduction produces a highly fluorescent HBT-amino fluorophore that produces an analyte-specific response. Measurement conditions: PBS Buffer (10 mM, pH = 7.4) containing 1 mM CTAB.

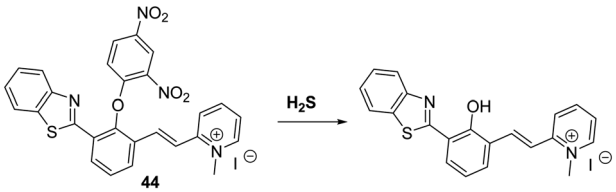

Scheme 40 A H_2S-mediated S_NAr cleavage endows probe **44** with an ability to detect H_2S with good selectivity. Measurement conditions: PBS/ACN (50 : 50) pH = 7.4.

Zeng *et al.* developed a HBT-derived long-wavelength fluorescent probe **44** functionalised with a H_2S-responsive 2,4-dinitrophenyl ether unit. In this case exposure to H_2S results in nucleophilic aromatic substitution at the 2,4-dinitrophenyl fragment. This, in turn, releases the free phenol of the fluorophore and enables the ESIPT process to take place (Scheme 40). The net result is a large increase in the fluorescence intensity, ascribed to emission from the keto form (λ_{em} = 620 nm). A large Stokes shift (240 nm) is also observed. Probe **44** was shown to be highly selective for H_2S over a range of biologically relevant analytes; however, it did respond to high concentrations of GSH and Cys (*ca.* 10 mM and 1 mM, respectively).[116a] Mahapatra and co-workers developed a similar fluorescent probe that was shown to reversibly detect S^{2-} and Zn^{2+} ions once the 2,4-dinitrophenol ether unit was removed.[116b] The same group have developed an ESIPT probe that can be used to detect picric acid an explosive and environmental pollutant.[116c]

Homocysteine (HCys)

Homocysteine (HCys) is a naturally occurring amino thiol that is exclusively derived from the demethylation of methionine (Met). Free HCys is either re-methylated to Met facilitated by folate and vitamin B_{12} as cofactors or transformed into cysteine (Cys) *via* a condensation reaction with serine catalysed by cystathionine β-synthase with vitamin B_6 acting as a co-factor. Due to the structural similarity with Met, HCys can enter the first step of protein synthesis and is recognised by 'methionyl t-RNA synthetase' (MetRS). However, the error-editing activity of MetRS prevents the incorporation of HCys into proteins. As a by-product of this error-editing process, HCys thiolactone (HTL) is formed. HTL can non-enzymatically modify proteins through the irreversible covalent attachment to lysine residues known as 'protein *N*-homocysteinylation'.[117,118] This results in structural alterations, loss of enzymatic function, and induces protein aggregation. Elevated levels of HCys (hyperhomocysteinemia) have been associated with pregnancy disorders, cardiovascular, and neurodegenerative diseases.[119–121] This provides a particular incentive to generate probes for this neutral species.

Tang *et al.* developed a simple HBI-based fluorescent probe **45** for the selective detection of HCys over other amino acids, including Cys and GSH (Scheme 41). HCys and Cys have previously been shown to form thiazolidine and thiazine adducts in the presence of aldehydes. By exploiting this reactivity, probe **45** was capable of distinguishing between HCys and Cys. This selectivity was ascribed to the formation of 5- and 6-membered heterocycles in an analyte-specific sense, chemistry that effected the ESIPT emission to differing extents. As a result of **45** demonstrating excellent selectivity, probe **45** was used in cellular imaging experiments. Probe **45** was shown to detect intracellular HCys in MCF-7 cells, leading to the suggestion that it might find utility in biological applications.[122]

Cysteine (Cys)

Cysteine (Cys) is a biologically significant thiol-containing amino acid that plays a vital role in a number of biological processes including protein synthesis, cellular detoxification, and metabolism. However, abnormal levels of Cys are associated with a number of health problems, including cancer, neurological disorders, and motor neuron diseases.[123–127] Therefore, the development of an analytical tool for the detection of Cys over other thiol-containing biologically important species is highly desirable.

The ability of the thiol group of Cys to undergo conjugate addition reactions to acrylate esters, with concomitant intramolecular amide formation has been exploited to create turn on ESIPT-based fluorescent probes whose phenolic group are protected by Cys-reactive acrylate fragments. Strongin *et al.* reported an acrylate-functionalised HMBT fluorescent probe **46**,

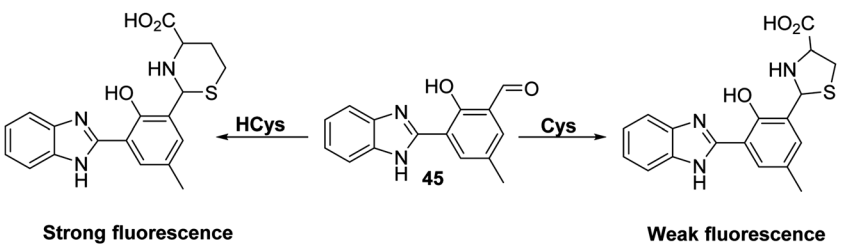

Scheme 41 A HBI-based fluorescent probe **45** that was found to display differing responses to HCys and Cys. Measurement conditions: HEPES/EtOH (9 : 1) pH = 7.4.

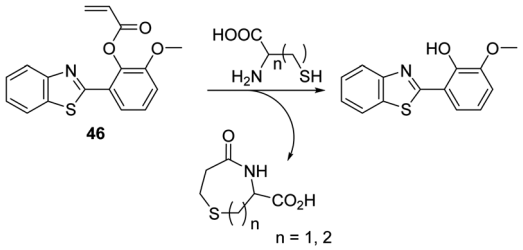

Scheme 42 An acrylate functionalised HMBT fluorescent probe **46** that allows for the selective detection of Cys and HCys. Measurement conditions: HEPES/EtOH (8 : 2) – pH = 7.4.

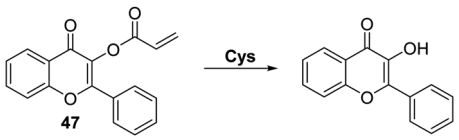

Scheme 43 An acrylate functionalised 3-hydroxyflavone fluorescent probe **47**. This system was found to permit the ratiometric detection of Cys in human mesenchymal stem cells (hMSCs). Measurement conditions: HEPES/ACN (50 : 50) pH = 7.4.

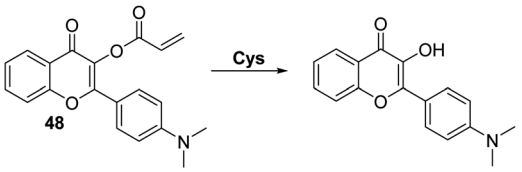

Scheme 44 An acrylate functionalised dimethylamino 3-hydroxyflavone fluorescent probe **48**. This system allowed for the ratiometric detection of Cys in human mesenchymal stem cells (hMSCs). Measurement conditions: PBS/DMSO (7.5 : 2.5), pH = 7.4.

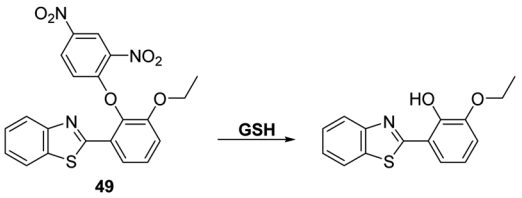

Scheme 45 A HBT-based fluorescent probe **49** for the detection of GSH catalysed by CTAB. Measurement conditions: HEPES buffer, 20 mM, pH = 7.4 containing 1 mM CTAB.

which was used to detect cysteine (Cys) and homocysteine (HCys) in EtOH/PBS (8 : 2) (Scheme 42). The presence of very low concentrations of Cys/HCys (LOD = 0.11 and 0.18 μM, respectively) resulted in thiol-based conjugate addition to the acrylate group of probe **46** resulting a subsequent amino cyclisation reaction; this afforded the HMBT fluorophore and the respective lactam and gave rise to a large change in the ratiometric emission intensity (I_{487}/I_{377}). Probe **46** was found to possess excellent selectivity for Cys/HCys over other biologically relevant amino acids. Moreover, probe **46** was shown to be capable of discriminating Cys over HCys due to disparities in the rate of 7- *vs.* 8-membered ring-formation, a difference that was reflected in different spectroscopic and kinetic profiles for each analyte.[128]

Pang and co-workers prepared a related acrylate-functionalised flavone-based fluorescence probe **47** that allowed for the selective detection of Cys over other biological thiols. Exposure of **47** produced a large ratiometric change in the fluorescence intensity, with a lower detection limit of <1 μM being observed (Scheme 43). Probe **47** was shown to exhibit excellent selectivity over other α-amino acids. This permitted its use in cellular imaging experiments, where it was shown to have low cytotoxicity and good cell permeability.[129]

Similarly, Feng and co-workers reported an acrylate modified dimethylamino-flavone-based fluorescent probe **48** for Cys. This particular system demonstrated Cys-mediated acrylate cleavage within 5 min at low concentrations of Cys (LOD = 0.2 μM) (Scheme 44). A large ratiometric change in fluorescence intensity (I_{550}/I_{471}) and a large Stokes shift (>130 nm) were observed. Probe **48** was found to display excellent selectivity over other amino acids and could be used to detect intracellular levels of Cys in HeLa cells.[130]

Glutathione (GSH)

GSH is a natural tripeptide (γ-L-glutamyl-L-cysteinyl-glycine), which mainly exists in its thiol reduced form (GSH) over its corresponding disulphide-oxidised (GSSG) form.[131] GSH is present in millimolar concentrations in most cells, where it functions as an antioxidant. Elevated levels of GSH are often seen under conditions of oxidative stress and, in fact, the susceptibility of cells towards ROS/RNS species is strongly correlated with intracellular GSH levels.[132,133] Moreover, dysregulation of GSH homeostasis is associated with a number of diseases, including AIDS, liver damage, cancer, and neurodegenerative diseases.[134–136]

Chen *et al.* reported a 2,4-dinitrophenyl ether HBT-based fluorescent probe **49** for the detection of GSH. In the presence of CTAB exposure of probe **49** to GSH results in cleavage of the 2,4-dinitrophenyl group to release the ESIPT fluorophore and an increase in the fluorescence intensity (15-fold) at 485 nm (Scheme 45). The presence of CTAB and the resulting formation of micelles was believed helpful in catalysing the nucleophilic aromatic substitution reaction between GSH and probe **49** by maximising the hydrophobic and electrostatic interactions between the positive charge of CTAB and the negative charge of the carboxylate groups of GSH. Probe **49** proved effective in detecting low concentrations of GSH (LOD = 0.81 μM). It also displayed excellent selectivity over other amines, including HCys and Cys. This selectivity was rationalized in terms of GSH having a negatively charged carboxylate group. Probe **49** was use to image exogenously added GSH in HeLa cells, thus demonstrating its potential utility in biological applications.[137]

Hydrogen peroxide (H_2O_2)

Hydrogen peroxide (H_2O_2) is a weak oxidant and a weak nucleophile that is able to diffuse freely across cell membranes and into cells. H_2O_2 is known to be critical to a number of physiological processes, including cell proliferation, differentiation, apoptosis, and cell signalling.[138] However, the accumulation of H_2O_2 has been implicated in a number of pathological

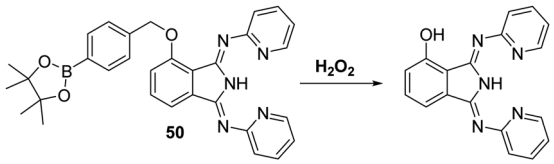

Scheme 46 A boronic ester functionalised ESIPT fluorescent probe **50**. This system permitted the detection of hydrogen peroxide in 4T1 cells. Measurement conditions: PBS buffer, 10 mM, pH = 7.4 containing 1 mM CTAB.

conditions, including cancer, aging, and neurodegenerative diseases.[139–142] There is thus a demand for fluorescent probes that might permit the selective detection and quantification of H_2O_2 in biological milieus.

A commonly employed strategy for the detection of H_2O_2 involves the H_2O_2-mediated oxidation of functionalized aryl boronates to their corresponding phenols thereby generating a fluorescence response.[143] Song *et al.* developed a fluorescent probe **50** for the detection of H_2O_2 *via* functionalisation of the phenol group of the ESIPT dye, 1,3-bis(bispyridin-2-ylimino)-isoindolin-4-ol, with an aromatic boronate ester unit. This functionalisation blocks the ESIPT process (Scheme 46). Addition of H_2O_2 to probe **50** in PBS (pH = 7.4) containing CTAB produced a large fluorescence increase (54-fold) and a remarkably large Stokes shift (217 nm). Probe **50** was shown to display sensitivity towards H_2O_2 (LOD = 9.4 nM) and to react fully within 60 min in the presence of 80 equiv. of H_2O_2. Probe **50** was found to have excellent selectivity for H_2O_2 over other ROS/RNS species as well as other biologically relevant analytes. Probe **50** was shown to be membrane permeable in 4T1 cells, which were imaged successfully in the presence of exogenous H_2O_2.[144]

Singh *et al.* developed a 'two-step surveillance' ESIPT HBT-based probe **51** for the detection of H_2O_2 where photolysis ($\geq$410 nm) allowed for the release of the anticancer drug chlorambucil (Scheme 47). Nanoformulation was carried out to produce nanoparticles containing probe **51** that provided for relatively good penetration and retention in cancer cells. Initially, the ESIPT process is blocked by the presence of a benzyl boronic ester; however, exposure to H_2O_2 results in oxidative cleavage and gives rise to a large ratiometric change in the fluorescence intensity (I_{518}/I_{448}). Subsequent exposure of probe **51** to visible light ($\geq$410 nm) leads to release of chlorambucil, as monitored by reverse-phase high-performance liquid chromatography (RP-HPLC). Remarkably, exposure of probe **51** to visible light ($\geq$410 nm) led to a decrease in the fluorescence intensity of the keto emission (518 nm) with only a fluorescence emission at 450 nm being observed. Probe **51** was shown to be membrane permeable which allowed it to be used to image ratiometrically H_2O_2 in HeLa cells (blue to green). Subjecting HeLa cells containing probe **51** to irradiation for 15 min was found to produce change in the colour of the emitted light from green to blue. This colour change was taken as evidence of chlorambucil release. Further support for this conclusion came from the enhanced cytotoxicity of probe **51** upon irradiation as inferred from an MTT assay.[145]

Yan *et al.* developed a mitochondria-targetable NIR fluorescent probe **52** for the detection of H_2O_2. In this case, exposure of the probe to the analyte results in a decrease in the emission intensity at 539 nm and an increase in the emission intensity at 669 nm. A large Stokes shift of 357 nm is also seen (Scheme 48). Probe **52** was shown to have high sensitivity for H_2O_2 (LOD = 0.59 μM) and good selectivity over other ROS/RNS species, as well as other biologically relevant analytes. Probe **52** was found to localise in the mitochondria of A549 cells where it could be used to image both exogenous and endogenous H_2O_2.[146]

Li and co-workers have developed a clever dual functional theranostic probe **53** that generates a fluorescence response and releases a therapeutic agent in the presence of H_2O_2 (Scheme 49). Probe **53** is comprised of HBT whose phenolic group is esterified with an aspirin moiety that blocks the ESIPT process. Probe **53** was shown to detect H_2O_2 at low concentrations (LOD = 2.5 μM) and with good selectivity over other reactive species, including $ONOO^-$. Probe **53** was used to image

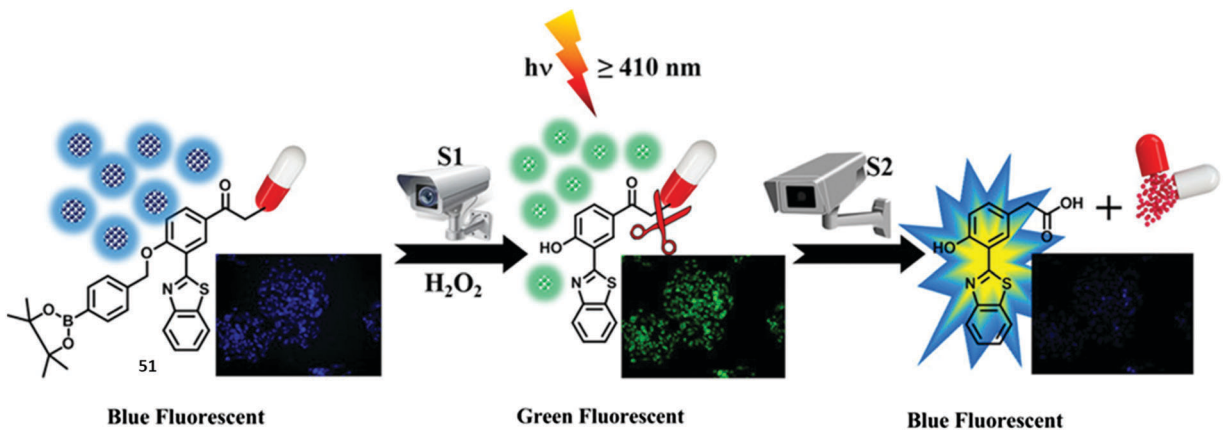

Scheme 47 A 'two-step surveillance' ESIPT HBT fluorescent probe **51** that allows for the detection of hydrogen peroxide and the irradiation-triggered release of chlorambucil with a corresponding change in fluorescence emission. Measurement conditions: not reported. Reproduced with permission from (*ACS Appl. Mater. Interfaces*, 2017, **9**, 28180–28184). Copyright (2017) American Chemical Society.

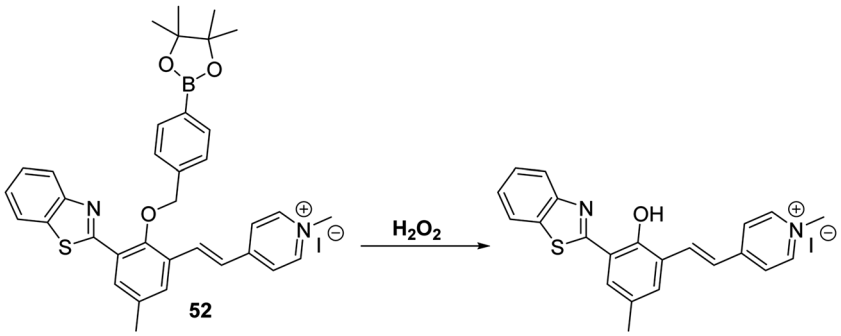

Scheme 48 A NIR-mitochondria targeting ESIPT fluorescent probe **52** that allows for the ratiometric detection of hydrogen peroxide in A549 cells. Measurement conditions: HEPES/ACN (50 : 50) pH = 7.4.

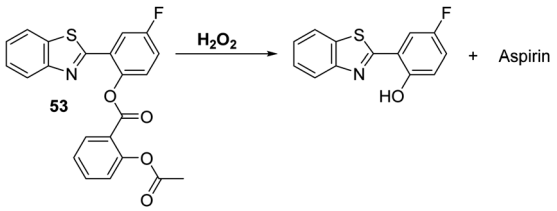

Scheme 49 A hydrogen peroxide responsive theranostic probe **53** that allows for endothelial injury imaging and protection. Measurement conditions: PBS/EtOH (50 : 50) pH = 7.4.

H_2O_2 in EA.hy926 endothelial cells. It was also shown to alleviate endothelial injury, with the endothelial-protective effect of probe **53** being demonstrated in terms of reduced thrombosis formation in zebrafish models.[147]

Nitric oxide (NO)

Nitric oxide (NO) is a small signalling molecule that is generated by three different nitric oxide synthases (NOS) that catalyse the oxidative conversion of L-arginine to L-citrulline. NO is known to mediate many physiological processes, such as neurotransmission, blood pressure regulation, smooth muscle relaxation, and immune regulation. However, uncontrolled NO production can lead to nitrosative stress, which is implicated in neurodegenerative diseases and ischemic-reperfusion injury.[75,76,148,149] Therefore, the development of fluorescence-based probes for NO could provide useful tools allowing for its direct detection and real-time monitoring in biological environments.

Yoon and co-workers developed a simple HBT-based fluorescent probe **54** for the selective and ratiometric detection of NO (Scheme 50). Initially, probe **54** exhibited a fluorescence emission peak at 470 nm due to the ESIPT process. However, the presence of NO resulted in the formation of a longer wavelength benzo[*c*]cinnoline derivative leading to a ratiometric change in fluorescence intensity (I_{560}/I_{470}). The formation of a benzo[*c*]cinnoline derivative was confirmed by mass spectrometry. Probe **54** displayed good selectivity and sensitivity (LOD = 17 nM) for NO over other relevant analytes. It was also shown to be cell permeable and could be used to image exogenously added 1,1-diethyl-2-hydroxy-2-nitroso-hydrazine (DEA NONOate – an NO donor) in HeLa cells.[150]

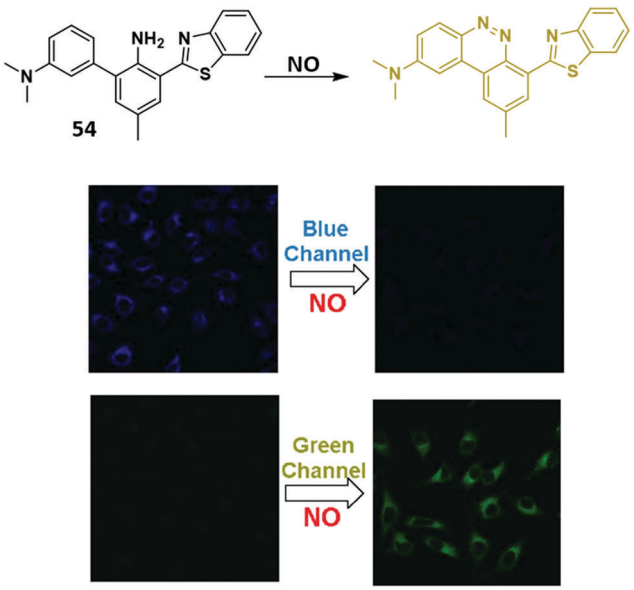

Scheme 50 An ESIPT fluorescent probe **54** for the ratiometric detection of NO *via* formation of a benzo[*c*]cinnoline derivative. Measurement conditions: PBS buffer (1.0 mM, pH = 7.4). Reproduced with permission from (*Sens. Actuators, B*, 2018, **259**, 347–353). Copyright (2018) Elsevier.

Nitroxyl (HNO)

Nitroxyl (HNO) is the one-electron reduced form of NO that demonstrates a unique chemical and biological profile compared to NO. HNO exists in two electronic forms, a singlet and triplet state. Biologically, ^{1}HNO is a small neutral molecule ($pK_a \approx 11.4$), which allows it to freely cross cell membranes and engage in several redox reactions with biological reductants and oxidants. HNO has been found to have a number of beneficial physiological properties therefore HNO is emerging in the literature as a potential pharmacological agent. Some of these properties include increasing cardiac output, protective effects against myocardial ischemia injury, and anticancer properties.[151–155] Therefore, the development of a fluorescent probe for its detection could provide a suitable tool for understanding the role in biological systems.

In 2009, King *et al.* reported that HNO can react with *ortho*-triarylphosphines methyl benzoates to give the corresponding phosphine oxides and an aza-ylide (Scheme 51).[156] The resulting

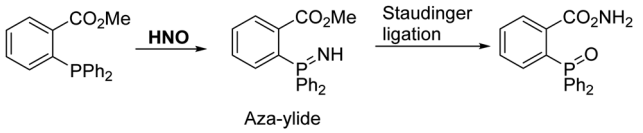

Scheme 51 HNO induced Staudinger ligation developed by King *et al.*[156] Reaction conditions: 3 : 1 CD_3CN/Tris buffer.

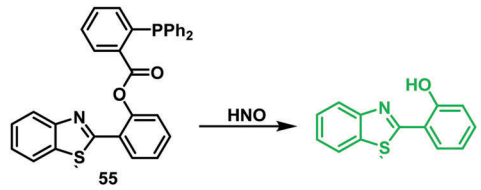

Scheme 52 A HNO-reactive diphenylphosphine-based ESIPT fluorescent probe **55**. This system permitted the ratiometric detection of HNO in HeLa cells. Measurement conditions: PBS/ACN (7 : 3) pH = 7.4.

intermediate can rearrange to afford an amide and a phosphine oxide (Staudinger ligation).

Yin and co-workers employed this reactivity to develop the first ESIPT fluorescent probe **55** functionalised with a HNO-reactive diphenylphosphinobenzoyl group (Scheme 52). As expected, addition of sodium trioxodinitrate – $Na_2N_2O_3$ (Angeli's salt) as a HNO donor (0–30 μM) gave a ~9.5 fold ratiometric change in fluorescence (I_{460}/I_{380}). Probe **55** exhibited high sensitivity (LOD = 0.98 μM) and selectivity for HNO and was used to image HNO in HeLa cells (Fig. 5).[157]

Zhu *et al.* developed a flavone-based fluorescent probe **56** for HNO. This was achieved by functionalising the hydroxyl group of flavone with an HNO-cleavable diphenylphosphinobenzoyl recognition unit (Scheme 53). Probe **56** was shown to exhibit a selective response to HNO over other biological oxidants and reductants and to permit the rapid detection of HNO (LOD = 0.13 μM). Importantly, probe **56** could be used to detect HNO

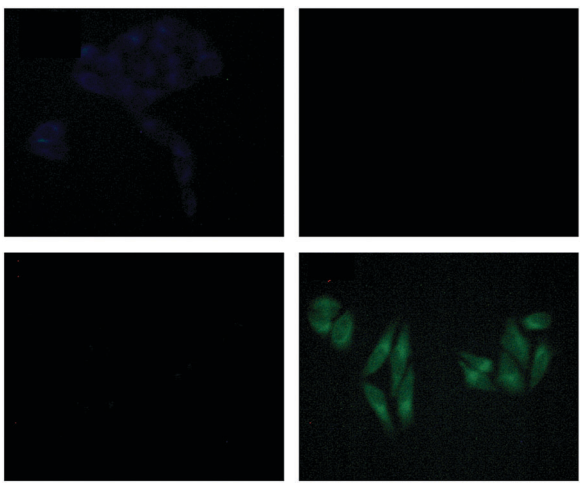

Fig. 5 Results of cellular imaging experiments involving HeLa cells incubated with probe **55**. The images were recorded with and without the addition of Angeli's salt. Adapted with permission from (*Anal. Methods*, 2015, **7**, 3883–3887). Copyright (2015) The Royal Society of Chemistry.

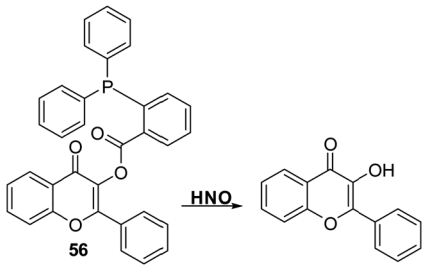

Scheme 53 A diphenylphosphine-based 3-hydroxyflavone fluorescent probe **56** that could be used for the detection of HNO in aqueous media and in serum. Measurement conditions: PBS/EtOH (6 : 4), pH = 7.3.

in complex biological samples (serum) demonstrating its potential utility in clinical applications.[158]

Ozone (O_3)

Ozone (O_3) is located in the stratosphere, where its presence acts to protect the Earth from harmful UV light. However, in the lower troposphere, O_3 is known to be harmful and has been associated with the onset of respiratory diseases.[159] In addition, it is known that antibodies can catalyse the production of the previously unknown oxidant, dihydrogen trioxide (H_2O_3) and O_3 from $^1O_2$, for the purpose of immune defense.[160] For these reasons, the development of fluorescent probes for the detection of O_3 is highly desirable from both a health and safety perspective and to gain a greater understanding of its biological function.

Wang *et al.* have reported a simple HBT-based fluorescent probe **57** for the detection of O_3. The ESIPT process of probe **57** is initially blocked through alkylation of the phenol group of HBT with 4-bromo-1-butene. O_3 reacts with the terminal alkene to afford an aldehyde that undergoes β-elimination to release the HBT fluorophore and acrolein (Scheme 54). This cleavage process liberates the phenol group turning on the ESIPT process. This in turn leads to a large increase in the fluorescence intensity. Probe **57** was shown to exhibit high sensitivity for O_3 (LOD = 34 nM) and an excellent selectivity for O_3 over other ROS/RNS species. In addition, filter paper impregnated with probe **57** was found capable of detecting qualitatively various concentrations of O_3, thus demonstrating its potential utility as a tool for monitoring environmental levels of O_3.[161]

Hydrazine (NH_2NH_2)

Hydrazine (NH_2NH_2) is a chemical reagent that is widely used in the pharmaceutical, chemical, aerospace, and agricultural

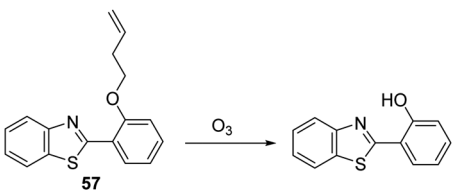

Scheme 54 1-Butene-functionalised HBT fluorescent probe **57** that permits the rapid detection of ozone. Measurement conditions: PBS buffer, 10 mM, pH = 7.1.

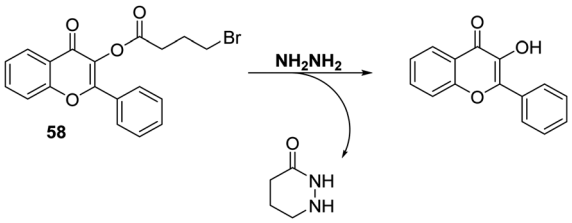

Scheme 55 3-Hydroxyflavone probe **58**, a system that permits the rapid detection of hydrazine in HeLa cells. Measurement conditions: PBS/DMSO (1 : 9) pH = 7.0.

industries.[162–164] However, it is highly toxic, displaying mutagenic and carcinogenic effects that can cause serious damage to major organs and the central nervous system.[165–167] Therefore, it is vital to have analytical methods that allow its detection since these could allow for its monitoring in the event of accidental release into the environment.

Zhu and co-workers functionalised a flavone fluorophore with 4-bromobutyric acid to produce probe **58**. As prepared the ESIPT process in probe **58** is blocked and only the enol-derived emission is observed (Scheme 55). However, addition of NH_2NH_2 to a DMSO/H_2O (9 : 1, v/v) solution of probe **58** results in nucleophilic substitution of bromide and subsequent amino-carbonyl cyclisation onto the ester to release the flavone fluorophore. This results in a large increase in the fluorescence intensity ($\sim$55 fold increase) due to the formation of the keto form. Probe **58** was shown to have high sensitivity for NH_2NH_2 (LOD = 0.15 μM) and excellent selectivity over other amine-containing analytes. Probe **58** could be used to image exogenously added NH_2NH_2 in living HeLa cells.[168] It could also be formulated into test strips that permitted the qualitative detection of different concentrations of NH_2NH_2 under conditions of UV light irradiation.

Recently, Huang and co-workers functionalised a HMBT fluorophore with acetic anhydride to afford probe **59**, wherein the inherent ESIPT process is blocked (Scheme 56). Addition of NH_2NH_2 to a PBS buffer solution containing 1 mM CTAB and probe **59** resulted in the nucleophilic cleavage of the acetate group and release of the HMBT fluorophore. This engendered a large ratiometric fluorescence response (I_{480}/I_{371}). Probe **59** was found to possess high sensitivity for hydrazine and excellent selectivity over other nucleophilic anionic species. Moreover, renewable test strips impregnated with probe **59** were developed; these proved capable of qualitatively and quantitatively detecting NH_2NH_2 in aqueous media or in the gaseous state. These strips were thought to exploit the solid state emitting nature of this specific ESIPT fluorophore, a feature seen in several other systems.[9] The protocol embodied in the test strips containing **59** is relatively unexplored and it was suggested that it could be used for the real time monitoring of NH_2NH_2 gas released from various sources, including those ostensibly contributing to air pollution (Scheme 56).[169]

Phosgene ($COCl_2$)

Phosgene ($COCl_2$) is a colourless and highly toxic gas that was used as a chemical weapon during World War I. Exposure to

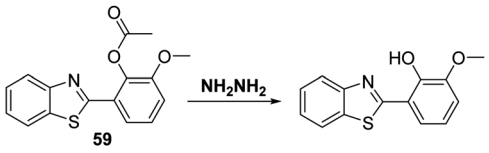

Scheme 56 Acetate-functionalised HMBT fluorescent probe **59**. This system was found to allow for the ratiometric detection of aqueous and gaseous hydrazine in the solid state and in aqueous media. Measurement conditions: PBS buffer, 10 mM, pH = 7.4 containing 1 mM CTAB.

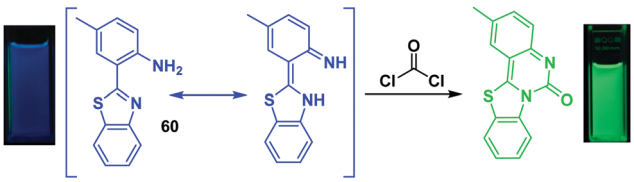

Scheme 57 An ESIPT fluorescent probe **60** that acts as an effective detection system for phosgene. Measurement conditions: $CHCl_3$ and NEt_3. Adapted with permission from (*Anal. Chem.*, 2017, **89**, 12596–12601). Copyright (2017) American Chemical Society.

$COCl_2$ results in serious damage to the lungs and respiratory tract leading to asphyxia, pulmonary emphysema, and death.[170,171] However, $COCl_2$ is still widely used in industry for the synthesis of pesticides and pharmaceuticals;[172] therefore, $COCl_2$ is a potential threat to human health and safety and so the availability of fluorescent probes for its detection is highly desirable.

Yoon and co-workers developed a colorimetric and ratiometric fluorescent probe **60** for the selective detection of $COCl_2$ (Scheme 57). Initially, probe **60** has a fluorescence emission at 445 nm due to an ESIPT effect. Exposure to $COCl_2$ results in the carbamoylation of probe **60** to form a tetracyclic urea (structure confirmed by ^{1}H NMR spectroscopy and mass spectrometry) characterized by a fluorescence emission feature at 496 nm. Reaction of $COCl_2$ with probe **60** also results in a colorimetric change (colourless to yellow) and a ratiometric change in the fluorescence intensity (I_{495}/I_{445}). High sensitivity and selectivity was observed for phosgene in chloroform and in the gas phase. Probe **60** could be incorporated into filter papers giving test strips that could be used for the qualitative detection of different concentrations of $COCl_2$.[173]

Boronic acids (R-B(OH)$_2$)

Boronic acids (R-B(OH)$_2$) are one of the most commonly used compounds in synthetic organic and medicinal chemistry. They also represent a functional group that can be used as a recognition unit for the sensing of biological analytes.[143,174,175] This provides a cogent rationale to develop probes for boronic acids. Their availability might allow the progress of an organic transformation that employs a boronic acid to be monitored readily or permit its presence as a contaminant in a pharmaceutical process to be detected more easily.

Raines and co-workers developed a quinolone-based fluorescent probe **61** that was able to bind and detect boronic-acid functionalised compounds selectively *via* disruption of an ESIPT process (Scheme 58). Probe **61** was shown to be able to

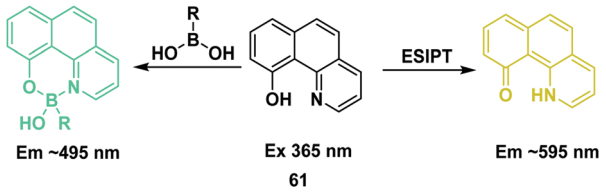

Scheme 58 An ESIPT fluorescent probe **61** for boronic acids that could allow for the direct monitoring of the progress of certain organic reactions. Measurement conditions: probe **61** spotted on TLC plates.

detect phenylboronic acid over a range of 0–20 μM. A 1 mM solution of probe **61** was developed by this group as a dip for the visualisation of boronic acids spotted onto TLC plates. In addition, probe **61** was used to detect the presence of *m*-aminophenylboronic acid on agarose functionalised beads, thus demonstrating its potential utility in materials chemistry applications.[176a] Similarly, Mahapatra and co-workers developed an ESIPT probe that can be used to detect perborate.[176b]

ESIPT fluorescence based sensors for biomacromolecules

Esterases

Esterases represent a broad class of enzymes that catalyse the hydrolysis of esters that are all-important in biology and which play a central role in biotechnology, including food processing, production of alcohol, cellular signalling, material transport, and metabolism.[177,178] Therefore, the development of a fluorescent probe for the detection of esterase activity is a particularly attractive goal since it could provide new tools for use in manufacturing and biological analysis.

Li *et al.* reported a flavone-based fluorescent probe **62** that could be used to evaluate esterase activity *via* fluorescence emission monitoring and ^{19}F NMR spectroscopy (Scheme 59). Initially, the ESIPT process of probe **62** was blocked by an acetate group; however addition of an esterase results in hydrolysis of the acetate group and release of the flavone fluorophore. This release results in an enhancement in the fluorescence intensity at 510 nm (~27 fold) which is ascribed to the presence of the

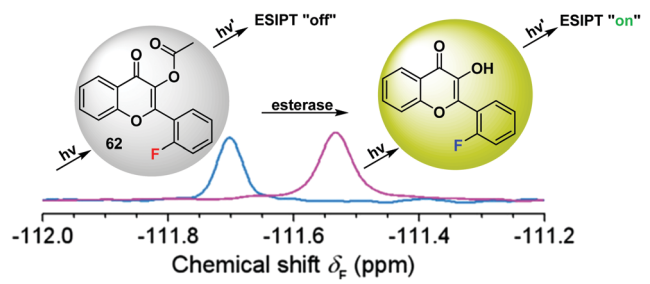

Scheme 59 A fluorinated 3-hydroxyflavone probe **62** that allows for the detection of esterase activity *via* fluorescence emission monitoring and ^{19}F NMR spectroscopy. Measurement conditions: not reported. Adapted with permission from (*Mater. Chem. Front.*, 2018, **2**, 1201–1206). Copyright (2018) the Chinese Chemical Society (CCS), Hong Kong University of Science and Technology, and the Royal Society of Chemistry.

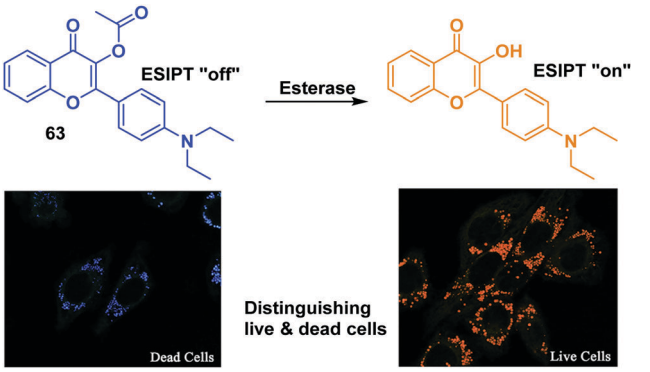

Scheme 60 A 3-hydroxyflavone-based fluorescent probe **63** that permits the discrimination between live and dead cells. Measurement conditions: 1,4-dioxane. Adapted with permission from (*Anal. Chem.*, 2018, **90**, 998–1005). Copyright (2018) American Chemical Society.

more emissive keto tautomer. ^{19}F NMR spectral studies provided further evidence that hydrolysis of the acetate group had occurred. Specifically, the fluorine signal of the probe was seen to shift from δ_F −111.57 to −111.69 ppm upon treatment with an esterase. The combination of these two detection methods, enabled probe **62** to be used for the real-time detection of esterase. In fact, probe **62** allowed for the confocal fluorescence imaging of esterase activity in HeLa cells.[179]

Li and co-workers developed a flavone-based probe **63** that is capable of discriminating between live and dead cells. Its efficacy depends on the fact that cellular esterases are normally inactive inside dead cells (Scheme 60). Probe **63** contains an esterase cleavable acetate group that only exhibits an enol tautomer emission at 440 nm. Esterase-mediated acetate hydrolysis in live HeLa cells, results in a keto tautomer-derived emission at 570 nm being turned on. Two-photon spectroscopic analysis of probe **63** revealed that it is capable of detecting dead tumour cells that had been killed *via* pre-treatment with H_2O_2 and UV. Probe **63** could also be used to discriminate between live and dead zebrafish, thus demonstrating its use as a potentially powerful visualising agent for use in molecular biological applications.[180]

Human carboxylesterase (CE)

Mammalian carboxylesterases are a multigene family of α/β-hydrolase enzymes that are widely distributed throughout the body. They catalyse the hydrolysis of a range of structurally diverse exogenous and endogenous substances (*e.g.*, fatty acid esters, toxins, and drugs). In humans, most carboxylesterases have been identified as carboxylesterase 1 (CE1) and carboxylesterase 2 (CE2), which differ in terms of their distribution throughout the body. CE2 is the major carboxylesterase isoform found in the intestine where it mediates the hydrolysis of most oral ester prodrugs. This means it is an important biomarker for determining first-pass metabolism of a drug of interest. In addition, CE2 is believed to be overexpressed in human colon cancer tissue, thus making CE2 an important biomarker. Being able to detect it could aid in the development of new prodrugs and advance our understanding its role in disease.[181–183]

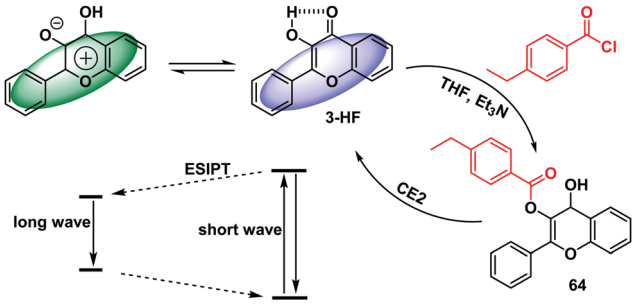

Scheme 61 A 3-hydroxyflavone based fluorescent probe **64** that allows for the monitoring of human carboxylesterase 2 (CE2) activity in HeLa cells. Measurement conditions: PBS buffer solution PBS/ACN – (50 : 50).

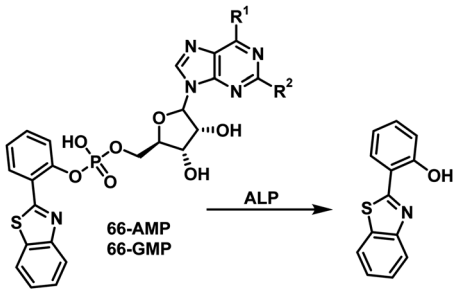

Scheme 63 Nucleotide monophosphate-functionalised fluorescent probes **66-AMP** and **66-GMP** developed for the selection detection of ALP. Measurement conditions: PBS buffer (100 mM, pH = 7.4).

Yang *et al.* have developed a flavone-based fluorescent probe **64** for the selective and sensitive detection of human carboxylesterase 2 (CE2) activity (Scheme 61). The inherent ESIPT process for probe **64** is blocked through functionalisation of the hydroxyl unit of the flavone fluorophore with a 4-ethylbenzoyl chloride unit. Addition of CE2 to probe **64** results in a colorimetric change (clear to light yellow) and a ratiometric change in the fluorescence intensity (I_{528}/I_{392}). Probe **64** was shown to display high sensitivity with a limit of detection for CE2 activity that was lower than 0.5 μg mL^{-1}. Excellent selectivity over other hydrolase enzymes, including CE1, was also seen. Probe **64** could be used to evaluate the activity of a series of different CE2 inhibitors and to image CE2 activity in HeLa cells.[184]

Phosphatases

Alkaline phosphatase (ALP) is an enzyme that catalyses the dephosphorylation of a range of biological substrates, including phosphorylated proteins, nucleic acids, and other small molecules. More importantly, ALP is an important biomarker in medical diagnostics as changes in expression levels of ALP are associated with a range of pathological processes.[185–187]

Wu *et al.* reported a phosphorylated flavone-based fluorescent probe **65** that allows for the detection of ALP based on the modulation of its inherent ESIPT effect (Scheme 62). The phosphate group of probe **65** functions as an ESIPT blocking agent and as a recognition unit for ALP, with only enol emission being observed for the parent probe. ALP can hydrolyse the phosphate group to generate a free hydroxyl group resulting in an ESIPT process being turned on as reflected in a strong keto form-based emission signal. Probe **65** exhibited excellent selectivity for ALP activity over other phosphatase enzymes and proved capable of detecting very low levels of activity (0.032 U L^{-1}). Probe **65** could be used to detect endogenous ALP levels in human serum samples and to be internalised into HeLa cells where it could be used to image endogenous ALP activity.[188]

Han *et al.* have developed two HBT-based fluorescent probes **66-AMP** functionalised with the nucleotides adenosine monophosphate (AMP) and **66-GMP** guanosine monophosphate (GMP), with the aim of achieving greater selectivity for phosphatase activity (Scheme 63). Initially, both probes displayed enol emission due to the ESIPT process being blocked. However, in the presence of ALP a large increase in fluorescence emission intensity at 512 nm was observed corresponding to emission from the keto form. Both probes displayed an excellent selectivity for ALP over other types of phosphatase. The biological potential of these probes was demonstrated by imaging endogenous ALP activity in real time in both HeLa cells and a zebrafish model.[189]

More specifically, Kim and co-workers developed an effective fluorescent probe **67** for the detection of protein tyrosine phosphatase-MKP-6 (PTP MKP-6) activity (Scheme 64). PTP MKP-6 is thought to inhibit the apoptosis of gastric cancer cells; therefore, the ability to detect low levels of MKP-6 activity is potentially important for early cancer diagnosis.[190,191] Probe **67** was prepared by phosphorylating the phenol group of HBT resulting in the inhibition of the ESIPT process. Remarkably, probe **67** was shown to be a highly selective substrate for PTP MKP-6 with phosphate hydrolysis resulting in a significant increase in the keto form-derived emission. The selectivity of this phosphatase activity was confirmed through addition of

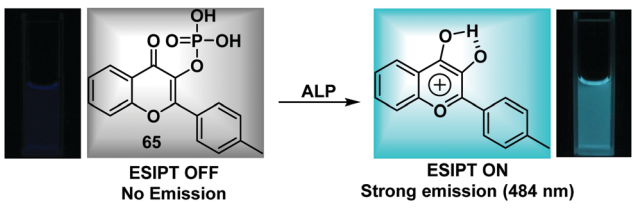

Scheme 62 A 3-hydroxyflavone probe **65** for the monitoring and imaging of ALP activity in HeLa cells. Measurement conditions: Tris–HCl/DMSO (8 : 2). Adapted with permission from (*Sens. Actuators, B*, 2015, **220**, 720–726). Copyright (2015) Elsevier.

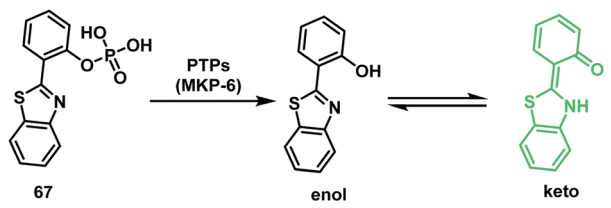

Scheme 64 An HBT-based fluorescent probe **67** for the selective detective of protein tyrosine phosphatase (PTP) activity. Measurement conditions: 20 mM Tris buffer (pH 8.0) containing NaCl (150 mM), 0.01% TritonX-100, DTT (5 mM), and BSA (5 μM).

sodium vanadate which is a known inhibitor of PTP MKP-6; under these latter conditions no fluorescence emission was observed.

Nitroreductases (NTR)

Hypoxia is an important condition found in many solid tumours which is caused by the limited availability of molecular oxygen in bodily tissues and is a state that has long been associated with tumour development.[192,193] Nitroreductase enzymes (NTR) are flavin-based oxidoreductases that catalyse the reduction of nitro-aromatics to their corresponding amino groups. NTRs can be divided into two functional classes: Type I NTRs – oxygen insensitive and Type II NTRs that only function under extreme hypoxic conditions.[194,195] Therefore, owing to the enhanced activity of Type II NTRs under hypoxic conditions the development of fluorescent probes for NTR detection is of particular importance in cancer research and diagnosis.

Wang and co-workers reported a NTR fluorescent probe **68** for the selective detection of nitroreductase (NTR) activity. In this probe, ESIPT activity is blocked *via* attachment to the known hypoxic trigger 4-nitroimidazole (Scheme 65). Addition of NTR and nicotinamide adenine dinucleotide (NADH) leads to catalytic reduction of the nitro group, cleavage of the benzylic ether bond, and release of an activated ESIPT fluorophore. Probe **68** was shown to be sensitive towards NTR activity (LOD = 63 ng mL^{-1}) as reflected in a significant enhancement in its fluorescence intensity at 560 nm. Probe **68** was shown to have an excellent selectivity for NTR over other reductants, such as dithiothreitol and other biologically relevant analytes. Probe **68** was found to be cell permeable and capable of detecting changes in the levels of oxygen in HeLa cells, presumably *via* differences in NTR activity.[196]

Proteases

Proteases are important enzymes responsible for protein catabolism that generate amino acids through the hydrolysis of amide bonds. Proteases regulate and control the activity of many proteins, modulate protein–protein interactions, and contribute to cellular signalling. They are known to influence cell proliferation, DNA replication and transformation, wound repair, inflammation, necrosis, and apoptosis. Moreover, changes in proteolytic activity have been associated with a number of pathological conditions, such as cancer, neurodegenerative disorders, inflammation, and cardiovascular disease.[197] As a result, proteases are important biomarkers for drug delivery and diagnostics. Thus, the development of fluorescence based probes to evaluate protease activity is viewed as a highly desirable research objective.[198]

Hasserodt *et al.* developed a rapid response system for the detection of leucine aminopeptidase (LAP) using the hydroxyphenylquinazoline (HPQ) fluorescent probes **69** and **70**. These two probes undergo self-immolative 1,2-diamine-based cyclisation in the presence of LAP to release insoluble HPQ and the corresponding cyclic urea (Scheme 66). Probe **70** exploits the Thorpe–Ingold effect, which facilitates rapid cyclisation to release HPQ. Additionally, the charge present in the leucine recognition unit ensures good aqueous solubility for both probes. In fact, a high OFF–ON detection sensitivity for LAP was seen with no false positive signals being observed over the course of 24 hours.[199]

ESIPT probes for interrogating biomolecular interactions

Biological macromolecular recognition depends on the formation of multiple protein–protein and protein–nucleic acid interactions. Therefore, the development of fluorescence-based probes that can selectively interrogate these processes could prove useful.[200]

Mely and co-workers have exploited the environmentally sensitive nature of flavone ESIPT dyes to evaluate the microenvironments of single and double-stranded DNA fragments. In their work, they designed and developed flavone-based fluorescent probes, such as **71** and **72**, that were functionalised with a polycationic spermine unit (Fig. 6). Upon binding to a double-stranded DNA (dsDNA), a *ca.* 16-fold ratiometric change in fluorescence intensity was seen for probes **71** and **72**. This increase in fluorescence intensity is believed to result from intercalation of the probes into dsDNA, a binding event that serves to shield them effectively from water molecules. Both probes exhibited a smaller change in ratiometric fluorescence intensity in the presence of single-stranded DNA (ssDNA). This finding was considered consistent with the higher degree of exposure to water molecules expected in the case of ssDNA relative to dsDNA. Importantly, probes **71** and **72** can thus be used discriminate between ssDNA and dsDNA, a finding that

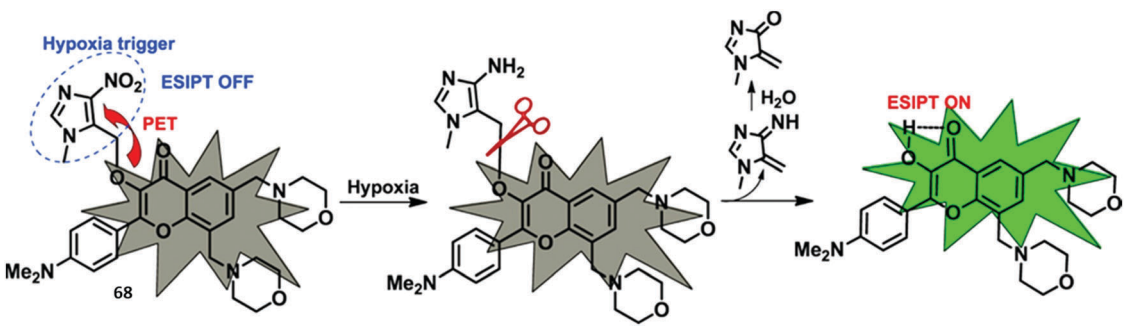

Scheme 65 A 4-nitroimidazole functionalised 3-hydroxyflavone fluorescent probe **68** capable of detecting of nitroreductase activity at various oxygen levels in HeLa cells. Measurement conditions: PBS buffer (10 mM) containing 0.5% DMSO. Reproduced with permission from (*Dyes Pigm.*, 2016, **131**, 145–153). Copyright (2016) Elsevier.

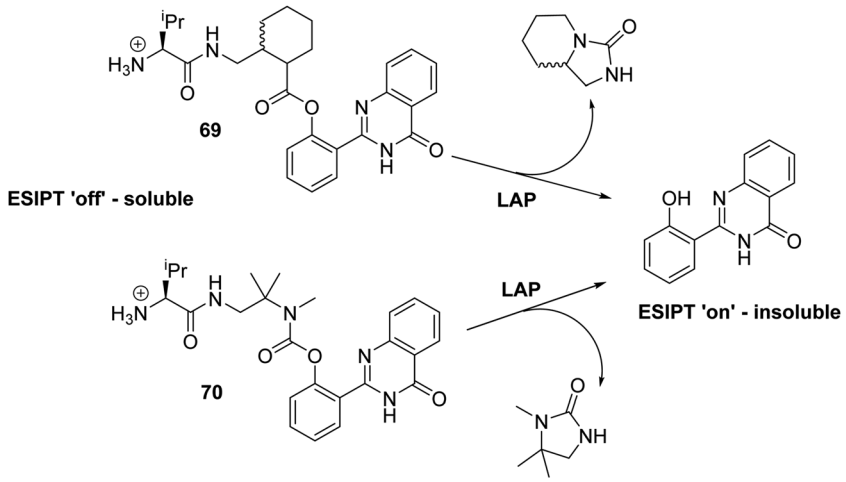

Scheme 66 Leucine-functionalised HPQ fluorescent probes **69** and **70** that were developed to allow for the rapid and selective detection of LAP. Measurement conditions: pH = 7.5.

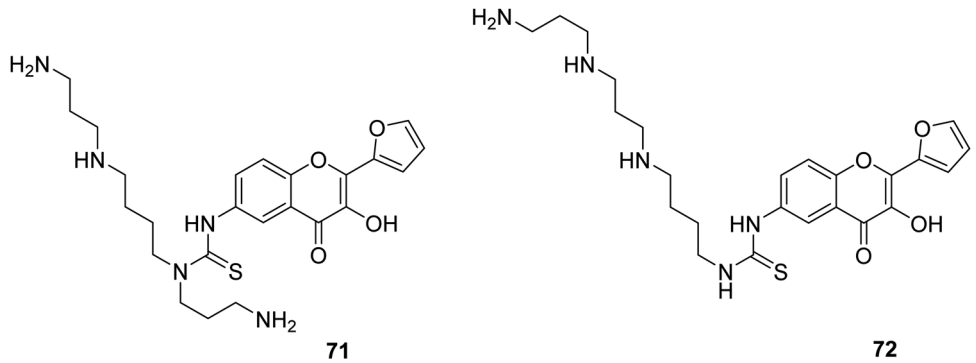

Fig. 6 3-Hydroxyflavone probes **71** and **72** used for the interrogation of DNA binding. Measurement conditions: PBS buffer pH 7.0.

was viewed as underscoring the potential utility of these probes in exploring DNA–protein interactions.[201]

Mely and co-workers further targeted peptide–oligonucleotide interactions by means of probe **73** that consists of the flavone ESIPT fluorophore covalently attached to the N-terminus of a peptide corresponding to the Zn-finger recognition domain of HIV-1 nucleocapsid protein (NC) – Fig. 7. Addition of the target oligonucleotides (ODN) to the probe-labelled peptide **73** gives rise to a large change in the ratiometric fluorescence intensity. The ratiometric response was found to be dependent upon the ODN sequence, a finding that enabled the peptide–ODN binding parameters to be determined for multiple ODN binding sites. This work provides a platform technology that illustrates how ESIPT dye-labelled peptides could be used to investigate peptide–ODN interactions.[202]

More recently, Mely and co-workers reported new probe systems **74–77** that display higher ratiometric sensitivity to solvent polarity (Fig. 8). These systems were covalently attached to the

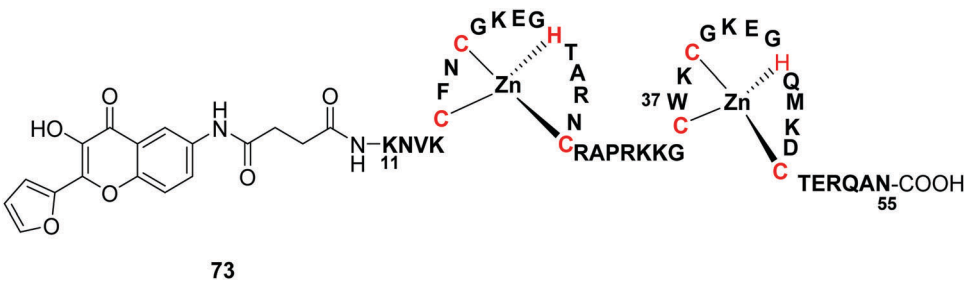

Fig. 7 3-Hydroxyflavone fluorophore functionalised with the N-terminus of a peptide corresponding to the zinc finger domain of the HIV-1 nucleocapsid protein (NC) for interrogation of site specific interactions of peptide–oligonucleotide interactions (ODN). Measurement conditions: PBS buffer pH 7.0.

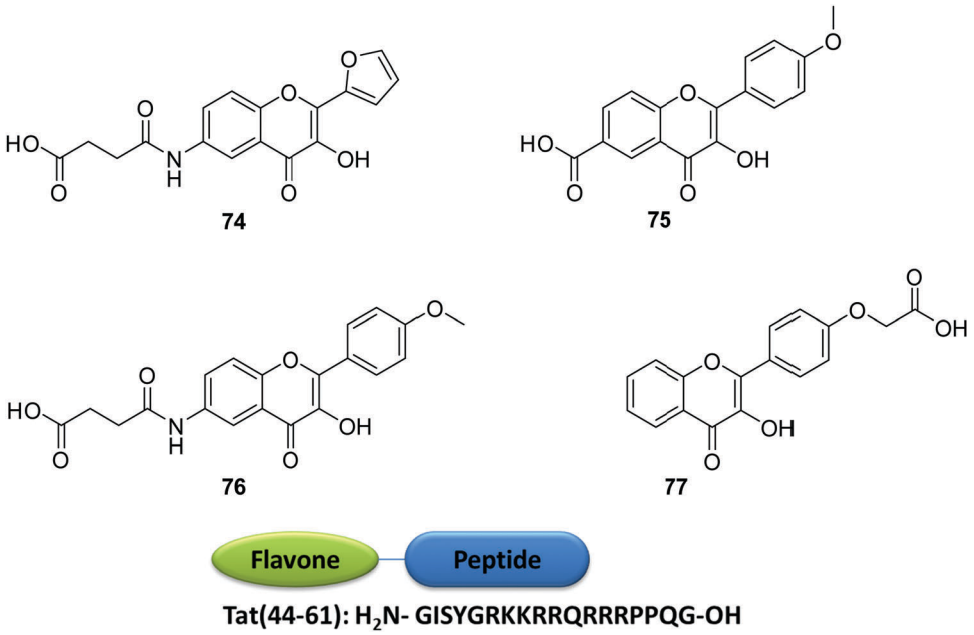

Fig. 8 3-Hydroxyflavone fluorophores that were covalently linked to the N-terminus of Tat (**44–61**) peptide for the interrogation of protein–ODN interactions. Measurement conditions: PBS buffer. (10 mM, pH = 7.0 and 30 mM NaCl).

N-terminus of a Tat (**44–61**) peptide that corresponded to the binding domain of the HIV-1 Tat protein. These ESIPT labelled-peptides produced dramatic ratiometric changes in the fluorescence intensity and could be used to investigate hydration levels in the vicinity of the peptide/oligonucleotide complex, revealing a solvation trend that decreases in the following order short ssDNAs ≫ long ssDNAs > DNA hairpins > dsDNAs.[203]

Exploiting the environmentally sensitive nature of ESIPT fluorophores, Mely and co-workers developed a dodecyl functionalised 3-hydroxyflavone probe **78**. This system is selectively incorporated into the outer leaflet of cell plasma membranes and can monitor changes in the outer membrane lipid content occurring during the initial steps of cell apoptosis (Scheme 67). It was found that probe **78** underwent a real time ratiometric

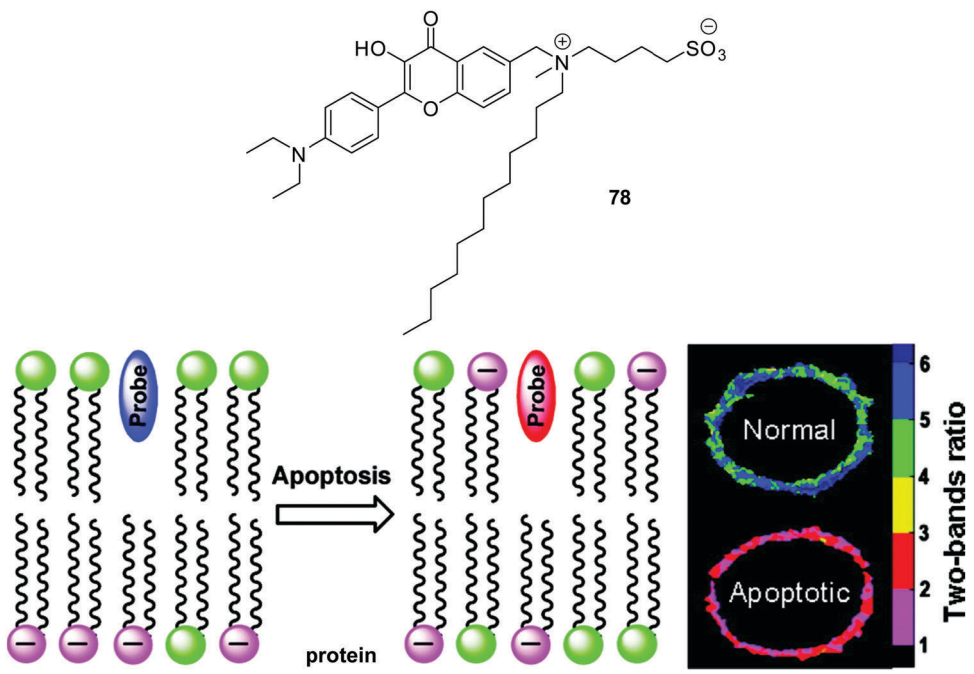

Scheme 67 A dodecyl functionalised 3-hydroxyflavone probe **78**. This system is incorporated into cell membranes and may be used to monitor changes in the lipid membrane content during the early stages of apoptosis. Measurement conditions: lipid. Adapted with permission from (*J. Am. Chem. Soc.*, 2007, **129**, 2187–2193). Copyright (2007) American Chemical Society.

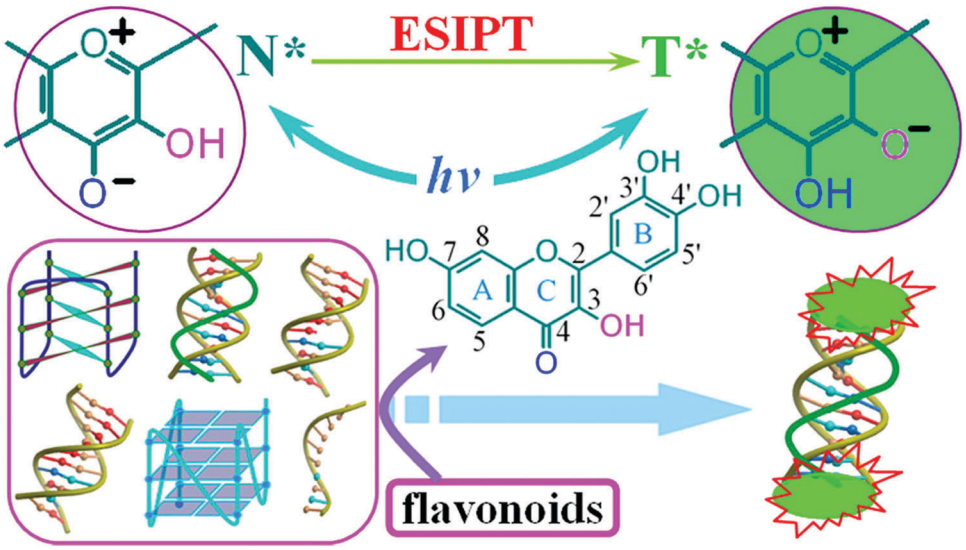

Scheme 68 A natural flavonoid, Fisetin (FIS), allows for the ratiometric detection of triplex DNA. Measurement conditions: PBS buffer (100 mM, pH 5.9). Reproduced with permission from (*Anal. Chem.*, 2015, **87**, 11620–11624). Copyright (2015) American Chemical Society.

change in its fluorescence during the course of apoptosis. Probe **78** could be used to monitor cellular events involving changes in the membrane content, such as those that occur during uncontrolled cell division. Therefore, it was suggested that probe **78** could be used to monitor cancer metathesis at the molecular level and hence evaluate the efficacy of anticancer drugs.[205]

Triplex DNA is formed *via* the sequence-selective recognition of the major groove of a dsDNA by an additional third strand of DNA. DNA triplexes have been shown to have a number of biological activities, including regulation of gene expression, DNA damage and repair. Additionally, triplex DNA has received considerable attention due to its importance in gene regulation, as a molecular switch, and for sensor development. Shao and co-workers screened a number of flavone-based probes for binding to triplex DNA. The natural flavonoid Fisetin (FIS) was found to undergo a large ratiometric change in the fluorescence intensity (I_{538}/I_{460}) in the presence of triplex DNA (Scheme 68). FIS was shown to have excellent selectivity for triplex DNA relative to ssDNA, dsDNA, i-motifs, and DNA/RNA G-quadruplexes. In fact, FIS was shown to stabilise the triplex DNA structure *via* a 2 : 1 interaction with both sequence termini.[204]

Membrane proteins normally contain a large number of transmembrane α-helices, whose expression levels often differ between normal and diseased cells.[206] Liu *et al.* designed an HBT-based fluorescent probe **79** whose keto emission levels were shown to correlate positively with the α-helix content of proteins (Scheme 69). Probe **79** was found to accumulate in cell membranes, where its fluorescence output could be used to detect the presence of the α-helices of membrane proteins. The changes in fluorescence output could be used to distinguish between healthy and prostate cancerous cells since the latter are typically characterized by higher levels of membrane proteins. Therefore, this system could be used as a possible diagnostic tool for the early detection of prostate cancer.[207]

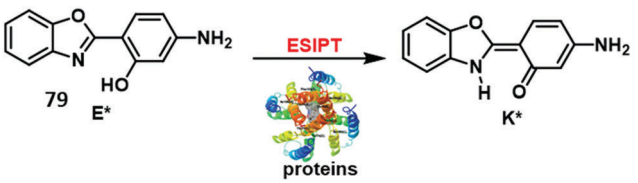

Scheme 69 A HBT-based fluorescent probe **79** for the detection of α-helix content of proteins. Measurement conditions: Tris–HCl buffer (100 mM, pH = 7.4, 150 mM NaCl). Adapted with permission from (*Org. Biomol. Chem.*, 2014, **12**, 5250–5259). Copyright (2014) the Royal Society of Chemistry.

Pang and co-workers prepared a flavone-based fluorescent probe **80** that was functionalised with a lysosome-directing morpholine unit (Fig. 9). The environmental sensitivity of probe **80**, meant that its fluorescence emission intensity at 560 nm increased ~75 fold on moving from polar to non-polar medium. Co-localisation studies confirmed that the probe could be used for the selective visualisation of lysosomes affording 'wash-free' stains that could be used for the real time imaging of lysosomes (Fig. 9).[208]

Fluorescence based sensors with a combined fluorescence mechanism

Combination of fluorescence mechanisms such as ESIPT with photoinduced electron transfer (PET), or ESIPT with aggregation induced emission (AIE), enables the favourable attributes of both processes to be combined to overcome the limitations of many ESIPT dyes.

PET-based fluorescent probes result in a significant change in fluorescence intensity ('off to on', or 'on to off') in the presence of a target analyte with the emission wavelength remaining unchanged.[209] Therefore, the combination of PET

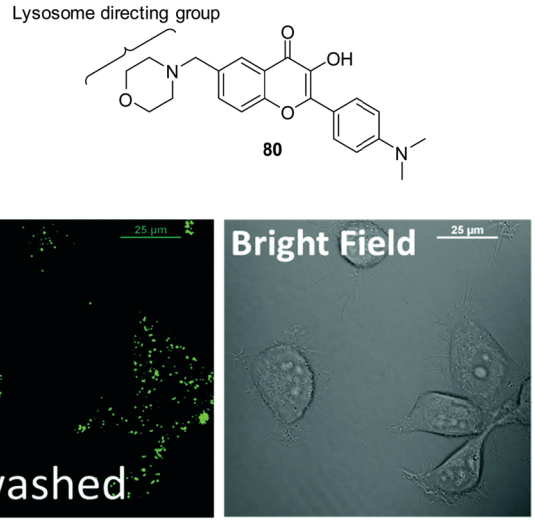

Fig. 9 A lysosomal-targeted ESIPT probe **80** that may be used for the imaging of lysosomes. Measurement conditions: n/a. Adapted with permission from (*J. Mater. Chem. B*, 2018, **6**, 5050–5058). Copyright (2018) the Royal Society of Chemistry.

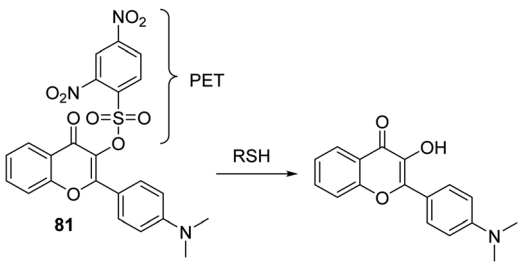

Scheme 70 A combined PET + ESIPT fluorescent probe **81** that proved effective for the detection of biological thiols. Measurement conditions: PBS/EtOH (6 : 4) – pH = 7.4.

and ESIPT can afford a fluorescent probe that exhibits a dual emission spectrum with amplified sensitivity and selectivity.[210a,210b] Wang and co-workers reported a flavone-based fluorescent probe **81** functionalised with the PET fluorescence quenching unit DNBS (dinitrobenzenesulfonyl) (Scheme 70). As prepared, probe **81** is non-fluorescent, due to PET. However, addition of biological thiols (Cys, HCys, and GSH) results in S_NAr cleavage of the dinitroaryl group. This produces a free phenol and gives rise to a large fluorescence response. Probe **81** demonstrated excellent selectivity for biological thiols and could be used to image these analytes in HeLa cells.

Strongin and co-workers reported a HBT rhodol thioester fluorescent probe **82**. This system exploits the fluorescence emission of a combined PET + ESIPT construct to distinguish between GSH and Cys/Hcy (Scheme 71). Addition of Cys/Hcy to probe **82** results in a tandem native chemical ligation (NCL) reaction that affords a deconjugated spirolactam. This NCL reaction results in the quinone of the rhodol unit being transformed into a phenolic group and triggers an ESIPT process that affords a large increase in the fluorescence emission intensity at 454 nm (ESIPT on, no PET). Conversely, addition of GSH, only results in a transthioesterification reaction; this prevents the intramolecular PET process and leads to a large fluorescence response at 587 nm (ESIPT off, no PET). Probe **82** was shown to image biological thiols in HepG2 cells successfully, thus demonstrating its potential for use in biological applications.[211]

AIE is a unique fluorescence phenomenon that was discovered by Tang *et al.*, wherein a weakly fluorescent probe in the solution state becomes highly fluorescent in the aggregate state. It thus stands in contrast to the traditional self-quenching that occurs for fluorophores at high concentrations.[212] AIE normally results in fluorescent probes with a high signal-to-noise ratio and excellent photostability. However, AIE probes generally require good solubility in water in order to ensure a low background signal. ESIPT + AIE probes rely on an intramolecular proton transfer event to induce a change in the fluorescence intensity associated with the ESIPT process but can be designed to favour the formation of aggregates, thus enhancing an AIE-based signal.

Tang *et al.* reported a phosphorylated chalcone derived fluorescent probe **83** that combines the AIE + ESIPT mechanism and allows for the visualization of ALP activity in living cells (Scheme 72). As prepared, probe **83** is water soluble and emits at 539 nm in aqueous buffer. However, the addition of ALP results in a ratiometric change in the fluorescence emission (I_{641}/I_{539}) due to phosphate hydrolysis and aggregation of the resultant phenol product (which is also responsible for the ESIPT effect). Probe **83** was shown to be sensitive towards ALP activity (LOD = 0.15 mU mL^{-1}) over a range of 0–150 mU mL^{-1}. These attributes allowed it to be used to map ALP activity in HeLa cells.[213]

Zhang and co-workers designed and developed a novel AIE + ESIPT probe **84**. This system combines in one molecular construct tetraphenylethene (TPE), a classic AIE luminogen, and the ESIPT fluorophore HBT (Scheme 73). This combination was expected to the synergistic benefit of both fluorescence mechanisms, namely a high solid-state fluorescence quantum yield (Φ_F = 0.97) and a large Stokes shift (>200 nm). In the case of **84**, functionalisation with DNBS afforded a probe that was suitable for the imaging biothiols in cells. In fact, probe **84** displayed high sensitivity (LOD = 72 nM) and excellent selectivity over other biologically relevant analytes.[214]

Lin and co-workers reported an aggregate based AIE + ESIPT fluorescent probe **85** for SO_2/SO_3^{2-}-that contains a leuvinate ester as a SO_3^{2-}-reactive unit (Scheme 74). As prepared probe **85** is weakly emissive at 422 nm. However, exposure to an aqueous solution of SO_3^{2-} results in the leuvinate ester being cleaved and gives rise to a large ratiometric change in the fluorescence emission intensity (I_{567}/I_{470}). The formation of aggregates was confirmed using dynamic light scattering (DLS), experiments that revealed the formation of aggregates with an average size of 60 nm. Probe **85** exhibited high sensitivity (LOD = 0.9 μM), and was able to detect SO_2 ratiometrically in live cells and zebrafish models.[215]

Singh and co-workers designed an AIE + ESIPT imaging agent/prodrug probe **86** for the real-time monitoring of drug

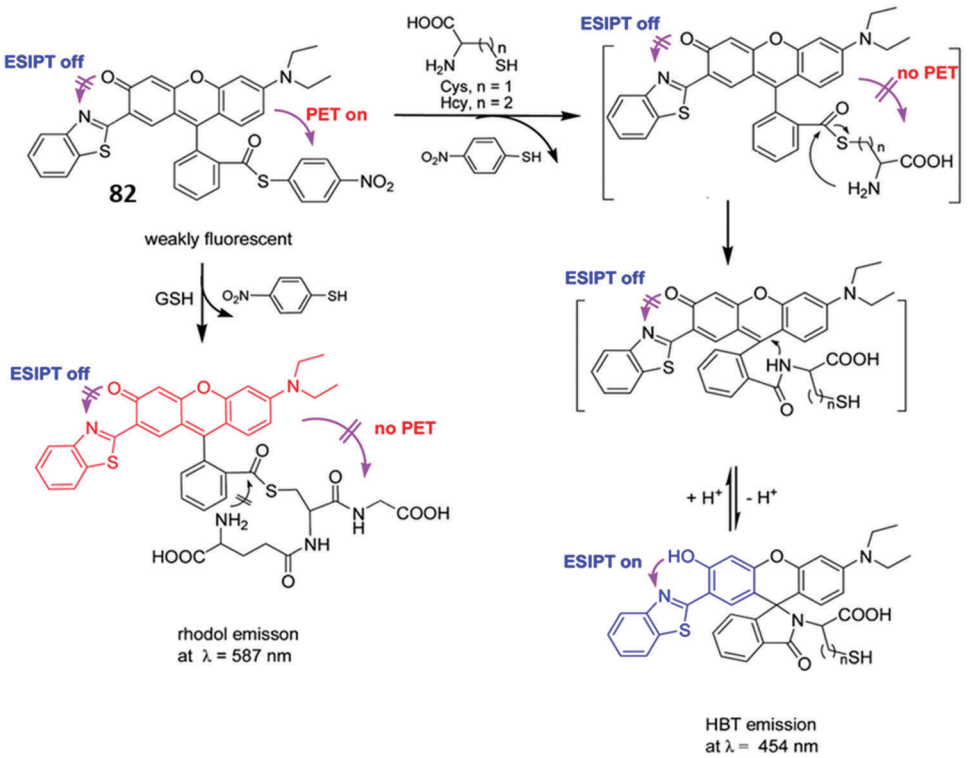

Scheme 71 An ESIPT-PET rhodol-HBT fluorescent probe **82** that allows for the discrimination between GSH and Cys/HCys. Measurement conditions: PBS/DMF (7 : 3) – pH 7.4. Reproduced with permission from (*Chem. Sci.*, 2014, **5**, 2177–2183). Copyright (2014) the Royal Society of Chemistry.

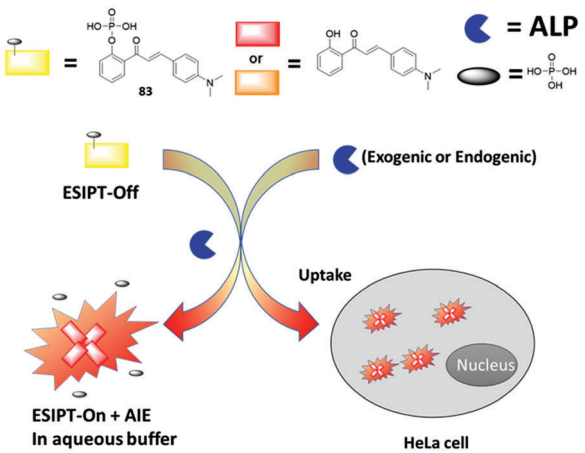

Scheme 72 A combined AIE + ESIPT fluorescent probe **83** that allows for the monitoring of ALP activity in HeLa cells. Measurement conditions: Tris–HCl buffer (pH = 9.2). Reproduced with permission from (*ACS Appl. Mater. Interfaces*, 2014, **6**, 17245–17254). Copyright (2014) American Chemical Society.

release (Scheme 75). This AIE + ESIPT drug delivery system (DDS) displayed a number of ideal properties, including: (i) excitation: >410 nm; (ii) drug release only occurring from an aggregated state, and (iii) a ratiometric response to photoactivation. Probe **86** contains two drug molecules and was formulated into nanoparticles to enhance selectivity, permeability, and retention in tumour cells. Irradiation for 5 minutes resulted in significant cytotoxicity, a finding ascribed to the photoinduced release of the drug molecules. This putative release was accompanied by a ratiometric change in the observed fluorescence in HeLa cells.[216]

Zhang and co-workers developed a novel solid-state AIE + ESIPT fluorophore (HTPQ and TPE), probe **87**, whose phenolic unit was functionalised with a phosphate unit to inhibit the ESIPT processes (Scheme 76). Exposure to ALP resulted in phosphate hydrolysis, a conversion that produced an insoluble fluorophore that aggregated after a short period of time to produce a 100-fold fluorescence increase in the emission intensities at 550 nm. The insoluble diffusion-resistant properties of the cleavage product of probe **87**, enabled ALP to be successfully visualised at the cell membranes of HeLa cells. Probe **87** was also used to visualise different ALP activity levels in Saos-2 and U-2OS osteosarcoma cells, thus enabling the role of ALP in the development of physiological and pathological processes to be determined.[217]

Hu *et al.* developed an AIE + ESIPT HPQ-based fluorescent probe **88** that was designed to allow for the enzymatic detection of β-galactosidase (β-Gal). This is an enzyme that catalyses the hydrolysis of oligosaccharides containing β-galactoside linkages. Overexpression of β-Gal is widely recognised as a biomarker for cell senescence and primary ovarian cancer.[218,219] The inherent ESIPT process of probe **88** was blocked through attachment of galactose to the phenolic unit of HPQ. In the presence of β-Gal, the galactose unit of probe **88** is cleaved turning on the ESIPT process, whilst allowing the formation of aggregates resulting

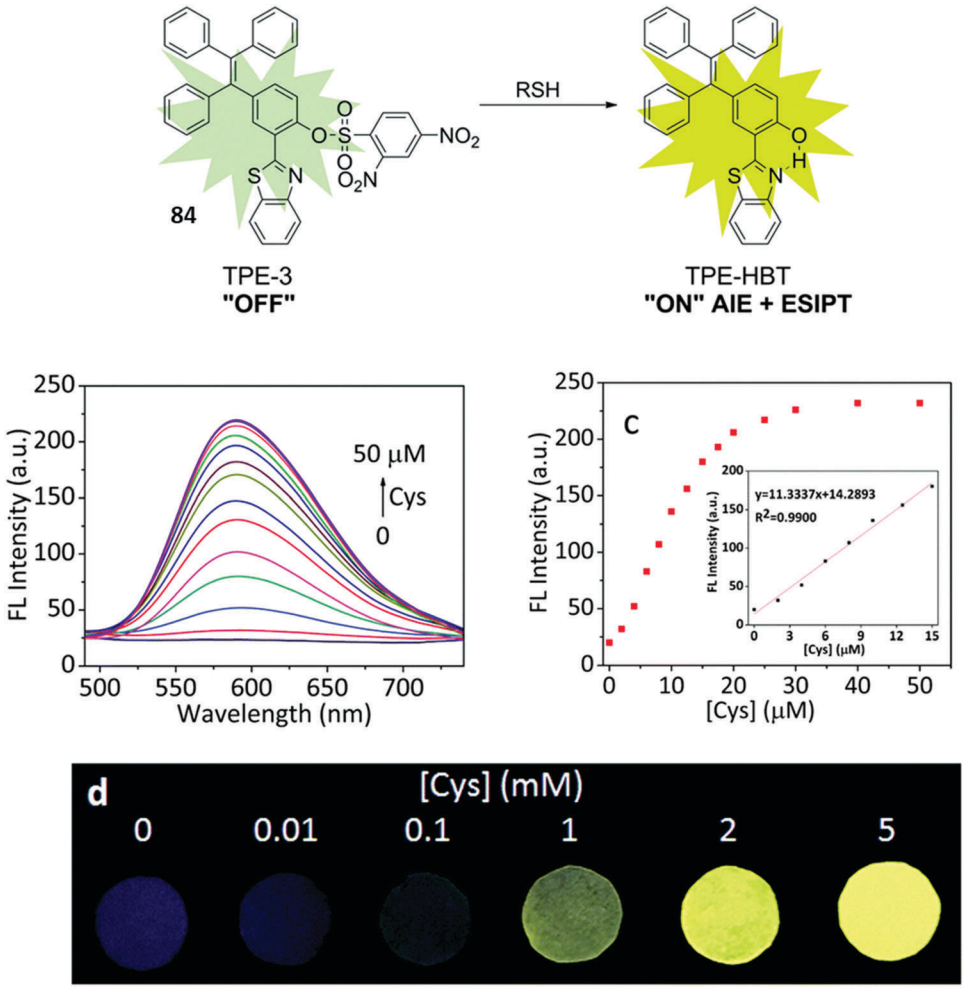

Scheme 73 An AIE + ESIPT fluorescent probe **84** that permits the detection of biological thiols. Measurement conditions: PBS/DMSO (5.5/4.5) – pH = 7.4. Reproduced with permission from (*J. Mater. Chem. B*, 2017, **5**, 7736–7742). Copyright (2017) the Royal Society of Chemistry.

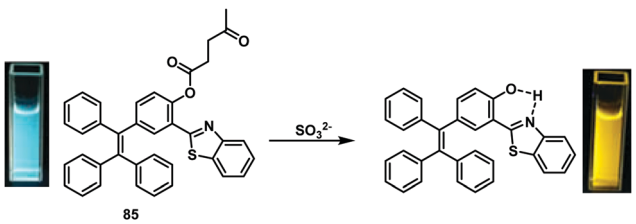

Scheme 74 A leuvinate-functionalised combined AIE + ESIPT fluorescent probe **85** that allows for the detection of SO_3^{2-} in live cells and zebrafish models. Measurement conditions: PBS buffer solution, pH = 7.4. Adapted with permission from (*J. Mater. Chem. B*, 2018, **6**, 1973–1983). Copyright (2018) the Royal Society of Chemistry.

in a large increase in fluorescence emission intensity at 495 nm (Scheme 77). Probe **88** was used successfully for imaging β-Gal activity in OVCAR-3 cells with the insoluble nature of HPQ resulting in the fluorophore being retained in living cells. These are features that make this probe particularly suitable for intracellular imaging applications.[220]

Liu and co-workers developed a salicylaldehyde-derived azine fluorescent probe **89** that was designed to display both an AIE and an ESIPT response to β-Gal (Scheme 78). Upon addition of β-Gal, the galactose recognition units were cleaved. This activated an ESIPT process whilst also producing aggregates, as evidenced by the strong enhancement in fluorescence emission (820 fold) and a large Stokes shift (190 nm). Probe **89** was shown to display high sensitivity (LOD = 0.014 U mL^{-1}) and excellent selectivity for β-Gal activity. Its cellular retention and use in imaging of C6/LacZ cells was aided by administrating it as a colloidal solution.[221]

Liu and co-workers reported a morpholine-functionalised salicylaldehyde azine fluorescent probe **90** for the *in situ* visualisation of lysosomal esterase activity. As prepared, the acetate groups present in probe **90** serve to block the ESIPT process but also act as recognition units for esterases (Scheme 79). Treatment with esterase results in generation of free phenol groups and a 'turning on' of the ESIPT process, as well as aggregate formation. The net result is a large increase in the fluorescence emission intensity at 532 nm (Stokes shift = 176 nm). Probe **90** was shown to target lysosomes and to produce an enzyme-dependent fluorescence response in MCF-7 cells within 8 min. Additionally, probe **90** was found capable of tracking lysosome

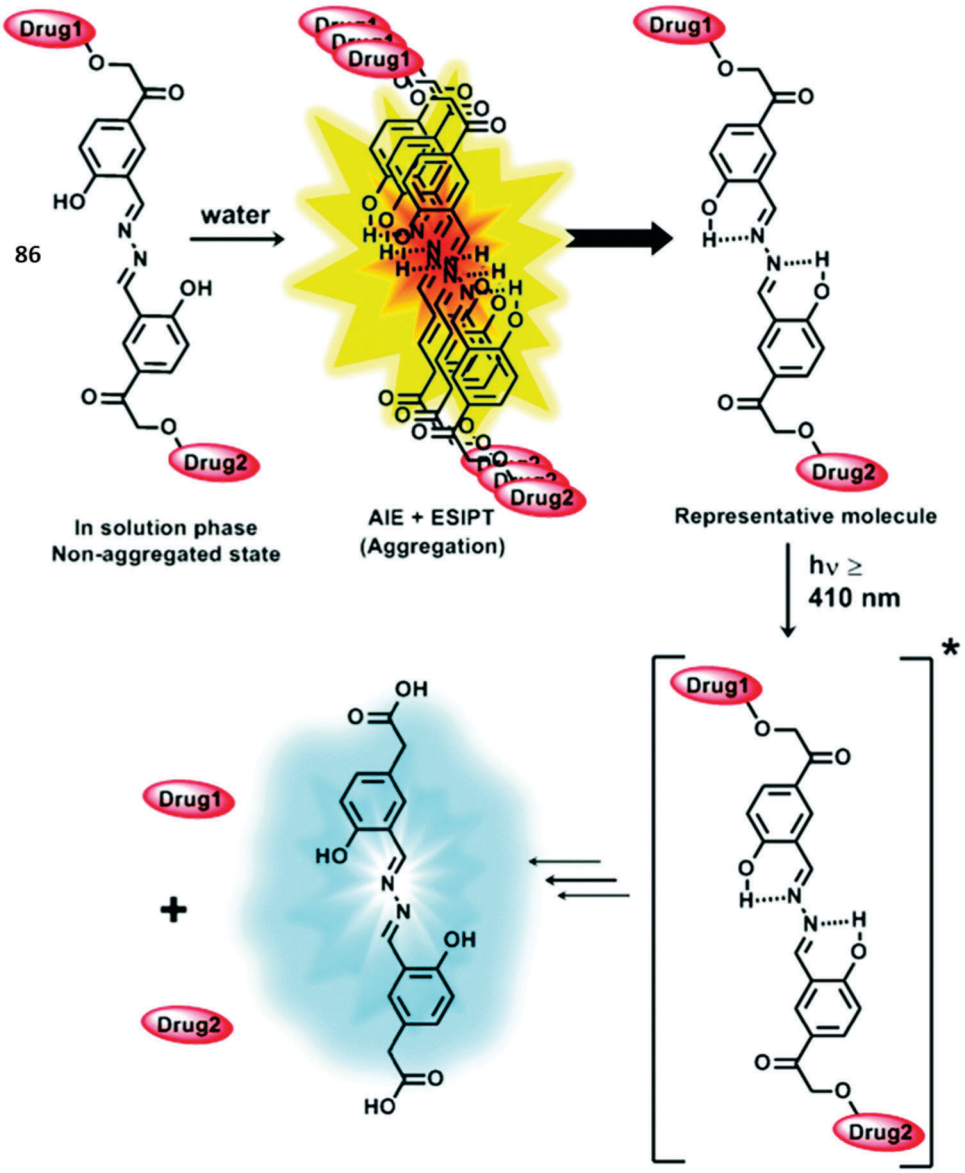

Scheme 75 An AIE + ESIPT imaging probe **86** that releases two separate drugs under conditions of UV irradiation. Drug 1 = chlorambucil, Drug 2 = ferulic acid. Measurement conditions: aqueous solution. Reproduced with permission from (*Chem. Commun.*, 2018, **54**, 168–171). Copyright (2018) the Royal Society of Chemistry.

movements over time in the presence of chloroquine, an agent that is known to induce the movement of lysosomes.[222]

Tong reported a salicylaldehyde azine-derived fluorescent probe **91** that contains a hydroxyl ESIPT donor masked by a Cys-reactive acryloyl group. Addition of Cys results in hydrolysis of the acrylate group and release the AIE + ESIPT fluorophore (Scheme 80). Probe **91** was shown to permit the selective detection of Cys over the 0–30 μM concentration with a limit of detection as low as 0.46 μM. This probe also proved capable of measuring concentrations of Cys in fetal bovine serum.[223]

Yoon and co-workers reported a similar *p*-methoxy-salicylaldehyde azine-derived fluorescent probe **92** that has both hydroxyl units of the ESIPT unit protected with Cys-reactive acryloyl groups. Addition of Cys caused the cleavage of both acryloyl groups and formation of aggregates. This resulted in a large increase in the fluorescence intensity at 505 nm. A large Stokes shift of 165 nm is also observed (Scheme 81). Probe **92** displayed excellent selectivity towards Cys over other biothiols (HCys and GSH) and could be used to detect Cys selectively in HeLa cells.[224]

Jiang and co-workers developed a Schiff base fluorescent probe **93** containing two phenolic groups. In the presence of CN^-, this system undergoes an oxidative cyclization to form HBO (Scheme 82). Probe **93** displayed a strong fluorescence emission intensity in the presence of CN^- in a micellar environment due to a combined ESIPT process and AIE effect. Probe **93** was shown to display excellent selectivity and high sensitivity for CN^- with a LOD = 0.59 μM. Notably, this latter value is lower

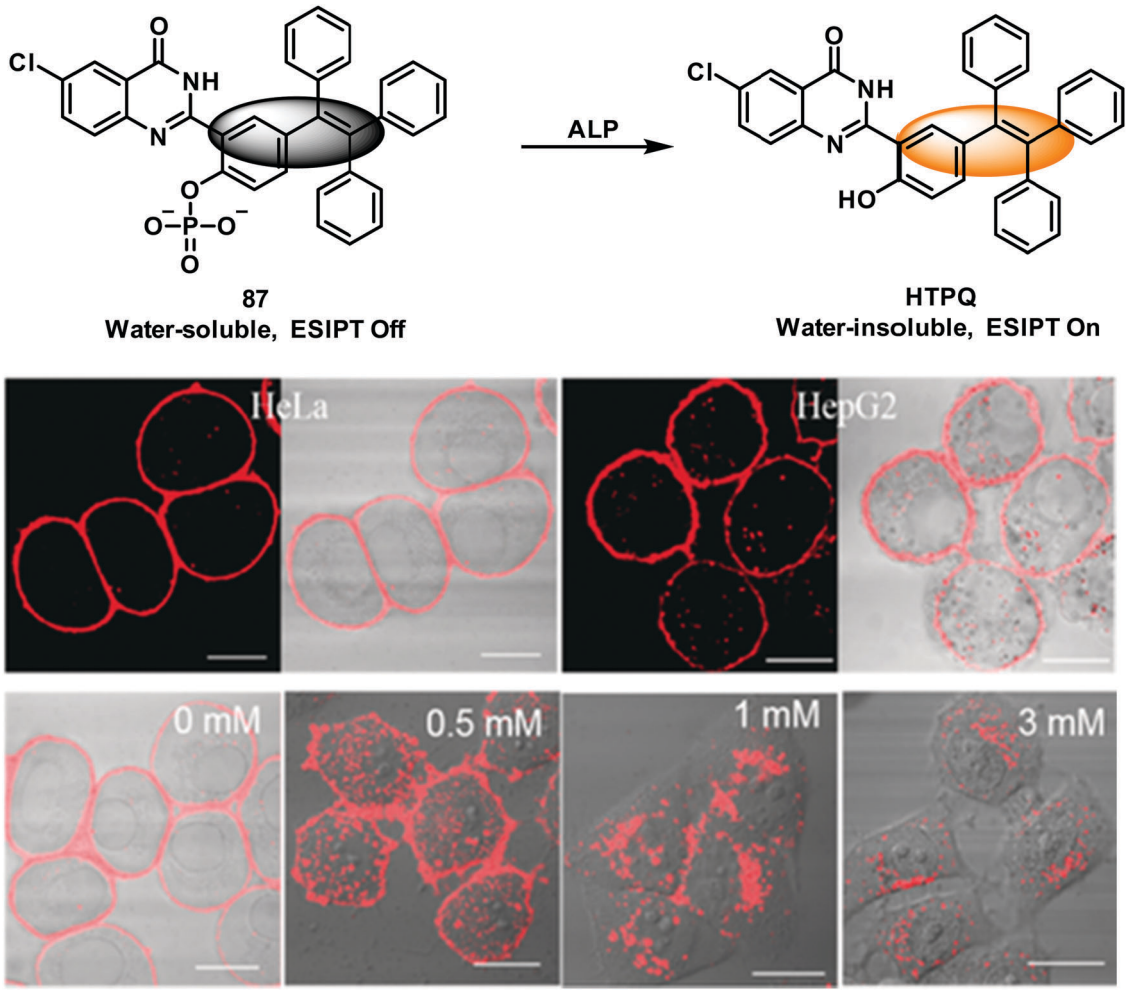

Scheme 76 An AIE + ESIPT fluorescent probe **87** developed to allow the detection of ALP. This system precipitates and localises within cells upon hydrolysis. Measurement conditions: TBS (10 mM, pH = 8.0). Adapted with permission from (*Angew. Chem., Int. Ed.*, 2017, **56**, 11788–11792). Copyright (2017) John Wiley and Sons.

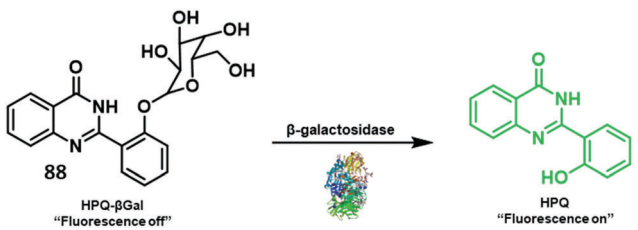

Scheme 77 An AIE + ESIPT fluorescent probe **88** that allows for the monitoring of β-galactosidase activity in live cells. Measurement conditions: PBS buffer (5 mM, pH = 7.3). Adapted with permission from (*Dyes Pigm.*, 2018, **156**, 100–107). Copyright (2018) Elsevier.

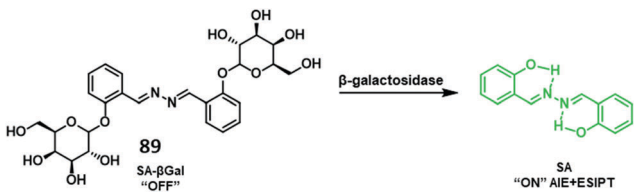

Scheme 78 A salicylaldehyde azine AIE + ESIPT probe **89** developed to allow for the monitoring of β-galactosidase activity in C6/LacZ cells. Measurement conditions: PBS buffer (10 mM, pH = 7.4).

than the WHO guideline for CN^- in drinking water (1.9 μM). Finally, test papers were prepared based on **93** that enabled the practical detection of CN^-.[225]

Attachment of an electron acceptor to an ESIPT fluorophore can afford near infrared (NIR) probes that can be used to carry out ratiometric sensing at lower emission energies. Probes with longer excitation/emission wavelengths minimise background auto-fluorescence from proteins and photodamage to biological samples. They also permit far greater tissue penetration, a feature that is useful in the *in vivo* imaging of tissues.

Zhao and co-workers reported an ESIPT + FRET based fluorescent probe **94** for the endogenous detection of bisulfite (HSO_3^-) in liver cancer cells. This system incorporates an ESIPT flavone fluorophore conjugated to a hemicyanine moiety and displays a high FRET efficiency (Fig. 10). Addition of HSO_3^-/SO_3^{2-} results in a decrease in fluorescence emission at 590 nm

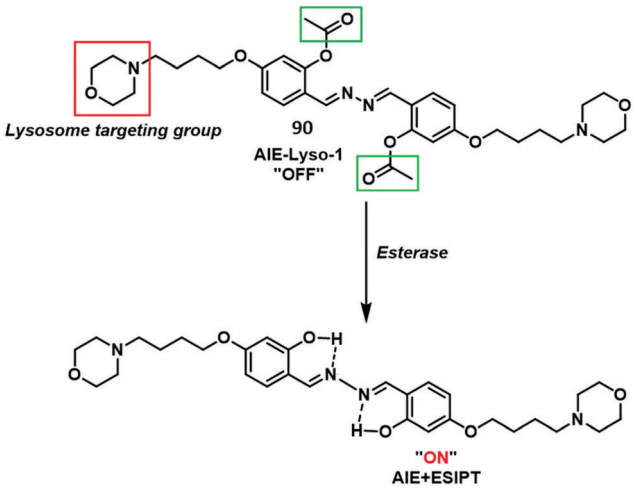

Scheme 79 An AIE + ESIPT probe **90** that allows for the monitoring of lysosomal esterase activity in MCF-7 cells. Measurement conditions: PBS buffer solution (pH = 7.4). Reproduced with permission from (*J. Mater. Chem. B*, 2014, **2**, 3438–3442). Copyright (2014) the Royal Society of Chemistry.

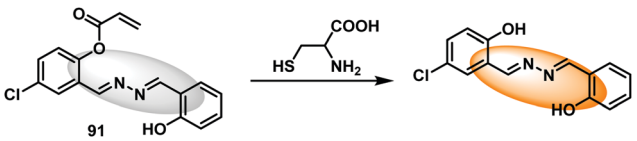

Scheme 80 An AIE + ESIPT-based fluorescent probe **91** for the detection of cysteine. Measurement conditions: PBS/DMSO (7 : 3) – pH = 7.4.

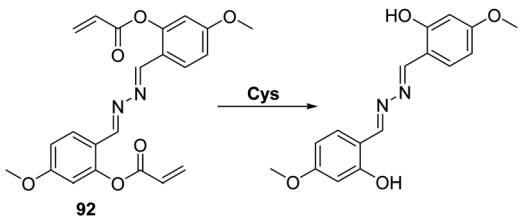

Scheme 81 A *p*-methoxy-salicylaldehyde azine-derived fluorescent based probe **92** that combines AIE + ESIPT mechanisms. It has been used to detect Cys in HeLa cells. Measurement conditions: PBS buffer (10 mM, pH = 7.4, 1% DMSO).

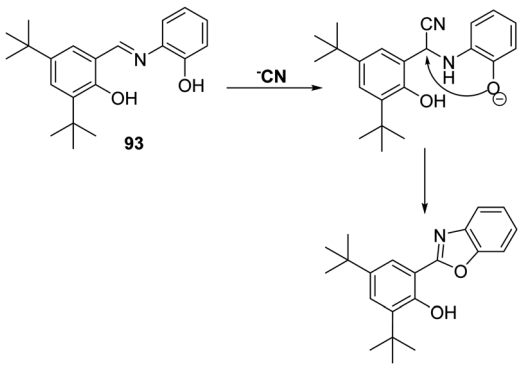

Scheme 82 Schiff-base fluorescent probe **93**. This system undergoes a cyanide anion-induced oxidative cyclisation to form an active ESIPT fluorophore, HBO. Measurement conditions: H_2O containing CTAB.

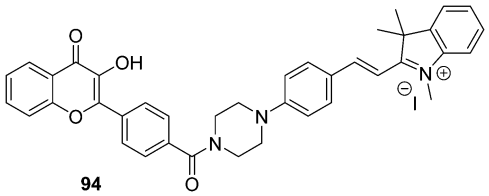

Fig. 10 A FRET + ESIPT-based fluorescent probe **94** for the detection of bisulfite in HepG2 cells. Measurement conditions: PBS/DMF (7.5 : 2.5) – pH = 7.4.

and a concomitant increase in the emission intensity at 530 nm. This is ascribed to the nucleophilic attack of SO_3^{2-} at the alkene bond of the hemicyanine moiety, resulting in emission from the keto form of the flavone being turned on. Probe **94** was shown to have good sensitivity (LOD = 16 nM) and to produce a large ratiometric change in the fluorescence intensity (I_{530}/I_{590}) upon exposure to HSO_3^-/SO_3^{2-} over a 1.5–22.5 μM concentration range. This allowed it to be used to image endogenous levels in HepG2 cells.[226]

Feng *et al.* reported a long-wavelength HBT–hemicyanine hybrid, probe **95**. This system combines intramolecular charge transfer (ICT) and ESIPT effects and was found to give rise to a rapid colorimetric and ratiometric fluorescence response upon exposure to the bisulfite anion (Scheme 83). Conjugate addition of HSO_3^- to the alkene functionality in **95** eliminates the ICT pathway, resulting in only the ESIPT emission of the HBT being observed. Probe **95** was shown to detect HSO_3^- with good sensitivity in aqueous solution. A linear response was seen over a 0–25 μM concentration range, with a detection limit of 56 nM being determined. This probe could be used to detect exogenous HSO_3^- in food samples and HeLa cells.[227]

Pang *et al.* developed a near-infrared (NIR) lysosomal fluorescent probe **96** that could be used to monitor pH levels (Scheme 84).[228]

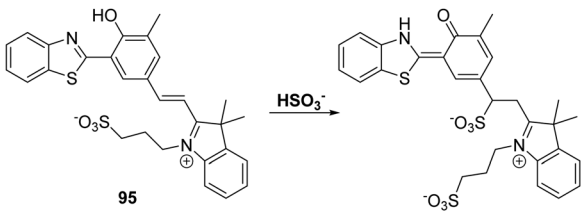

Scheme 83 A combined ICT + ESIPT fluorescent probe **95** for the detection of HSO_3^-. Measurement conditions: PBS/EtOH (6 : 4) – pH = 7.4.

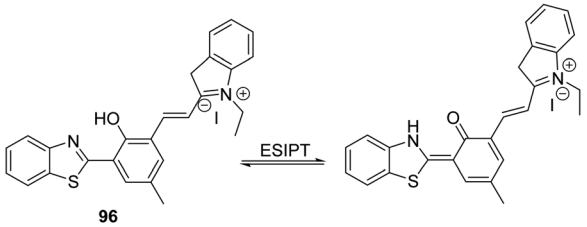

Scheme 84 A NIR-lysosomal targeting ESIPT + FRET probe **96** for the imaging of lysosomes in normal human lung fibroblast cells. Measurement conditions: H_2O at various pH.

This ESIPT probe exhibits a large Stokes shift 234 nm with a NIR-emission (tautomer = 700 nm). The phenolic proton is proposed to act as a switch and to provide a strong fluorescence emission at pH 5 that could be used to selectively visualise lysosome organelles.

Conclusion

Excited State Intramolecular Proton Transfer (ESIPT) is a unique four-level photochemical process that relies on extremely fast enol to keto phototautomerization ($k_{ESIPT} > 10^{12}$ s^{-1}) pathways to enable fluorescence based detection of reactive analytes. As a result of this rapid photochemical process, ESIPT fluorophores exhibit a number of particularly attractive attributes that have been used in the design of fluorescent probes. ESIPT-based probes have been designed to enable ratiometric detection of a specific analyte. This is a key attribute that provides direct information on the concentration of the analyte in question without the need for calibration. Moreover, the ESIPT emission is readily influenced by the environment. As a consequence, it is often found that the presence of polar and hydrogen bond donating solvents results in an inhibition of the ESIPT process with no keto (K*) emission being observed. This property could be viewed as a disadvantage. However, this property has been used to help image a range of biomacromolecules. A specific example includes the development of ESIPT-fluorophores functionalised with the lysosome-directing morpholine group by Pang and co-workers as discussed above. In an aqueous biological environment, the probes were non-fluorescent. Once they entered the hydrophobic pocket of lysosomes a large fluorescence increase was observed. Co-localisation studies confirmed that the probes were selective for the visualisation of lysosomes and effective as 'wash-free' stains thus making them suitable imaging agents for the real time monitoring.

A particularly interesting and exciting development has been the combination of ESIPT with other fluorescence mechanisms. The systems produced as the result of this intellectual and chemical linking generally combine the favourable attributes of both mechanisms and override many of the limitations of ESIPT. Aggregate induced emission (AIE), where systems are weakly fluorescent in solution but highly fluorescent when aggregated, has emerged as a promising complement to ESIPT. Specifically, the combination of AIE and ESIPT can be used to overcome the environmentally sensitive nature of the ESIPT process, since the formation of aggregates favours the sensitive nature of the ESIPT emission. Similarly, the attachment of an additional fluorophore to an ESIPT fluorophore (ESIPT and FRET) enables the development of longer wavelength/near infrared (NIR) probes that show promise for the detection of biologically relevant analytes *in vivo*. Lastly, the use of photoinduced electron transfer (PET)-based fluorescent probes can produce systems that display significant changes in the fluorescence intensity ('off to on' or 'on to off') in the presence of a target analyte with the emission wavelength remaining unchanged. This can give rise to amplified sensitivity and selectivity.

Overall, ESIPT is emerging an important sensing mechanism for the detection of biologically and/or environmentally important species. In this review, we have selected representative examples up to and including work published by August 2018. While not fully comprehensive in its coverage, an effort has been made to be as thorough as possible while focusing on examples that we hope will allow the reader to appreciate the unique aspects of ESIPT and how it can be used for the development of fluorescence-based probes. We believe that ESIPT fluorophores will continue to provide an important foundation on which to build. We further predict that its use in combination with other fluorescence mechanisms will allow new probes to be constructed that overcome the limitations of many current detection methods while allowing for the development of an ever-increasing number of practical fluorescence based sensors and imaging agents.[229] It is our hope that this review will inspire the readers to take up the challenge of these new, not-yet-conceived probes.

''There's Nature and she's going to come out the way She is. So therefore when we go to investigate we shouldn't predecide what it is we're looking for only to find out more about it. Now you ask: ''Why do you try to find out more about it?'' If you began your investigation to get an answer to some deep philosophical question, you may be wrong. It may be that you can't get an answer to that particular question just by finding out more about the character of Nature. But that's not my interest in science; my interest in science is to simply find out about the world and the more I find out the better it is...'' Richard P. Feynman (1918–1988)

Abbreviations

3-HF	3-Hydroxyflavone
α	Alpha
β	Beta
β-Gal	Beta-galactosidase
δ	Delta, chemical shift
μM	Micromolar
ACN	Acetonitrile
Ag^+	Silver ion
AIE	Aggregation induced emission
Al^{3+}	Aluminium ion
ALP	Alkaline phosphatase
AMP	Adenosine monophosphate
Angeli's salt ($Na_2N_2O_3$)	Sodium trioxodinitrate
Ar	Aryl
Ba^{2+}	Barium ion
BBB	Blood brain barrier
Br	Bromine
Ca^{2+}	Calcium ion
Cd^{2+}	Cadmium ion
CD_3CN	Deuterated acetonitrile
CE	Human carboxylesterase
CE1	Human carboxylesterase 1
CE2	Human carboxylesterase 2

CH_3COO^-	Acetate ion
Cl^-	Chloride anion
ClO^-	Hypochlorite anion
CN^-	Cyanide anion
Co^{2+}	Cobalt ion
$COCl_2$	Phosgene
Cr	Chromium
Cr^{3+}	Chromium ion
CTAB	Cetyl trimethylammonium bromide
$Cu^{+/2+}$	Copper ion
Cys	Cysteine
DEA NONOate	1,1-Diethyl-2-hydroxy-2-nitroso-hydrazine
DLS	Dynamic light scattering
DMF	Dimethylformamide
DMN	Diaminomaleonitrile
DMSO	Dimethylsulfoxide
DNA	Deoxyribose nucleic acid
DNBS	Dinitrobenzenesulfonyl
DPA	Dipicolylamine
DPBS	Dulbecco's phosphate buffer saline
dsDNA	Double stranded DNA
E	Enol
Er^{3+}	Erbium ion
ESIPT	Excited state intramolecular proton transfer
Et	Ethyl
EtOH	Ethanol
F^-	Fluoride ion
$Fe^{2+/3+}$	Iron ion
FIS	Fisetin
FRET	Förster resonance energy transfer
Gd^{2+}	Gadolinium ion
GMP	Guanosine monophosphate
GSH	Glutathione
h	Hours
H^+	Proton
HBI	2-(2′-Hydroxyphenyl)benzimidazole
HBO	2-(2-Hydroxyphenyl)-benzoxazole
HBT	2-(2-Hydroxyphenyl)-benzothiazole
HCys	Homocysteine
HEPES	4-(2-Hydroxyethyl)-1-piperazine-ethanesulfonic acid
Hg^{2+}	Mercury ion
HIV	Human immunodefiency virus
HMBT	2-(2′-Hydroxy-3′-methoxyphenyl)-benzothiazole
hMSCs	Human mesenchymal stem cells
HNO	Nitroxyl ion
HO^-	Hydroxyl anion
H_2O	Water
H_2O_2	Hydrogen peroxide
H_2O_3	Dihydrogen trioxide
HOCl	Hypochlorite
$H_2PO_4^-$	Dihydrogen phosphate
HPQ	Hydroxyphenylquinazoline
H_2S	Hydrogen Sulphide
HSO_3^-	Bisulfite ion
HTL	Homocysteine thiolactone
I	Intensity
ICT	Intramolecular charge transfer
K	Keto
K^+	Potassium ion
KNO_3	Potassium nitrate
KO_2	Potassium superoxide
LAP	Leucine aminopeptidase
LOD	Limit of detection
Me	Methyl
MeOH	Methanol
Met	Methionine
MetRS	Methionyl t-RNA synthetase
Mg^{2+}	Magnesium ion
Min	Minutes
mL	Millilitres
mM	Millimolar
Mn^{2+}	Manganese ion
MPO	Myeloperoxidase
MTT	3-(4,5-Dimethylthiazol-2-yl)-2,5-diphenyltetrazolium bromide
mU	MilliUnits
Na^+	Sodium ion
NaCl	Sodium chloride
NADH	Nicotinamide adenine dinucleotide
$Na_2N_2O_3$	Angeli's salt
NC	Nucleocapsid protein
NCL	Native chemical ligation
Nd^{3+}	Neodymium ion
NEt_3	Triethylamine
N_2H_4	Hydrazine
Ni^{2+}	Nickel ion
NIR	Near-infrared
nm	Nanometres
nM	Nanomolar
NMR	Nuclear magnetic resonance
NO	Nitric oxide
NOS	Nitric oxide synthase
NTR	Nitroreductase
$^1O_2$	Singlet Oxygen
O_2	Oxygen
O_2^-	Superoxide
O_3	Ozone
OAc	Acetate
ODN	Oligonucleotides
OH	Hydroxyl radical
OMe	Methoxy
$ONOO^-$	Peroxynitrite
Pb^{2+}	Lead ion
PBS	Phosphate buffer saline
PCR	Polymerase chain reaction
Pd	Palladium
Pd^{2+}	Palladium ion
PET	Photoinduced electron transfer

Ph	Phenyl
ppm	Parts per million
ppb	Parts per billion
PTP	Protein tyrosine phosphatase
PPi	Pyrophosphate
R	Unspecified generic group
R-B(OH)$_2$	Boronic acids
RNS	Reactive nitrogen species
ROS	Reactive oxygen species
RP-HPLC	Reverse-phase high-performance liquid chromatography
RPT	Reverse proton transfer
S	Sulfur
S^{2-}	Sulfide
S_NAr	Nucleophilic aromatic substitution
SO_2	Sulfur dioxide
SO_3^{2-}	Sulfite ion
ssDNA	Single stranded DNA
Tat	Trans-activator of transcription
TBDMS	*tert*-Butyldimethylsilyl
TBDPS	*tert*-Butyldiphenyllsilyl ether
TBS	Tris-buffered saline
THF	Tetrahydrofuran
TLC	Thin layer chromatography
TPE	Tetraphenylethene
UV	Ultraviolet
WHO	World Health Organisation
Yb^{3+}	Ytterbium ion
Zn^{2+}	Zinc ion

Conflicts of interest

There are no conflicts to declare.

Acknowledgements

ACS thanks the EPSRC for a studentship. LW wishes to thank China Scholarship Council and the University of Bath for supporting his PhD work in the UK. ACS, LW, SDB and TDJ would like to thank the EPSRC and the University of Bath for funding. TDJ wishes to thank the Royal Society for a Wolfson Research Merit Award and Sophia University for a visiting professorship. HHH, XPH, HT thank the Natural Science Foundation of China (No. 21788102, 21722801 and 21572058), the Program of Introducing Talents of Discipline to Universities (B16017) and the Shanghai Rising-Star Program (16QA1401400) (XPH) for generous financial support. BZT thanks the National Natural Science Foundation of China (21788102) and the Innovation and Technology Commission of Hong Kong (ITC-CNERC14SC01) for financial support. JY acknowledges a grant from the National Creative Research Initiative programs of the National Research Foundation of Korea (NRF) funded by the Korean government (MSIP) (No. 2012R1A3A2048814). JLS thanks the National Institutes of Health (RGM103790A) and the Robert A. Welch Foundation (F-0018) for support. We would like to thank Lauren Gwynne and Bethany L. Patenall for proof reading the manuscript.

References

1 D. Wu, A. C. Sedgwick, T. Gunnlaugsson, E. U. Akkaya, J. Yoon and T. D. James, *Chem. Soc. Rev.*, 2017, **46**, 7105–7123.
2 (*a*) Y. N. Hong, J. W. Y. Lam and B. Z. Tang, *Chem. Soc. Rev.*, 2011, **40**, 5361–5388; (*b*) W. Sun, S. Guo, C. Hu, J. Fan and X. Peng, *Chem. Rev.*, 2016, **116**(14), 7768–7817.
3 A. C. Sedgwick, H. H. Han, J. E. Gardiner, S. D. Bull, X. P. He and T. D. James, *Chem. Sci.*, 2018, **9**, 3672–3676.
4 A. C. Sedgwick, H. H. Han, J. E. Gardiner, S. D. Bull, X. P. He and T. D. James, *Chem. Commun.*, 2017, **53**, 12822–12825.
5 A. C. Sedgwick, A. Hayden, B. Hill, S. D. Bull, R. B. P. Elmes and T. D. James, *Front. Chem. Sci. Eng.*, 2018, **12**, 311–314.
6 A. C. Sedgwick, J. E. Gardiner, G. Kim, M. Yevglevskis, M. D. Lloyd, A. T. A. Jenkins, S. D. Bull, J. Yoon and T. D. James, *Chem. Commun.*, 2018, **54**, 4786–4789.
7 A. Weller, *Naturwissenschaften*, 1955, **42**, 175–176.
8 J. Z. Zhao, S. M. Ji, Y. H. Chen, H. M. Guo and P. Yang, *Phys. Chem. Chem. Phys.*, 2012, **14**, 8803–8817.
9 V. S. Padalkar and S. Seki, *Chem. Soc. Rev.*, 2016, **45**, 169–202.
10 J. E. Kwon and S. Y. Park, *Adv. Mater.*, 2011, **23**, 3615–3642.
11 J. S. Wu, W. M. Liu, J. C. Ge, H. Y. Zhang and P. F. Wang, *Chem. Soc. Rev.*, 2011, **40**, 3483–3495.
12 P. T. Chou, Y. C. Chen, W. S. Yu, Y. H. Chou, C. Y. Wei and Y. M. Cheng, *J. Phys. Chem. A*, 2001, **105**, 1731–1740.
13 M. T. Ignasiak, C. Houee-Levin, G. Kciuk, B. Marciniak and T. Pedzinski, *ChemPhysChem*, 2015, **16**, 628–633.
14 D. Ghosh, S. Batuta, S. Das, N. A. Begum and D. Mandal, *J. Phys. Chem. B*, 2015, **119**, 5650–5661.
15 S. J. Schmidtke, D. F. Underwood and D. A. Blank, *J. Am. Chem. Soc.*, 2004, **126**, 8620–8621.
16 M. J. Paterson, M. A. Robb, L. Blancafort and A. D. DeBellis, *J. Am. Chem. Soc.*, 2004, **126**, 2912–2922.
17 E. Hadjoudis and I. M. Mavridis, *Chem. Soc. Rev.*, 2004, **33**, 579–588.
18 Y. Nakane, T. Takeda, N. Hoshino, K. Sakai and T. Akutagawa, *J. Phys. Chem. A*, 2015, **119**, 6223–6231.
19 N. Sarkar, K. Das, S. Das, A. Datta, D. Nath and K. Bhattacharyya, *J. Phys. Chem.*, 1995, **99**, 17711–17714.
20 K. Das, N. Sarkar, A. K. Ghosh, D. Majumdar, D. N. Nath and K. Bhattacharyya, *J. Phys. Chem.*, 1994, **98**, 9126–9132.
21 M. H. Lee, J. S. Kim and J. L. Sessler, *Chem. Soc. Rev.*, 2015, **44**, 4185–4191.
22 W. Aoi and Y. Marunaka, *BioMed Res. Int.*, 2014, 598986, DOI: 10.1155/2014/598986.
23 P. Swietach, R. D. Vaughan-Jones, A. L. Harris and A. Hulikova, *Philos. Trans. R. Soc., B*, 2014, **369**, DOI: 10.1098/rstb.2013.0099.
24 V. S. Patil, V. S. Padalkar, K. R. Phatangare, V. D. Gupta, P. G. Umape and N. Sekar, *J. Phys. Chem. A*, 2012, **116**, 536–545.
25 V. S. Patil, V. S. Padalkar, A. B. Tathe and N. Sekar, *Dyes Pigm.*, 2013, **98**, 507–517.

26 Y. P. Chan, L. Fan, Q. H. You, W. H. Chan, A. W. M. Lee and S. M. Shuang, *Tetrahedron*, 2013, **69**, 5874–5879.
27 D. J. Colacurcio and R. A. Nixon, *Ageing Res. Rev.*, 2016, **32**, 75–88.
28 A. Kogot-Levin, M. Zeigler, A. Ornoy and G. Bach, *Pediatr. Res.*, 2009, **65**, 686–690.
29 B. Winchester, A. Vellodi and E. Young, *Biochem. Soc. Trans.*, 2000, **28**, 150–154.
30 Q. Q. Wang, L. Y. Zhou, L. P. Qiu, D. Q. Lu, Y. X. Wu and X. B. Zhang, *Analyst*, 2015, **140**, 5563–5569.
31 Y. Kato, S. Ozawa, C. Miyamoto, Y. Maehata, A. Suzuki, T. Maeda and Y. Baba, *Cancer Cell Int.*, 2013, **13**, DOI: 10.1186/1475-2867-13-89.
32 S. Barman, S. K. Mukhopadhyay, M. Gangopadhyay, S. Biswas, S. Dey and N. D. P. Singh, *J. Mater. Chem. B*, 2015, **3**, 3490–3497.
33 H. Rubin, *BioEssays*, 2005, **27**, 311–320.
34 M. Liu, X. Yu, M. Li, N. X. Liao, A. Y. Bi, Y. P. Jiang, S. Liu, Z. C. Gong and W. B. Zeng, *RSC Adv.*, 2018, **8**, 12573–12587.
35 N. Singh, N. Kaur, R. C. Mulrooney and J. F. Callan, *Tetrahedron Lett.*, 2008, **49**, 6690–6692.
36 J. M. Berg and Y. G. Shi, *Science*, 1996, **271**, 1081–1085.
37 S. L. Sensi, P. Paoletti, A. I. Bush and I. Sekler, *Nat. Rev. Neurosci.*, 2009, **10**, 780–791.
38 S. Alam and S. L. Kelleher, *Nutrients*, 2012, **4**, 875–903.
39 C. T. Chasapis, A. C. Loutsidou, C. A. Spiliopoulou and M. E. Stefanidou, *Arch. Toxicol.*, 2012, **86**, 521–534.
40 S. K. Ghosh, P. Kim, X. A. Zhang, S. H. Yun, A. Moore, S. J. Lippard and Z. Medarova, *Cancer Res.*, 2010, **70**, 6119–6127.
41 Y. Q. Xu and Y. Pang, *Chem. Commun.*, 2010, **46**, 4070–4072.
42 L. J. Tang, M. J. Cai, P. Zhou, J. Zhao, K. L. Zhong, S. H. Hou and Y. J. Bian, *RSC Adv.*, 2013, **3**, 16802–16809.
43 F. J. Huo, Q. Wu, J. Kang, Y. B. Zhang and C. X. Yin, *Sens. Actuators, B*, 2018, **262**, 263–269.
44 M. An, B. Y. Kim, H. Seo, A. Helal and H. S. Kim, *Spectrochim. Acta, Part A*, 2016, **169**, 87–94.
45 R. A. Festa and D. J. Thiele, *Curr. Biol.*, 2011, **21**, R877–R883.
46 C. Cheignon, M. Tomas, D. Bonnefont-Rousselot, P. Faller, C. Hureau and F. Collin, *Redox Biol.*, 2018, **14**, 450–464.
47 D. J. Waggoner, T. B. Bartnikas and J. D. Gitlin, *Neurobiol. Dis.*, 1999, **6**, 221–230.
48 D. Maity, V. Kumar and T. Govindaraju, *Org. Lett.*, 2012, **14**, 6008–6011.
49 C. Y. Yang, Y. Chen, K. Wu, T. Wei, J. L. Wang, S. S. Zhang and Y. F. Han, *Anal. Methods*, 2015, **7**, 3327–3330.
50 H. Wang, D. L. Shi, J. Li, H. Y. Tang and Y. Guo, *Sens. Actuators, B*, 2018, **256**, 600–608.
51 Y. M. Shen, X. Y. Zhang, C. X. Zhang, Y. Y. Zhang, J. L. Jin and H. T. Li, *Spectrochim. Acta, Part A*, 2018, **191**, 427–434.
52 S. Okamoto and L. D. Eltis, *Metallomics*, 2011, **3**, 963–970.
53 G. Papanikolaou and K. Pantopoulos, *Toxicol. Appl. Pharmacol.*, 2005, **202**, 199–211.
54 T. A. Rouault, *Nat. Chem. Biol.*, 2006, **2**, 406–414.
55 I. De Domenico, D. M. Ward and J. Kaplan, *Nat. Rev. Mol. Cell Biol.*, 2008, **9**, 72–81.
56 B. Kuzu, M. Tan, Z. Ekmekci and N. Menges, *J. Lumin.*, 2017, **192**, 1096–1103.
57 J. F. Wang, Y. B. Li, N. G. Patel, G. Zhang, D. M. Zhou and Y. Pang, *Chem. Commun.*, 2014, **50**, 12258–12261.
58 P. B. Tchounwou, W. K. Ayensu, N. Ninashvili and D. Sutton, *Environ. Toxicol.*, 2003, **18**, 149–175.
59 M. Harada, *Crit. Rev. Toxicol.*, 1995, **25**, 1–24.
60 M. Santra, B. Roy and K. H. Ahn, *Org. Lett.*, 2011, **13**, 3422–3425.
61 B. Gu, L. Y. Huang, N. X. Mi, P. Yin, Y. Y. Zhang, X. M. Tu, X. B. Luo, S. L. Luo and S. Z. Yao, *Analyst*, 2015, **140**, 2778–2784.
62 J. Kielhorn, C. Melber, D. Keller and I. Mangelsdorf, *Int. J. Hyg. Environ. Health*, 2002, **205**, 417–432.
63 J. C. Wataha and C. T. Hanks, *J. Oral Rehabil.*, 1996, **23**, 309–320.
64 B. Liu, H. Wang, T. S. Wang, Y. Y. Bao, F. F. Du, J. Tian, Q. B. A. Li and R. K. Bai, *Chem. Commun.*, 2012, **48**, 2867–2869.
65 T. T. Chen, T. W. Wei, Z. J. Zhang, Y. H. Chen, J. Qiang, F. Wang and X. Q. Chen, *Dyes Pigm.*, 2017, **140**, 392–398.
66 T. Gao, P. F. Xu, M. H. Liu, A. Y. Bi, P. Z. Hu, B. Ye, W. Wang and W. B. Zeng, *Chem. – Asian J.*, 2015, **10**, 1142–1145.
67 W. F. Luo, J. Li and W. S. Liu, *Org. Biomol. Chem.*, 2017, **15**, 5846–5850.
68 R. A. Terkeltaub, *Am. J. Physiol.: Cell Physiol.*, 2001, **281**, C1–C11.
69 W. H. Chen, Y. Xing and Y. Pang, *Org. Lett.*, 2011, **13**, 1362–1365.
70 M. D. Brand, C. Affourtit, T. C. Esteves, K. Green, A. J. Lambert, S. Miwa, J. L. Pakay and N. Parker, *Free Radical Biol. Med.*, 2004, **37**, 755–767.
71 M. Hayyan, M. A. Hashim and I. M. AlNashef, *Chem. Rev.*, 2016, **116**, 3029–3085.
72 K. Niizuma, H. Yoshioka, H. Chen, G. S. Kim, J. E. Jung, M. Katsu, N. Okami and P. H. Chan, *Biochim. Biophys. Acta, Mol. Basis Dis.*, 2010, **1802**, 92–99.
73 G. W. Kim, T. Kondo, N. Noshita and P. H. Chan, *Stroke*, 2002, **33**, 809–815.
74 D. P. Murale, H. Kim, W. S. Choi and D. G. Churchill, *Org. Lett.*, 2013, **15**, 3946–3949.
75 P. Pacher, J. S. Beckman and L. Liaudet, *Physiol. Rev.*, 2007, **87**, 315–424.
76 J. S. Beckman and W. H. Koppenol, *Am. J. Physiol.*, 1996, **271**, C1424–C1437.
77 P. Ascenzi, A. di Masi, C. Sciorati and E. Clementi, *BioFactors*, 2010, **36**, 264–273.
78 H. Ischiropoulos and J. S. Beckman, *J. Clin. Invest.*, 2003, **111**, 163–169.
79 P. Sarchielli, F. Galli, A. Floridi and V. Gallai, *Amino Acids*, 2003, **25**, 427–436.
80 D. A. Wink, Y. Vodovotz, J. Laval, F. Laval, M. W. Dewhirst and J. B. Mitchell, *Carcinogenesis*, 1998, **19**, 711–721.
81 X. Li, R.-R. Tao, L.-J. Hong, J. Cheng, Q. Jiang, Y.-M. Lu, M.-H. Liao, W.-F. Ye, N.-N. Lu, F. Han, Y.-Z. Hu and Y.-H. Hu, *J. Am. Chem. Soc.*, 2015, **137**, 12296–12303.

82 A. Sikora, J. Zielonka, M. Lopez, J. Joseph and B. Kalyanaraman, *Free Radical Biol. Med.*, 2009, **47**, 1401–1407.
83 A. C. Sedgwick, X. L. Sun, G. Kim, J. Yoon, S. D. Bull and T. D. James, *Chem. Commun.*, 2016, **52**, 12350–12352.
84 L. Wu, Y. Wang, M. Weber, L. Liu, A. C. Sedgwick, S. D. Bull, C. Huang and T. D. James, *Chem. Commun.*, 2018, **54**, 9953–9956.
85 J. A. Bernstein, N. Alexis, C. Barnes, I. L. Bernstein, A. Nel, D. Peden, D. Diaz-Sanchez, S. M. Tarlo and P. B. Williams, *J. Allergy Clin. Immunol.*, 2004, **114**, 1116–1123.
86 H. Traboulsi, N. Guerrina, M. Iu, D. Maysinger, P. Ariya and C. J. Baglole, *Int. J. Mol. Sci.*, 2017, **18**, 243, DOI: 10.3390/ijms18020243.
87 T. M. Chen, J. Gokhale, S. Shofer and W. G. Kuschner, *Am. J. Med. Sci.*, 2007, **333**, 249–256.
88 X. B. Wang, J. B. Du and H. Cui, *Life Sci.*, 2014, **98**, 63–67.
89 S. Chen, P. Hou, J. X. Wang and X. Z. Song, *RSC Adv.*, 2012, **2**, 10869–10873.
90 A. Strzepa, K. A. Pritchard and B. N. Dittel, *Cell. Immunol.*, 2017, **317**, 1–8.
91 M. J. Davies, *J. Clin. Biochem. Nutr.*, 2011, **48**, 8–19.
92 S. J. Klebanoff, *J. Leukocyte Biol.*, 2005, **77**, 598–625.
93 B. S. van der Veen, M. P. J. de Winther and P. Heeringa, *Antioxid. Redox Signaling*, 2009, **11**, 2899–2937.
94 L. Chen, S. J. Park, D. Wu, H. M. Kim and J. Yoon, *Dyes Pigm.*, 2018, **158**, 526–532.
95 A. Manna and S. Goswami, *New J. Chem.*, 2015, **39**, 4424–4429.
96 C. C. Chang, F. Wang, J. Qiang, Z. J. Zhang, Y. H. Chen, W. Zhang, Y. Wang and X. Q. Chen, *Sens. Actuators, B*, 2017, **243**, 22–28.
97 L. Wu, Q. Yang, L. Liu, A. C. Sedgwick, A. J. Cresswell, S. D. Bull, C. Huang and T. D. James, *Chem. Commun.*, 2018, **54**, 8522–8525.
98 J. L. Way, *Annu. Rev. Pharmacol. Toxicol.*, 1984, **24**, 451–481.
99 R. Koenig, *Science*, 2000, **287**, 1737–1738.
100 M. K. Bera, C. Chakraborty, P. K. Singh, C. Sahu, K. Sen, S. Maji, A. K. Das and S. Malik, *J. Mater. Chem. B*, 2014, **2**, 4733–4739.
101 S. Goswami, A. Manna, S. Paul, A. K. Das, K. Aich and P. K. Nandi, *Chem. Commun.*, 2013, **49**, 2912–2914.
102 A. Ghosh, K. Mukherjee, S. K. Ghosh and B. Saha, *Res. Chem. Intermed.*, 2013, **39**, 2881–2915.
103 R. Hu, J. A. Feng, D. H. Hu, S. Q. Wang, S. Y. Li, Y. Li and G. Q. Yang, *Angew. Chem., Int. Ed.*, 2010, **49**, 4915–4918.
104 (*a*) S. Goswami, A. K. Das, A. Manna, A. K. Maity, H. K. Fun, C. K. Quah and P. Saha, *Tetrahedron Lett.*, 2014, **55**, 2633–2638; (*b*) A. K. Mahapatra, S. Mondal, S. K. Manna, K. Maiti, R. Maji, S. Samim, D. Mandal, M. R. Uddin and S. Mandal, *Supramol. Chem.*, 2016, **28**, 693–706.
105 S. D. Liu, L. W. Zhang, P. P. Zhou, Y. Yang and W. S. Wu, *Sens. Actuators, B*, 2018, **255**, 401–407.
106 C. Saravanan, S. Easwaramoorthi, C. Y. Hsiow, K. Wang, M. Hayashi and L. Wang, *Org. Lett.*, 2014, **16**, 354–357.
107 Y. K. Wu, X. J. Peng, J. L. Fan, S. Gao, M. Z. Tian, J. Z. Zhao and S. Sun, *J. Org. Chem.*, 2007, **72**, 62–70.
108 H. Kimura, *Antioxid. Redox Signaling*, 2010, **12**, 1111–1123.
109 R. Wang, *Antioxid. Redox Signaling*, 2010, **12**, 1061–1064.
110 M. Wang, J. Zhu, Y. Pan, J. D. Dong, L. L. Zhang, X. R. Zhang and L. Zhang, *J. Neurosci. Res.*, 2015, **93**, 487–494.
111 R. Wang, *Physiol. Rev.*, 2012, **92**, 791–896.
112 Z. Xu, L. Xu, J. Zhou, Y. F. Xu, W. P. Zhu and X. H. Qian, *Chem. Commun.*, 2012, **48**, 10871–10873.
113 H. A. Henthorn and M. D. Pluth, *J. Am. Chem. Soc.*, 2015, **137**, 15330–15336.
114 V. S. Lin, A. R. Lippert and C. J. Chang, *Redox Biol.*, 2015, **554**, 63–80.
115 J. Y. Zhang and W. Guo, *Chem. Commun.*, 2014, **50**, 4214–4217.
116 (*a*) P. F. Xu, M. H. Liu, T. Gao, H. L. Zhang, Z. W. Li, X. Y. Huang and W. B. Zeng, *Tetrahedron Lett.*, 2015, **56**, 4007–4010; (*b*) P. Karmakar, S. Manna, S. S. Ali, U. N. Guria, R. Sarkar, P. Datta, D. Mandal and A. K. Mahapatra, *New J. Chem.*, 2018, **42**, 76–84; (*c*) K. Maiti, A. K. Mahapatra, A. Gangopadhyay, R. Maji, S. Mondal, S. S. Ali, S. Das, R. Sarkar, P. Data and D. Mandal, *ACS Omega*, 2017, **2**, 1583–1593.
117 G. S. Sharma, T. Kumar, T. A. Dar and L. R. Singh, *Biochim. Biophys. Acta*, 2015, **1850**, 2239–2245.
118 K. Karolczak and B. Olas, *Physiol. Res.*, 2009, **58**, 623–633.
119 P. Ganguly and S. F. Alam, *Nutr. J.*, 2015, **14**, DOI: 10.1186/1475-2891-14-6.
120 U. Hubner, I. Koch, U. Retzke and W. Herrmann, *Geburtshilfe Frauenheilkd.*, 2003, **63**, 990–998.
121 M. P. Mattson and T. B. Shea, *Trends Neurosci.*, 2003, **26**, 137–146.
122 L. J. Tang, J. Z. Shi, Z. L. Huang, X. M. Yan, Q. Zhang, K. L. Zhong, S. H. Hou and Y. J. Bian, *Tetrahedron Lett.*, 2016, **57**, 5227–5231.
123 N. Mohorko, A. Petelin, M. Jurdana, G. Biolo and Z. Jenko-Praznikar, *BioMed Res. Int.*, 2015, **2015**, 418681.
124 P. B. E. Woolsey, *J. Altern. Complement. Med.*, 2008, **14**, 1159–1164.
125 J. Lin, I. M. Lee, Y. Q. Song, N. R. Cook, J. Selhub, J. E. Manson, J. E. Buring and S. M. Zhang, *Cancer Res.*, 2010, **70**, 2397–2405.
126 L. J. Wang, P. Y. Lin, L. Yu, Y. C. Huang, C. C. Wu, S. T. Hsu, C. C. Chen, C. Mian-Yoon, C. H. Lin and C. F. Hung, *Schizophr. Res.*, 2018, **192**, 391–397.
127 X. F. Wang and M. S. Cynader, *J. Neurosci.*, 2001, **21**, 3322–3331.
128 X. F. Yang, Y. X. Guo and R. M. Strongin, *Angew. Chem., Int. Ed.*, 2011, **50**, 10690–10693.
129 B. Liu, J. F. Wang, G. Zhang, R. K. Bai and Y. Pang, *ACS Appl. Mater. Interfaces*, 2014, **6**, 4402–4407.
130 Y. Liu, D. H. Yu, S. S. Ding, Q. Xiao, J. Guo and G. Q. Feng, *ACS Appl. Mater. Interfaces*, 2014, **6**, 17543–17550.
131 S. C. Lu, *Mol. Aspects Med.*, 2009, **30**, 42–59.
132 J. S. Armstrong, K. K. Steinauer, B. Hornung, J. M. Irish, P. Lecane, G. W. Birrell, D. M. Peehl and S. J. Knox, *Cell Death Differ.*, 2002, **9**, 252–263.
133 M. Nakamura, V. H. Thourani, R. S. Ronson, D. A. Velez, X. L. Ma, S. Katzmark, J. Robinson, L. S. Schmarkey,

Z. Q. Zhao, N. P. Wang, R. A. Guyton and J. Vinten-Johansen, *Circulation*, 2000, **102**, 332–338.
134 N. Ballatori, S. M. Krance, S. Notenboom, S. J. Shi, K. Tieu and C. L. Hammond, *Biol. Chem.*, 2009, **390**, 191–214.
135 G. Y. Wu, Y. Z. Fang, S. Yang, J. R. Lupton and N. D. Turner, *J. Nutr.*, 2004, **134**, 489–492.
136 C. B. Pocernich and D. A. Butterfield, *Biochim. Biophys. Acta, Mol. Basis Dis.*, 2012, **1822**, 625–630.
137 X. T. Ren, F. Wang, J. Lv, T. W. Wei, W. Zhang, Y. Wang and X. Q. Chen, *Dyes Pigm.*, 2016, **129**, 156–162.
138 J. L. Martindale and N. J. Holbrook, *J. Cell. Physiol.*, 2002, **192**, 1–15.
139 K. J. Barnham, C. L. Masters and A. I. Bush, *Nat. Rev. Drug Discovery*, 2004, **3**, 205–214.
140 T. Finkel and N. J. Holbrook, *Nature*, 2000, **408**, 239–247.
141 P. D. Ray, B. W. Huang and Y. Tsuji, *Cell. Signalling*, 2012, **24**, 981–990.
142 E. H. Sarsour, M. G. Kumar, L. Chaudhuri, A. L. Kalen and P. C. Goswami, *Antioxid. Redox Signaling*, 2009, **11**, 2985–3011.
143 E. W. Miller, A. E. Albers, A. Pralle, E. Y. Isacoff and C. J. Chang, *J. Am. Chem. Soc.*, 2005, **127**, 16652–16659.
144 X. J. Liu, H. H. Tian, L. Yang, Y. A. Su, M. Guo and X. Z. Song, *Sens. Actuators, B*, 2018, **255**, 1160–1165.
145 S. Biswas, J. Das, S. Barman, B. R. Pinninti, T. K. Maiti and N. D. P. Singh, *ACS Appl. Mater. Interfaces*, 2017, **9**, 28180–28184.
146 L. J. Tang, M. Y. Tian, H. B. Chen, X. M. Yan, K. L. Zhong and Y. J. Bian, *Dyes Pigm.*, 2018, **158**, 482–489.
147 C. K. Wang, J. Cheng, X. G. Liang, C. Tan, Q. Jiang, Y. Z. Hu, Y. M. Lu, K. Fukunaga, F. Han and X. Li, *Theranostics*, 2017, **7**, 3803–3813.
148 T. Malinski, *J. Alzheimer's Dis.*, 2007, **11**, 207–218.
149 U. Forstermann and W. C. Sessa, *Eur. Heart J.*, 2012, **33**, 829–837.
150 L. Chen, D. Wu and J. Yoon, *Sens. Actuators, B*, 2018, **259**, 347–353.
151 C. H. Switzer, W. Flores-Santana, D. Mancardi, S. Donzelli, D. Basudhar, L. A. Ridnour, K. M. Miranda, J. M. Fukuto, N. Paolocci and D. A. Wink, *Biochim. Biophys. Acta*, 2009, **1787**, 835–840.
152 T. Y. Dai, Y. Tian, C. G. Tocchetti, T. Katori, A. M. Murphy, D. A. Kass, N. Paolocci and W. D. Gao, *J. Physiol.*, 2007, **580**, 951–960.
153 M. Feelisch, *Proc. Natl. Acad. Sci. U. S. A.*, 2003, **100**, 4978–4980.
154 M. E. Shoman and O. M. Aly, *Curr. Top. Med. Chem.*, 2016, **16**, 2464–2470.
155 V. Shafirovich and S. V. Lymar, *Proc. Natl. Acad. Sci. U. S. A.*, 2002, **99**, 7340–7345.
156 J. A. Reisz, E. B. Klorig, M. W. Wright and S. B. King, *Org. Lett.*, 2009, **11**, 2719–2721.
157 H. M. Lv, Y. Chen, J. Lei, C. T. Au and S. F. Yin, *Anal. Methods*, 2015, **7**, 3883–3887.
158 X. D. Jin, X. L. Sun, X. Y. Di, X. Q. Zhang, H. Huang, J. N. Liu, P. W. Ji and H. J. Zhu, *Sens. Actuators, B*, 2016, **224**, 209–216.
159 B. Brunekreef and S. T. Holgate, *Lancet*, 2002, **360**, 1233–1242.
160 R. A. Lerner and A. Eschenmoser, *Proc. Natl. Acad. Sci. U. S. A.*, 2003, **100**, 3013–3015.
161 L. Yu, Y. Y. Li, H. Yu, K. Zhang, X. W. Wang, X. F. Chen, J. Yue, T. X. Huo, H. W. Ge, K. A. Alamry, H. M. Marwani and S. H. Wang, *Sens. Actuators, B*, 2018, **266**, 717–723.
162 U. Ragnarsson, *Chem. Soc. Rev.*, 2001, **30**, 205–213.
163 B. Toth, *In Vivo*, 2000, **14**, 299–319.
164 B. A. Aigner, U. Darsow, M. Grosber, J. Ring and S. G. Plotz, *Dermatology*, 2010, **221**, 300–302.
165 B. Ritz, Y. X. Zhao, A. Krishnadasan, N. Kennedy and H. Morgenstern, *Epidemiol.*, 2006, **17**, 154–161.
166 S. Garrod, M. E. Bollard, A. W. Nicholllst, S. C. Connor, J. Connelly, J. K. Nicholson and E. Holmes, *Chem. Res. Toxicol.*, 2005, **18**, 115–122.
167 S. D. Zelnick, D. R. Mattie and P. C. Stepaniak, *Aviat., Space Environ. Med.*, 2003, **74**, 1285–1291.
168 X. D. Jin, C. Z. Liu, X. M. Wang, H. Huang, X. Q. Zhang and H. J. Zhu, *Sens. Actuators, B*, 2015, **216**, 141–149.
169 Y. Wang, H. Xiang, R. Zhao and C. Huang, *Analyst*, 2018, **143**, 3900–3906.
170 D. Evison, D. Hinsley and P. Rice, *Br. Med. J.*, 2002, **324**, 332–335.
171 J. Borak and W. F. Diller, *J. Occup. Environ. Med.*, 2001, **43**, 110–119.
172 H. Babad and A. G. Zeiler, *Chem. Rev.*, 1973, **73**, 75–91.
173 L. Chen, D. Wu, J. M. Kim and J. Yoon, *Anal. Chem.*, 2017, **89**, 12596–12601.
174 W. L. Zhai, X. L. Sun, T. D. James and J. S. Fossey, *Chem. – Asian J.*, 2015, **10**, 1836–1848.
175 A. J. J. Lennox and G. C. Lloyd-Jones, *Chem. Soc. Rev.*, 2014, **43**, 412–443.
176 (*a*) M. R. Aronoff, B. VanVeller and R. T. Raines, *Org. Lett.*, 2013, **15**, 5382–5385; (*b*) A. K. Mahapatra, S. Mondal, S. K. Manna, K. Maiti, R. Maji, S. S. Ali, S. Mandal, M. R. Uddin and D. K. Maiti, *ChemistrySelect*, 2016, **1**, 375–383.
177 T. Panda and B. S. Gowrishankar, *Appl. Microbiol. Biotechnol.*, 2005, **67**, 160–169.
178 P. Glynn, *Biochem. J.*, 1999, **344**, 625–631.
179 J. Hu, K. Cheng, Q. Wu, D. S. Ding, C. G. Li and Z. Li, *Mater. Chem. Front.*, 2018, **2**, 1201–1206.
180 M. G. Tian, J. Sun, Y. H. Tang, B. L. Dong and W. Y. Lin, *Anal. Chem.*, 2018, **90**, 998–1005.
181 S. P. Sanghani, S. K. Quinney, T. B. Fredenburg, Z. J. Sun, W. I. Davis, D. J. Murry, O. W. Cummings, D. E. Seitz and W. F. Bosron, *Clin. Cancer Res.*, 2003, **9**, 4983–4991.
182 D. Liu, J. Gao, C. L. Zhang, X. H. Ren, Y. Liu and Y. J. Xu, *Pharmazie*, 2011, **66**, 888–893.
183 M. Hosokawa, *Molecules*, 2008, **13**, 412–431.
184 L. Feng, Z. M. Liu, J. Hou, X. Lv, J. Ning, G. B. Ge, J. N. Cui and L. Yang, *Biosens. Bioelectron.*, 2015, **65**, 9–15.
185 G. Abboud and N. Kaplowitz, *Drug Saf.*, 2007, **30**, 277–294.
186 E. Mornet, *Orphanet J. Rare Dis.*, 2007, **2**, DOI: 10.1186/1750-1172-2-40.

187 J. L. Millan and W. H. Fishman, *Crit. Rev. Clin. Lab. Sci.*, 1995, **32**, 1–39.
188 Q. H. Hu, F. Zeng, C. M. Yu and S. Z. Wu, *Sens. Actuators, B*, 2015, **220**, 720–726.
189 Y. Jia, P. Li and K. L. Han, *Chem. – Asian J.*, 2015, **10**, 2444–2451.
190 L. Bai, S. O. Yoon, P. D. King and J. L. Merchant, *Cell Death Differ.*, 2004, **11**, 663–673.
191 T. I. Kim, H. J. Kang, G. Han, S. J. Chung and Y. Kim, *Chem. Commun.*, 2009, 5895–5897.
192 J. M. Brown and W. R. William, *Nat. Rev. Cancer*, 2004, **4**, 437–447.
193 R. B. P. Elmes, *Chem. Commun.*, 2016, **52**, 8935–8956.
194 E. M. Williams, R. F. Little, A. M. Mowday, M. H. Rich, J. V. E. Chan-Hyams, J. N. Copp, J. B. Smaill, A. V. Patterson and D. F. Ackerley, *Biochem. J.*, 2015, **471**, 131–153.
195 G. N. Parkinson, J. V. Skelly and S. Neidle, *J. Med. Chem.*, 2000, **43**, 3624–3631.
196 W. P. Feng, Y. C. Wang, S. Z. Chen, C. Wang, S. X. Wang, S. H. Li, H. Y. Li, G. Q. Zhou and J. C. Zhang, *Dyes Pigm.*, 2016, **131**, 145–153.
197 C. Lopez-Otin and J. S. Bond, *J. Biol. Chem.*, 2008, **283**, 30433–30437.
198 B. Law and C. H. Tung, *Bioconjugate Chem.*, 2009, **20**, 1683–1695.
199 O. Thorn-Seshold, M. Vargas-Sanchez, S. McKeon and J. Hasserodt, *Chem. Commun.*, 2012, **48**, 6253–6255.
200 C. I. Cheng, Y. P. Chang and Y. H. Chu, *Chem. Soc. Rev.*, 2012, **41**, 1947–1971.
201 A. S. Klymchenko, V. V. Shvadchak, D. A. Yushchenko, N. Jain and Y. Mely, *J. Phys. Chem. B*, 2008, **112**, 12050–12055.
202 V. V. Shvadchak, A. S. Klymchenko, H. de Rocquigny and Y. Mely, *Nucleic Acids Res.*, 2009, **37**, e25, DOI: 10.1093/nar/gkn1083.
203 O. M. Zamotaiev, V. Y. Postupalenko, V. V. Shvadchak, V. G. Pivovarenko, A. S. Klymchenko and Y. Mely, *Bioconjugate Chem.*, 2011, **22**, 101–107.
204 Y. Wang, Y. H. Hu, T. Wu, X. S. Zhou and Y. Shao, *Anal. Chem.*, 2015, **87**, 11620–11624.
205 V. V. Shynkar, A. S. Klymchenko, C. Kunzelmann, G. Duportail, C. D. Muller, A. P. Demchenko, J. M. Freyssinet and Y. Mely, *J. Am. Chem. Soc.*, 2007, **129**, 2187–2193.
206 D. P. Ng, B. E. Poulsen and C. M. Deber, *Biochim. Biophys. Acta*, 2012, **1818**, 1115–1122.
207 N. Jiang, C. L. Yang, X. W. Dong, X. L. Sun, D. Zhang and C. L. Liu, *Org. Biomol. Chem.*, 2014, **12**, 5250–5259.
208 K. A. Bertman, C. S. Abeywickrama, H. J. Baumann, N. Alexander, L. Mcdonald, L. P. Shriver, M. Konopka and Y. Pang, *J. Mater. Chem. B*, 2018, **6**, 5050–5058.
209 A. P. de Silva, H. Q. N. Gunaratne, T. Gunnlaugsson, A. J. M. Huxley, C. P. McCoy, J. T. Rademacher and T. E. Rice, *Chem. Rev.*, 1997, **97**, 1515–1566.
210 (*a*) M. H. Lan, J. S. Wu, W. M. Liu, H. Y. Zhang, W. J. Zhang, X. Q. Zhuang and P. F. Wang, *Sens. Actuators, B*, 2011, **156**, 332–337; (*b*) A. Gangopadhyay, S. S. Ali, U. N. Guria, S. K. Samanta, R. Sarkar, P. Datta and A. K. Mahapatra, *New J. Chem.*, 2018, DOI: 10.1039/c8nj03369b.
211 X. F. Yang, Q. Huang, Y. G. Zhong, Z. Li, H. Li, M. Lowry, J. O. Escobedo and R. M. Strongin, *Chem. Sci.*, 2014, **5**, 2177–2183.
212 J. D. Luo, Z. L. Xie, J. W. Y. Lam, L. Cheng, H. Y. Chen, C. F. Qiu, H. S. Kwok, X. W. Zhan, Y. Q. Liu, D. B. Zhu and B. Z. Tang, *Chem. Commun.*, 2001, 1740–1741.
213 Z. G. Song, R. T. K. Kwok, E. G. Zhao, Z. K. He, Y. N. Hong, J. W. Y. Lam, B. Liu and B. Z. Tang, *ACS Appl. Mater. Interfaces*, 2014, **6**, 17245–17254.
214 Q. Chen, C. M. Jia, Y. F. Zhang, W. Du, Y. L. Wang, Y. Huang, Q. Y. Yang and Q. Zhang, *J. Mater. Chem. B*, 2017, **5**, 7736–7742.
215 Y. Liu, J. Nie, J. Niu, W. S. Wang and W. Y. Lin, *J. Mater. Chem. B*, 2018, **6**, 1973–1983.
216 S. Biswas, R. Mengji, S. Barman, V. Venugopal, A. Jana and N. D. P. Singh, *Chem. Commun.*, 2018, **54**, 168–171.
217 H. W. Liu, K. Li, X. X. Hu, L. M. Zhu, Q. M. Rong, Y. C. Liu, X. B. Zhang, J. Hasserodt, F. L. Qu and W. H. Tan, *Angew. Chem.*, 2017, **56**, 11788–11792.
218 S. K. Chatterjee, M. Bhattacharya and J. J. Barlow, *Cancer Res.*, 1979, **39**, 1943–1951.
219 G. P. Dimri, X. H. Lee, G. Basile, M. Acosta, C. Scott, C. Roskelley, E. E. Medrano, M. Linskens, I. Rubelj, O. Pereirasmith, M. Peacocke and J. Campisi, *Proc. Natl. Acad. Sci. U. S. A.*, 1995, **92**, 9363–9367.
220 W. G. Yang, X. X. Zhao, J. Zhang, Y. Zhou, S. M. Fan, H. Sheng, Y. Cao and Y. H. Hu, *Dyes Pigm.*, 2018, **156**, 100–107.
221 L. Peng, M. Gao, X. L. Cai, R. Y. Zhang, K. Li, G. X. Feng, A. J. Tong and B. Liu, *J. Mater. Chem. B*, 2015, **3**, 9168–9172.
222 M. Gao, Q. L. Hu, G. X. Feng, B. Z. Tang and B. Liu, *J. Mater. Chem. B*, 2014, **2**, 3438–3442.
223 H. L. Liu, X. Y. Wang, Y. Xiang and A. J. Tong, *Anal. Methods*, 2015, **7**, 5028–5033.
224 L. Cui, Y. Baek, S. Lee, N. Kwon and J. Yoon, *J. Mater. Chem. C*, 2016, **4**, 2909–2914.
225 C. S. Liang and S. M. Jiang, *Analyst*, 2017, **142**, 4825–4833.
226 D. P. Li, Z. Y. Wang, H. Su, J. Y. Miao and B. X. Zhao, *Chem. Commun.*, 2017, **53**, 577–580.
227 H. Y. Zhang, Z. J. Huang and G. Q. Feng, *Anal. Chim. Acta*, 2016, **920**, 72–79.
228 D. Dahal, L. McDonald, X. M. Bi, C. Abeywickrama, F. Gombedza, M. Konopka, S. Paruchuri and Y. Pang, *Chem. Commun.*, 2017, **53**, 3697–3700.
229 A. Sedgwick, W.-T. Dou, J.-B. Jiao, L. Wu, G. T. Williams, A. T. A. Jenkins, S. D. Bull, J. L. Sessler, X.-P. He and T. D. James, *J. Am. Chem. Soc.*, 2018, DOI: 10.1021/jacs.8b08457.